Pharmacognosy Program
Doctoral School of Pharmaceutical Sciences
University of Szeged

Isolation and structure elucidation of biological active compounds from *Euphorbia deightonii* and *Centrapalus pauciflorus*

Ph.D. Thesis

Muhammad Bello Saidu

Supervisor:
Dr. Dóra Rédei

Szeged, Hungary
2023

List of publications related to the thesis

I. **Saidu, M. B.,** Kúsz N., Tsai Y. C., Vágvölgyi, M., Berkecz, R., Kókai, D., Burián, K., Hohmann, J., Rédei, D.
Triterpenes and phenolic compounds from *Euphorbia deightonii* with antiviral activity against herpes simplex virus type-2
Plants (Basel) **11**, 764 (2022)

II. **Saidu, M. B,** Kúsz, N., Berkecz, R., Rácz, B., Spengler, G., Hohmann, J., Rédei, D.
Ingol, *ent*-atisane, and stachane-type diterpenoids from *Euphorbia deightonii* with multidrug resistance reversing activity
Phytochemistry **204**, 113344 (2022)

III. **Saidu, M. B.,** Krstić, G., Todorović, N., Berkecz, R., Ali, H., Zupkó, I., Hohmann, J., Rédei, D.
Monoterpenoid 5-methylcoumarins from *Centrapalus pauciflorus* with antiproliferative activity
Arabian Journal of Chemistry **16**, 104777 (2023)

IV. Krstić, G., **Saidu, M. B.,** Bombicz, P., De, S., Ali, H., Zupkó, I., Berkecz, R., Gallah, U. S., Rédei, D., Hohmann, J.
Pauciflorins A–E, unexpected chromone–monoterpene-derived meroterpenoids from *Centrapalus pauciflorus*
Journal of Natural Products **86**, 891–896 (2023)

Table of Contents

Abbreviations and symbols

1D	one-dimensional
2D	two-dimensional
Ac	acetyl
Ang	angelyl
Bz	benzoyl
COSY	correlated spectroscopy
FLC	flash-liquid chromatography
fr	fraction
G2PS	genes encoding 2-pyrone synthase
GGPP	geranylgeranyl diphosphate
HMBC	heteronuclear multiple-bond correlation spectroscopy
HPLC	high-performance liquid chromatography
HRESIMS	high-resolution electrospray ionization mass spectroscopy
HSQC	heteronuclear single-quantum coherence spectroscopy
HSV-2	*Herpes simplex* virus type 2
*i*Bu	isobutyryl
*i*Val	isovaleryl
JMOD	*J*-modulated spin-echo experiment
MDR	multidrug resistance
NOESY	nuclear overhauser effect spectroscopy
NP	normal phase
OCC	open-column chromatography
P-gp	permeability glycoprotein
PKR	polyketide reductase
PKS	polyketide synthase
PLC	preparative-layer chromatography
R_f	retention factor
RP	reversed phase
Sal	salicylyl
SEM	standard error of the mean
Tig	tigloyl
TLC	thin-layer chromatography
t_R	retention time
VLC	vacuum-liquid chromatography
δ	chemical shift

1. Introduction

Africa is home to what is considered the earth's 'second lungs' due to the biodiversity rich Congo basin, second only to Amazon forest in South America.[1,2] A study conducted by Klopper et al., suggested that there are over 45,000 plant species in Africa.[3,4] Since time immemorial, plants have always occupied the central role in the treatment of diseases in folk medicine worldwide, examples includes African Traditional Medicine, Chinese Medicine, Ayuverdic Medicine, Unani medicine and others forms of folk medicine obtained globally.[5,6] Recent studies have shown that about 60-80% of the world population rely on traditional medicine to meet their primary health care needs.[7–9] Some 25% of medical prescriptions globally are still directly or indirectly derived from plants. This ranges from use of crude preparations or extracts, to refined extracts and single molecular species. These encompasses herbal medicines, food supplements, botanical drugs, and medicinal prescriptions. Currently, there is an increased demand for plants as source of novel pharmacophores due to their chemical diversity and versatility which is unmatched by synthetic chemistry libraries. Despite the surge in synthetic medicine, half of the more than 850 drugs introduced in the past 20 years have been derived directly from plants.[10,11]

African plants are sources of some well-known conventional drugs: *Physostigma venenosum* (physostigmine),[12] *Catharanthus roseus* (vinblastine and vincristine),[13] *Tabernanthe iboga* (ibogaine),[14] and *Dioscorea* spp. (diosgenin).[15] Many plant species in Africa have not been investigated scientifically for their medicinal properties or to prove or reject the folklore claims on the therapeutic properties of these plants.[16]

1.1. Diterpenoids from *Euphorbia* species

Diterpenoids of *Euphorbia* species have attracted significant interest because of their remarkable chemical diversity and promising pharmacological activities, such as anti-inflammatory, antitumor, antiviral, and cocarcinogenic effects.[17,18]

Euphorbia diterpenoids are classified based on their biosynthetic pathway as higher and lower diterpenes. 'Lower diterpenes' (macrocyclic) are derived from a tetraprenyl pyrophosphate precursor through a 'head-to-tail' cyclization, and non-specific 'higher diterpenes', whose skeletons are formed by the classical 'concertina-like' cyclization like those of triterpenes. The distribution of lower diterpenes are restricted to Euphorbiaceae and Thymeleaceae families while the higher terpenes occur in many plant families.[19] Macrocyclic diterpenes are subdivided into jatrophane-, lathyrane-, ingenane-, daphnane-, tigliane-, myrsinane-, pepluane-, paraliane-, segetane- and rhamnopholane-types, and are major chemical constituents of the *Euphorbia* genus. These diterpenoids display

promising pharmacological activities, for instance cytotoxic, antibacterial, anti-influenza, anti-HIV, HIV latency reversal, anti-inflammatory and multidrug resistance (MDR) reversal effects. Higher diterpenes are subdivided into labdanes, clerodanes, stachane, abietanes, kauranes, and atisanes.[19,20]

1.2. Ingol derivatives

Ingol is the common name of 4,15-epoxy-3,7,8,12-tetrahydroxy-lathyr-5-en-14-one isolated from *Euphorbai ingens* in 1971 by Opferkuch and Hecker.[21] The hypothetical biosynthetic pathways of ingol-type diterpenoids follows that of macrocyclic diterpenes as shown in **Figure 1**. Recent studies have provided more insight on the cyclization processes and the enzymes involved. First, a reactive cembrene cation is formed from geranylgerany diphosphate by the loss of a diphosphate moiety. The cembrene cation formed is unstable and gets stabilized by the formation of cembranoids which readily undergoes cationic cyclization and subsequent Wagner-Meerwein rearrangements.[22,23] CYP450 enzymes catalyze a further series of oxidative reactions on the hydrocarbon skeleton.[24] The casbanes formed from the cembrene cation via loss of a proton and cyclization of the isopropyle group have been considered to be the precursors of a number of macrocyclic diterpenes.[25] Casbanes with a *trans* or *cis* disubstituted cyclopropane ring occur in the species of *Euphorbia*[26] as well as other Euphorbiaceae genera.[27–30] ''*Euphorbia* steroid'' was the first isolated macrocyclic diterpene. It was isolated from *E. lathyris*[31] in 1939 by Dublyanskaya and elucidation of its structure showed it is a tricyclic lathyrane diterpenoid called 6,17-epoxy-lathyrol.[32]

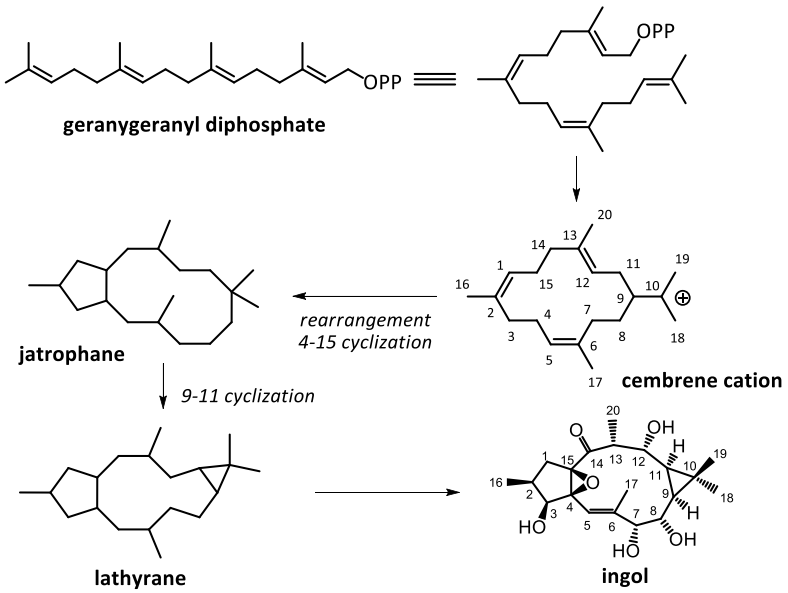

Figure 1. Hypothetical biosynthetic pathway of ingol.

Ingol diterpene is formed as a result of C-4, C-15 epoxy formation on lathyrane diterpene.[33] The most distinguishable feature of ingol among macrocyclic is the presence of 4, 15-epoxy group. Additionally, a keto group situated on C-14 is present and $\Delta^{(5,6)}$ olefine can be foundd in most ingols. There are five methyl groups usually located at C-2, C-6, C-13 and a *gem*-dimethyl group at C-10 in most of the ingols. The hydroxy group are basically found at C-3, C-7, C-8, C-12.[34–39] The unusual presence of hydroxy group on C-17 and C-19 have been reported in *E.* resinifera,[40] *E. antiquorum*,[41] *E. acrurensis*,[42] and *E. hermentiana*.[43] Ingol diterpenoids exist as polyesters. The common ester groups attached include acetyl, tiglyl, angelyl, benzyl, 2-methyl butyryl, *iso*-valeryl, and *iso*-butyryl. Acetyl group is the most common ester group attached to the ingol skeletal core. The types and positions of esters, and configurations of optically active carbons are responsible for variability observed in the ingol-type diterpenoids.

Lathyrane-type diterpenoids do not possess pro-inflammatory activity of phorbol esters.[44,45] Ingols have been reported to possess significant cytotoxic,[46,47] PGE_2-inhibitory,[33] vasoactive properties,[48] and low inhibition of RANKL-induced osteoclastogenesis.[49]

1.3. 5-methylcoumarins and 5-methylchromones of the plant family Asteraceae

Coumarins with methyl substitution at position 5 are rare in nature and have a restricted occurrence in the plant kingdom. They are mainly found from the members of tribes Vernonieae, Nassauvieae, Onoserideae and Mutisieae of the Asteraceae family, and occasionally from a few other taxa.[50,51] Unlike most coumarins that are synthesized through phenylpropanoid pathway, 5-methylcoumarins have been suggested to be derived through the acetate-malonate pathway *via* pentaketide intermediate.[52,53] The superfamily of type III polyketide synthases (PKSs) are key enzymes in generating the backbones of chalcones, stilbenes, chromones, pyrones and several other secondary metabolites in plants.[54,55]

Experiment on *Gerbera hybrida* was used to demonstrate the hypothetical biosynthetic pathway of 5-methylcoumarin (**Figure 2**). *G. hybrida* expresses three genes encoding 2-pyrone synthases (G2PS1–3). Polyketide synthases G2PS2 and G2PS3 are necessary for the biosynthesis of hydroxymethyl coumarin (HMC), and that a reductase enzyme is likely required to complete the pathway to HMC. It is biosynthesized *via* pentaketide with the starting acetate unit formed from acetyl CoA and the other four acetate units from malonyl CoA. The experiment involved the condensation of acetyl CoA and four units of malonyl CoA. The result is the formation of a reactive intermediate which is stabilized through the formation of 4-hydroxy-5-methylcoumarin.[52,53]

As soon as 4-hydroxycoumarin is formed, the prenylation of 5-methylcoumarins takes place immediately.[56] Majority of 5-methylcoumarins have the coumarin scaffold connected to terpene

moieties at C-3 and C-4 of the (α-pyrone moiety) coumarin scaffold.[57] The modification of the terpene component is the major source of variation in most 5-methylcoumarins. The terpene components could be hemiterpene (C_5), monoterpene (C_{10}) or sesquiterpene (C_{15}).[51] The terpene components of Onosorideae and Nassauvieae are mainly sesquiterpene units while those from Mutisieae and Vernonieae are mainly monoterpenes.[51,58–62] In the case of monoterpene component, its derivatives are modified to form one or two rings. Based on literature search, 5-methylcoumarins of Vernonieae tribe and Nassauvieae tribe are unique because many of its derivatives have terminal vinyl and methyl (of terpene unit) attached to C-3′ and this C-3′ is attached to C-3 of the coumarin scaffold.

The terpene substituted 5-methylcoumarins displayed great deal of stereochemistry due to present of α and β configuration forms of the same compounds.[58,59,63–65] Epoxy are sometimes formed between C–6′ and C-7′. [66–70] In some instances, the monoterpene is esterified with methyl group.

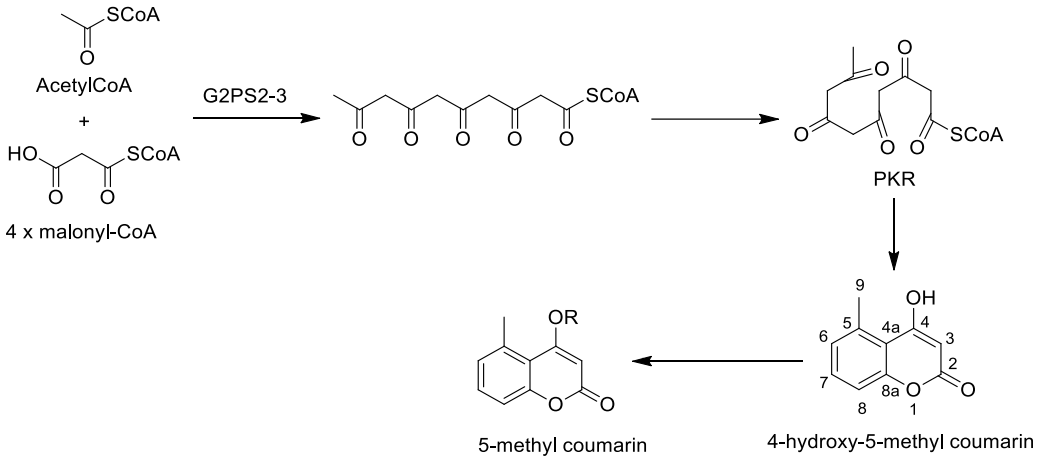

Figure 2. Hypothetical biosynthetic pathway of 5-methylcoumarins.

Ethuliacoumarin A from *Ethulia conyzoides* was the first discovered member of 5-methylcoumarins. This compound has a powerful anthelmintic and molluscicidal activities against *Biomphalaria glabrata* and *Bulinus truncates*.[60,68] Due to their restricted occurrence and few information on 5-methylcoumarins, there are little knowledge of their pharmacological activities. However, plants rich in 5-methylcoumarins have shown cytotoxic,[71] antiproliferative,[72,73] antifungal,[74] antiprotozoal,[75] antimicrobial,[76,77] antioxidant,[78,79] anti-inflammatory[80,81] and antidiabetic[82] activities.

Meroterpenoids are group of secondary metabolites derived from mixed biosynthetic pathways from hybrid polyketide or non-polyketide and terpenoid biosynthesis. They are widely produced by bacteria, algae, plants, and animals.[83–86] Cornforth in 1986 first used the word 'meroterpenoid' which was derived from the Greek word '*mero*' meaning 'fragment or part of' suggesting that the terpene component is part of a larger compound.[87–89] In this research, both 5-methylcoumarins and their isomers, 5-methylchromones can be grouped as meroterpenoid.

1.4. Botanical description and ethnobotanical uses of *Euphorbia deightonii*

Euphorbia is the largest genus in Euphorbiaceae family[90] and is attributed as the third most diverse plant genus in flowering plants accounting for about 2000 species.[91] Just like every genera in Euphorbiaceae, all flowers are unisexual and small in size. However, flowers of genus *Euphorbia* are even smaller and usually aggregated into clusters of flowers (inflorescence) known as a cyathium. *Euphorbia spp.* differ in features of their cyathium, which can show diverse and interesting modifications in different plants in the genus.[92,93–95] Cyathium is a cup-shaped flower cluster, which consist of a female flower with a single pistil surrounded by several male flowers having a single stamen each. The main defining feature of the cyathia is the involucre that surrounds each group of flowers. The involucre has one or more special glands on the upper rim which can vary in size and shape. There must be specialized leaves called cyathial leaves that surrounds the cyathium.[90,92]

Euphorbia deightonii Croizat (Euphorbiaceae) (**Table 1**) is a shrub that grows up to 6 m high. It does not have a distinct trunk but often, branches start right from the base of the plant. It is commonly grown as a hedge plant and its lowest branches are buried in the ground, thus, providing a thick barrier to the base. The 3–6 edged branch are up to 4.5 cm wide and are divided into elongations by constrictions. The wing-like edges are set with bay teeth at 2.5 cm from each other. Its bract are tinged and reddish, involucre glands are green, it has yellow flowers and its capsules are dull red. It is furnished with heavy spines up to 12 mm long. The plant produces white latex which has an irritant effect on wounds. It is native to West Tropical African countries like Nigeria, Senegal, Ghana, Ivory Coast, Benin, Burkina Faso, and Sierra Leone. In traditional medicine, It was used in the treatment of leprosy. Other uses include arrow poisoning during ancient wars, for ornamental purposes, as repellent in agro-horticulture and for production of gums and resins.[96,97]

1.5. Botanical description and ethnobotanical uses of *Centrapalus pauciflorus*

Genus *Centrapalus* belongs to Asteraceae family which is one of the largest plant families with over 1620 genera and 25000 species.[98,99] However, genus *Centrapalus* consists of nine species.[100,101] Members of the family have a unique inflorescence called capitulum, or head that are surrounded by bracts. Leaves are usually simple or compound, spiny or nonexistence.[102] The species are annual or perennial plants and rarely shrubs. The stems are erect, branched with alternate leaves.[103]

Centrapalus pauciflorus (syn. *Cacalia pauciflora* Kuntze, *Centrapalus galamensis* Cass., *Conyza pauciflora* Willd, *Vernonia afromontana* R.E.Fr., *V. coelestina* Schrad. ex D.C., *V. filisquama* M.G. Gilbert, *V. galamensis* (Cass.) Less., *V. galamensis* subsp. *afromontana* (R.E.Fr.) M.G. Gilbert, *V. galamensis* subsp. *filsquama* (M.G. Gilbert) C. Jeffrey, *V. galamensis* subsp. *gibbose* M.G. Gilbert, *V. galamensis* subsp. *lushotoensis* M.G. Gilbert, *V. galamensis* subsp. *mutomoensis* M.G. Gilbert, *V.*

galamensis subsp. *nairobensis* M.G. Gilbert, *V. pauciflora* (Wild.) Less., *V. petitiana* A. Rich., *V. senegalensis* Desf., *V. zernyi* Gilli)[104,105] belongs to the Asteraceae family (**Table 1**.). Its most used synonym is *V. galamensis* subsp. *galamensis*.[106] It is an annual or sometimes short-lived perennial herb with height range of 13-500 cm. It is erect and sometimes straggling, much-branched, with ribbed, finely to coarsely hairy stems. Leaves are sessile, sometimes rather crowded, elliptic, or linear to oblanceolate (3-25 cm long, 0.2-5 cm wide) with cuneate or attenuate base and serrated leaf margins. The leaves have bitter taste. Flowers are usually bisexual, fertile, and pink to violet blue in color. The fruit is a narrowly obovoid achene, with narrow ribs, and dark brown to black in colour.[107–110] It originated from Tropical Africa [111] In folk medicine, it is used in the treatment of malaria, diabetics, chest pain, external injury, cough and gastrointestinal diseases. For stomach pain, leaf pulp is mixed with water and the liquid is drunk.[112] For chest pain and lung pain, pounded leaves are dried and cooked in tea or porridge.[113]

Table 1. Taxonomic classification of the investigated species

Order	Euphorbiales	Asterales
Family	Euphorbiaceae	Asteraceae
Subfamily	Euphorbioideae	Vernoniodeae
Tribe	Euphorbieae	Vernonieae
Subtribe	Euphorbiinae	Centrapalinae
Genus	*Euphorbia*	*Centrapalus*
Species	*E. deightonii*	*C. pauciflorus*

2. Aims of the study

The objectives of my research were the isolation and structure determination of new natural compounds from *E. deightonii* and *C. pauciflorus*, and investigation of their biological activities. To achieve these objectives, the following steps were taken:

- Screening of *E. deightonii* for diterpenoids and *C. pauciflorus* for antiproliferative constituents.
- Preparing extracts from aerial parts of *E. deightonii* and leaves of *C. pauciflorus*
- Purification and isolation of compounds from *E. deightonii* and *C. pauciflorus* using a series and combination of chromatographic techniques such as OCC, VLC, FLC, HPLC, PLC and recrystallization methods.
- Structure elucidation of isolated compounds by use of data from advanced spectroscopic analysis of 1D and 2D NMR as well as HRMS.
- Evaluation of pharmacological activiities of isolated compounds (anti-HSV, anti-proliferative and cytotoxic effects).

3. Materials and methods

3.1. Plant materials

The aerial parts of *E. deightonii* (35 kg wet weight) and fresh leaves of *C. pauciflorus* were collected in August, 2018 from Zaria, Nigeria with their respective geographcal coordinates as (N 11°5'4.2252" E 7°45'44.172") and (N 11°7'19.758" E 7°43'23.1672"). The two plant materials were identified by Umar Gallah (Bioresource Department of National Research Institute for Chemical Technology, Zaria, Nigeria). The plant samples were subsequently cut into smaller pieces, air dried in the absence of sunlight and ground into powdered form. The powdered dried plant materials weighed 1.24 kg for *E. deightonii* and 548 g for *C. pauciflorus*. A voucher specimen (No. 918) for *E. deightonii* and (No. 897) for *C. pauciflorus* were deposited in the herbarium of the Department of Pharmacognosy, University of Szeged, Szeged, Hungary.

3.2. Preparation of extracts for phytochemical and pharmacological screenings

10 g of powdered each from the plant materials were percolated with MeOH (100 ml) at room temperature for a day. The concentrated extract were diluted with H_2O (30 ml) and were subjected to solvent-solvent partitioning with $CHCl_3$ (4 x 50 ml). Thereafter, the $CHCl_3$ soluble phase was separated on polyamide OCC (1 g) using a gradient system of methanol–water [1:4, 2:3, 3:2, 4:1 and 5:0 (250 ml each)] as eluent. Fractions obtained were concentrated via rotary vapour.

Screening of *E. deightonii* for diterpenoids: Fractions were monitored by thin layer chromatography (TLC) using mobile phases cyclohexane–EtOAc–EtOH (70:20:1) and $CHCl_3$:MeOH (98:2).

Screening of *C. pauciflorus* for antiproliferative potential: Samples from the fractions [MeOH–H_2O 1:4 (6.24 mg), 2:3 (5.32 mg) 3:2 (8.73 mg), 4:1 (8.76 mg), and 5:0 (7.89 mg)] were given to Department of Pharmacodynamics and Biopharmacy for screening their antiproliferative activities on HeLa, A2780, MCF-1, and 231 cell lines.

3.3. Extraction and purification of compounds from investigated species

3.3.1 Extraction

E. deightonii: The air-dried plant materials were grinded with a Bosch MKM 6000 grinder into powdered form affording 1240 g (*E. deightonii*) and 548 g (*C. pauciflorus*). The powdered plant materials were exhaustively extracted using percolation method with MeOH (29L for *E. deightonii*) and (45L for *C. pauciflorus*) at room temperature in a glass percolator (length 60 cm, diameter 15 cm). The two extracts were each concentrated *via* rotary vapor affording 218.2 g for *E. deightonii* and 133

g for *C. pauciflorus*. The concentrated extracts were diluted with H_2O (500 ml). Solvent–solvent partitioning was conducted on *E. deightonii* extract with $CHCl_3$ (6 x 500 ml). The $CHCl_3$ soluble phase was concentrated. 134 g of oily extract was obtained. On the other hand, solvent–solvent partitioning was conducted on *C. pauciflorus* extract with $CHCl_3$ (3 x 1000 ml). The $CHCl_3$ soluble phase was concentrated. 65.81 g of oily extract was obtained.

3.3.2 Chromatographic methods used in purification and isolation of compounds

Open-column chromatography (OCC): The $CHCl_3$ soluble fraction of *E. deightonii* extract was dissolved with $CHCl_3$ and pre-adsorbed onto 150 g polyamide (MP Polyamide, 50-160 µm, MP Biomedicals) and it was then subjected to a polyamide column (210 g stationary phase). Gradient mixtures of MeOH–H_2O [1:4, 3:2, 4:1 and 5:0 (6000 ml each) respectively] were used as mobile phase to elute the loaded sample. Weight of fractions obtained were MeOH–H_2O 1:4 (7.64 g), 3:2 (21.10 g), 4:1 (18.10 g), and 5:0 (2.00 g).

The same procedure was carried out on $CHCl_3$ soluble fraction of *C. pauciflorus* with 100 g polyamide used for sample preadsorbtion and 150 g polyamide as stationary phase. The column was eluted with MeOH–H_2O mixtures [1:4, 3:2, 2:3, 4:1 and 5:0 (5000 ml each) respectively]. Weight of fractions obtained were MeOH–H_2O 1:4 (10.80 g), 2:3 (12.33 g), 3:2 (14.00 g), 4:1 (15.10 g), and 5:0 (1.93 g) accordingly.

Vacuum-liquid chromatography (VLC): Silica gel (60 G, 15 µm, Merck) and RP silica gel (LiChroprep RP-18, 40-63 µm, Merck) were used. Each sample was dissolved in either $CHCl_3$ or CH_2Cl_2 and pre-adsorbed onto the silica using twice the weight of sample, then the organic solvent was completely removed via air chamber. The dry-packed columns were prepared by filling silica gel into glass filter funnels containing fritted discs (G3) at the bottom of the column. The VLC columns were eluted under gentle vacuum provided by a V-800 vacuum pump (Büchi). The collected fractions were combined in accordance with their chemical compositions as monitored by TLC (**Tables 2** and **5, Figures 3a–c** and **4a–c**).

Preparative layer chromatography (PLC): silica gel 60 coated aluminum plates with fluorescent indicator F_{254} (Merck 05715) were used. Separation was monitored under UV light at 254 nm and at 366 nm. Compounds were eluted from the scraped adsorbent with $CHCl_3$, and MeOH. The elutes were then filtered to remove the silica gel (**Tables 3** and **6, Figures 3a–c** and **4a–c**).

Thin layer chromatography (TLC): The obtained OCC and VLC fractions were monitored using TLC on silica gel 60 F_{254} (Merck 05554) and RP-18 modified silica gel F_{254s} (Merck 05559). Visualization methods: UV light at 254 nm and at 366 nm, spots were visualized by spraying with cc. H_2SO_4 followed by heating at 105 °C for 5 minutes.

High-performance liquid chromatography (HPLC):

Normal phase LiChrospher Si 60 (5 µm, 250 mm, 4 mm) and Luna Silica (2) 100 l (5 µm, 250 mm, 21.2 mm), and reversed phase Kinetex C_{18} 100 A (5 µm, 150 mm, 4.6 mm), Agilent ZORBAX ODS C-18 100A (5 µm, 250 mm, 9.4 mm) and Phenomenex Lux *i*-Amylose-1 (5 µm, 250 mm, 4.6 mm) columns were used. The eluted compounds were detected at 245 nm, 254 nm and 366 nm (**Tables 4** and **7**, **Figures 3a–c** and **4a–c**).

Table 2. VLC methods involved in the purification of compounds of *E. deightonii* (NP: normal phase, RP: reversed phase)

Method	Sorbent(g)	Eluent	Fractions (no. × ml)
NP 1	200	petroleum ether–EtOAc (9:1, 19:1, 8:2, 7:3 and 0:10; 1300 ml each)	130 × 50
NP 2	60	benzene–$CHCl_3$–diethyl ether (10:0:0, 9:1:0, 18:1:1, 18:3:2, 0:1:0, 0:0:1, 200 ml each)	55 × 20
NP 3–6	60	cyclohexane–$CHCl_3$–EtOH (10:0:0, 8:2:0, 6:4:0, 2:8:0, 8:2:2, 8:2:4, 8:2:8, 8:2:10, 250 ml each)	100 × 20
RP 1–3, 5–8	8.5	MeOH–H_2O (5:5, 6:4, 7:3, 8:2, 9:1, 0:10, 80 ml each)	46 × 10
RP 4	8.5	MeCN–H_2O (4:6, 5:5, 6:4, 7:3, 8:2, 9:1, 0:10, 80 ml each)	52 × 10

Table 3. PLC methods involved in the purification of compounds of *E. deightonii* (NP: normal phase)

Method	Phase	Eluent
A	NP	$CHCl_3$–acetone (100:0.8)
B, C	NP	*n*-hexane–EtOAc–MeOH (90:20:1.4)
D	NP	cyclohexane–$CHCl_3$–EtOH (80:20:10)
E–G	NP	$CHCl_3$–acetone (19:1)

Table 4. HPLC methods involved in the purification of compounds of *E. deightonii* (NP: normal phase, RP: reversed phase)

Method	Column	Eluent	Flow rate (ml/min)
NP 1–18	LiChrospher	*n*-hexane–EtOAc–MeOH (80:19:1)	1.0
NP 19, 20	LiChrospher	cyclohexane–EtOAc–MeOH (80:19:1)	1.0
RP 1–5, 7–9	Kinetex	MeOH–H_2O (70:30)	0.8
RP 6, 10	Luna	MeOH–H_2O (80:20)	0.8
RP 11	Luna	MeOH–H_2O (50:50)	0.8

Table 5. VLC and FLC methods involved in the purification of compounds of *C. pauciflorus* (NP: normal phase, RP: reversed phase)

Method	Sorbent (g)	Eluent	Fractions (no. × ml)
NP 7	150	cyclohexane–EtOAc–EtOH (9:1:0, 8:2:0, 7:3:0, 50:20:1.5, 50:20:3, 50:20:6, 50:20:9, 50:20:12, 50:20:15, 50:20:20, 50:20:40, 50:20:60, 50:20:80, 500 ml each)	109 × 55
NP 8, 10, 13, 14	40	cyclohexane–EtOAc (99:1, 98:2, 96:4, 94:6, 90:10, 80:20, 50:50, 0:100, 110 ml each),	20 × 50
NP 9, 11, 12	50	*n*-hexane–$CHCl_3$ (9:1, 8:2, 7:3, 6:4, 5:5, 4:6, 3:7, and 0:10, 110 mL each)	40 × 20
RP 9	17	MeOH–H_2O (4:6, 5:5, 6:4, 7:3, 8:2, 9:1, 110 mL each)	46 × 13
RF 1 (FLC)	40	gradient elution with MeOH–H_2O (3:7 to 10:0)	83 × 10

Table 6. PLC methods involved in the purification of compounds of *C. pauciflorus* (NP: normal phase)

Method	Phase	Eluent
H	NP	$CHCl_3$–acetone (100:2)
I	NP	$CHCl_3$–acetone (200:7)

Table 7. HPLC methods involved in the purification of compounds of *C. pauciflorus* (NP: normal phase, RP: reversed phase)

Method	Column	Eluent	Flowrate (ml/min)
NP 21, 37	ZORBAX	n-hexane–EtOAc (94:6)	1.0
NP 22, 25, 26, 29, 30, 35	LiChrospher	n-hexane–EtOAc–MeOH (80:19:1)	1.0
NP 23, 27	LiChrospher	n-hexane–EtOAc–MeOH (98:1:1)	1.0
NP 24	LiChrospher	n-hexane–EtOAc (88:12)	1.0
NP 28	LiChrospher	n-hexane–EtOAc–MeOH (90:8:2)	1.0
NP 31	LiChrospher	n-hexane–EtOAc (78:22)	1.0
NP 32	LiChrospher	n-hexane–EtOAc–MeOH (95:4:1)	1.0
NP 33	LiChrospher	n-hexane–EtOAc (80:20)	1.0
NP 34	LiChrospher	n-hexane–EtOAc–MeOH (90:9:1)	1.0
NP 36	LiChrospher	n-hexane–EtOAc (95:5)	1.0
RP 12, 24, 27	Kinetex	MeOH–H_2O (74:26)	0.7
RP 13, 20, 21	Kinetex	MeOH–H_2O (75:25)	0.7
RP 14	Kinetex	MeOH–H_2O (88:12)	0.7
RP 15, 26	Kinetex	MeOH–H_2O (70:30)	0.7
RP 16	Kinetex	MeOH–H_2O (65:35)	0.7
RP 17	Kinetex	MeOH–H_2O (90:10)	0.7
RP 18	Kinetex	MeCN–H_2O (70:30)	0.7
RP 19	Kinetex	MeCN–H_2O (47:53)	0.7
RP 22	Kinetex	MeOH–H_2O (85:15)	0.7
RP 23	Kinetex	MeCN–H_2O (gradient 75:25 to 81:19)	0.7
RP 25	Kinetex	MeOH–H_2O (68:32)	0.7

3.4. Characterization and structure determination of the isolated compounds

Mass spectroscopy: HRMS data were recorded on a Thermo Scientific Q-Exactive Plus Orbitrap mass spectrometer equipped with an ESI electrospray source and coupled with an Agilent 1100 HPLC system. The samples were measured with flow injection analysis method. The mass spectrometer was working in positive mode, and the scan mass range was set to *m/z* 150-2000 at a resolution of 140000. The data were acquired and processed with Thermo Xcalibur 4.0 software.

Nuclear magnetic resonance spectroscopy: NMR spectra were recorded in $CDCl_3$, CD_3OD, and C_5D_5N on a Bruker Avance DRX 500 spectrometer at 500 MHz (^1H) and 125 MHz (^{13}C). The signals of the residual solvents (δ_H 7.26, 3.31, and 8.74 ppm; δ_C 77.16, 49.00, and 150.35 ppm, respectively) were taken as references. Chemical shifts are expressed in parts per million (ppm) and coupling constant (*J*) values in Hz. The 2D data were acquired and processed with MestReNova *v*6.0.2-5475 and TopSpin 3.5pl7 software.

4. Results

4.1. Screening of *E. deightonii* for diterpenoid contents

Sample preparations were conducted as described in section **3.2.** As regards screening of polyamide fractions, TLC chromatograms of fraction eluted with MeOH–H_2O (3:2) showed deep brown colored spots which are indicative of diterpenoids [R_f values: 0.15-0.74 in cyclohexane–EtOAc–EtOH (60:20:2), $CHCl_3$–acetone (19:1) and petroleum ether–EtOAc (4:1)]. These ascertained the richness of diterpenoids in extracts of *E. deightonii*. Hence, this experiment was chemistry-guided with emphasis on isolation of diterpenoids.

4.2. Screening of *C. pauciflorus* for antiproliferative activity

*S*ample preparations were conducted as previously described in section **3.2.** As a result of the antiproliferative assay, it was established, that the fraction obtained with MeOH–H_2O (3:2) has the highest antiproliferative activity; it showed 44.2 ± 0.6%, 49.3 ± 0.9%, 54.6 ± 0.6% and 5.2 ± 0.5% inhibition at 10 mg/ml, and 70.7 ± 0.4%, 85.3 ± 1.0%, 63.7 ± 1.3%, and 68.2 ± 0.8% inhibition at 30 mg/ml against MCF-7, MDA-MB231, HeLa, and A2780 cells, respectively. Fraction eluted with MeOH–H_2O (3:2) was selected for further chromatographic analysis. Hence, this experiment is bioassay-guided fractionation.

4.3 Isolation of diterpenoids and polyphenols from *E. deightonii*

Extraction, solvent–solvent partitioning and polyamide OCC were done as described in section **3.3**. (**Figure 3a**). The diterpenoid-rich fraction MeOH–H_2O (3:2) (21.1 g) was separated on NP-VLC 1 which afforded 130 fractions (130 x 50 ml). The collected fractions were monitored by TLC, and those with similar profiles were combined, thereby affording twelve bulk fractions, A–L. The deep brown colored components were concentrated in bulk fractions G–K and these fractions were selected for further chromatographic separation.

Starting with bulk fraction G, it was further subjected to NP-VLC 2 which yielded G/a–c, fractions (**Figure 3b**). Purification of G/b and G/c were made on RP-VLC 2 and RP-VLC 1, respectively. G/b afforded G/b/I–III fractions while G/c afforded G/c/I–II. Further purification of G/b/II by PLC A resulted in the isolation of ED-1 (**28**) (8.4 mg). On the other hand, G/b/III was purified by RP-HPLC 1 and afforded ED-9 (**12**) (52.3 mg) and G/b/III/2–4. Further purification of G/b/III/3 by PLC B led to the isolation of ED-7 (**10**) (6.3 mg, R_f 0.33) and ED-8 (**11**) (35.9 mg, R_f 0.25). Meanwhile, G/b/III/2 and G/B/III/4 were purified by NP-HPLC 1 and NP-HPLC 2, respectively and resulted with the isolation of

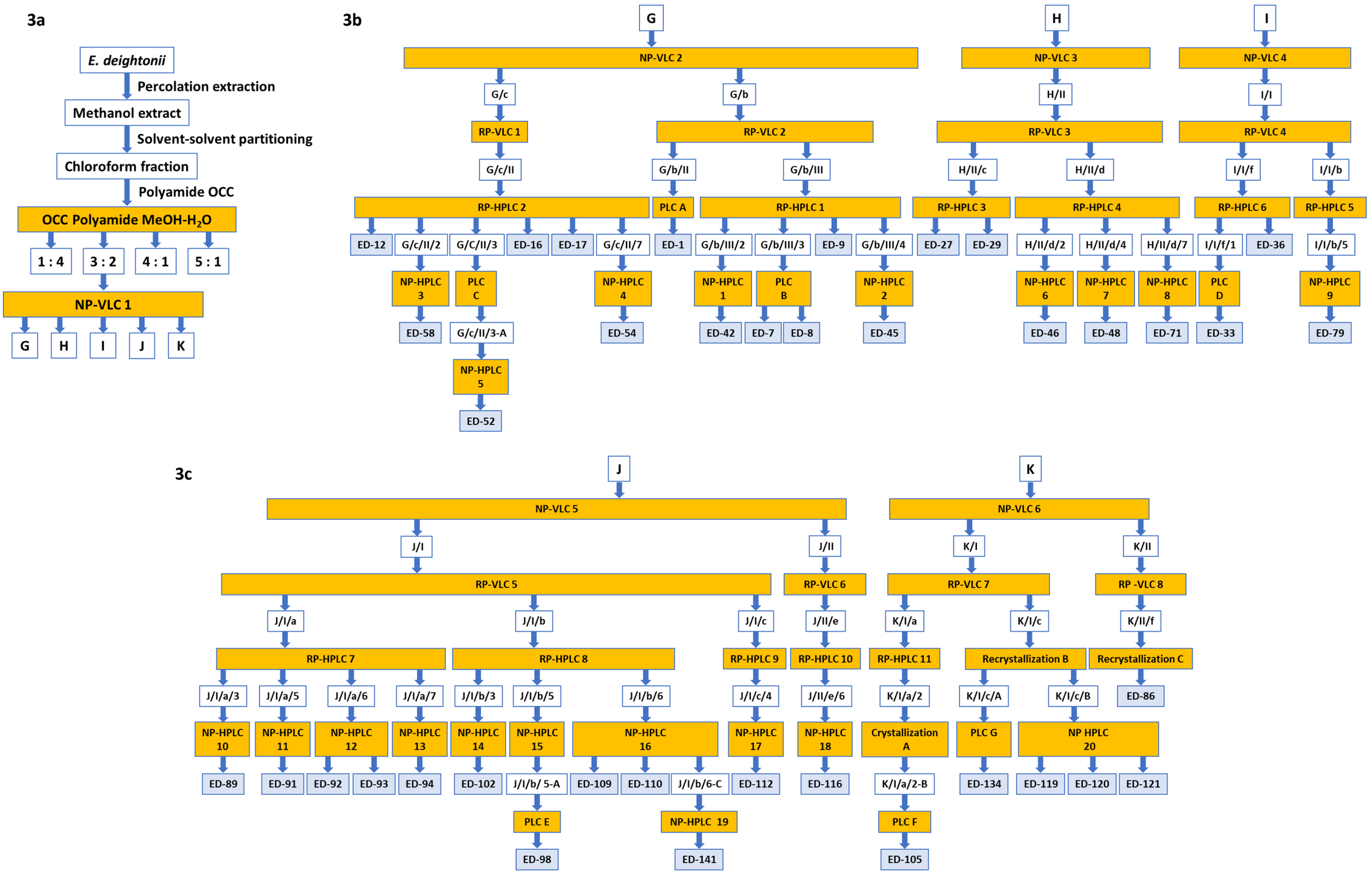

Figure 3. Isolation of compounds *E. deightonii.* **3a**: Extraction, solvent–solvent partition, OCC, and VLC 1; **3b**: Isolation of compounds from bulk fractions G–I; **3c**: Isolation of compounds from bulk fractions J and K.

ED-42 (**17**) (17.5 mg) and ED-45 (**27**) (2.4 mg) respectively. Similarly, G/c/II was purified by RP-HPLC 2 and afforded ED-12 (**13**) (18.9 mg), ED-16 (**14**) (25.5 mg), ED-17 (**15**) (11.0 mg), and fractions G/c/II/2, G/c/II/3, and G/c/II/7. Further purification of G/c/II/2 and G/c/II/7 by NP-HPLC 3 and NP-HPLC 4 afforded isolation of ED-58 (**2**) (1.1 mg) and ED-54 (**21**) (2.6 mg), respectively. Meanwhile, G/c/II/3 was purified by PLC C and gave G/C/II/3-A. Further purification of G/c/II/3-A by NP-HPLC 5 resulted in the isolation of ED-52 (**20**) (3.0 mg). Bulk fraction H was subjected to NP-VLC 3 and gave H/I–II. Separation of H/II by RP-VLC 3 afforded subfractions H/II/a–d. Purification of H/II/c by RP-HPLC 3 led to isolation of ED-27 (**16**) (3.5 mg) and ED-29 (**1**) (3.4 mg). Purification of H/II/d by RP-HPLC 4 gave H/II/d/1–7. H/II/d/2, H/II/d/4, and H/II/d/7 were purified by NP-HPLC 6, NP-HPLC 7, and NP-HPLC 8 respectively which led to the isolation of ED-46 (**18**) (2.2 mg), ED-48 (**19**) (1.6 mg) and ED-71 (**3**) (1.0 mg) respectively.

The bulk fraction I was subjected to NP-VLC 4 which gave fraction I/I which was further separated by RP-VLC 4 and afforded I/I/a–f. Purification of I/I/b by RP-HPLC 5 produced I/I/b/5 which was further purified by NP-HPLC 9 and resulted in the isolation of ED-79 (**4**) (1.2 mg). Similarly, I/I/f was purified by RP-HPLC 6 which afforded ED-36 (**33**) (5.1 mg), and I/I/f/1. Further purification of I/I/f/1 was conducted on PLC D and resulted in the isolation of ED-33 (**32**) (14.2 mg R_f 0.29).

The bulk fraction J was subjected to NP-VLC 5 which gave J/I–II (**Figure 3c**). J/I and J/II were separated on RP-VLC 5 and RP-VLC 6, respectively with gradient mixtures of MeOH–H_2O as eluent and afforded J/I/a–c and J/II/a–e, respectively. J/I/a, J/I/b, J/I/c and J/II/e were purified by RP-HPLC 7, RP-HPLC 8, RP-HPLC 9 and RP-HPLC 10, respectively and afforded J/I/a/1–7, J/I/b/1–6, J/I/c/1–4, and J/II/e/1–6, respectively. J/I/a/3, J/I/a/5, J/I/a/6, J/I/a/7, J/I/b/3, J/I/b/5, J/I/b/6, J/I/c/4 and J/II/e/6 were further purified by NP-HPLC 10, NP-HPLC 11, NP-HPLC 12, NP-HPLC 13, NP-HPLC 14, NP-HPLC 15, NP-HPLC 16, NP-HPLC 17 and NP-HPLC 18, respectively. As a consequence, J/I/a/3 resulted in the isolation of ED-89 (**22**) (1.6 mg), J/I/a/5 resulted in the isolation of ED-91 (**5**) (4.8 mg), J/I/a/6 resulted in the isolation of ED-92 (**23**) (10.9 mg) and ED-93 (**6**) (1.0 mg), J/I/a/7 resulted in the isolation of ED-94 (**24**) (4.8 mg), J/I/b/3 resulted in the isolation of ED-102 (**25**) (2.7 mg), J/I/b/5 gave J/I/b/5-A, J/I/b/6 affording ED-109 (**8**) (0.9 mg), ED-110 (**26**) (2.1 mg), and J/I/b/6-A, while J/I/c/4 resulted in the isolation of ED-112 (**9**) (1.2 mg) and J/II/e/6 afforded the isolation of ED-116 (**1**) (1.7 mg). Further purification of J/I/b/5-A on PLC E led to the isolation of ED-98 (**7**) (10.6 mg) while further purification of J/I/b/6-A by NP-HPLC 19 resulted in the isolation of ED-141 (**30**) (2.1 mg). The bulk fraction K was subjected to NP-VLC 6 and produced K/I–II fractions. K/I and K/II were further separated by RP-VLC 7 and RP-VLC 8, respectively and gave K/I/a–c and K/II/a–f, respectively. K/I/a was purified by RP-HPLC 11 affording K/I/a/1–2. K/I/a/2 formed precipitate when dissolved with *n*-hexane–EtOAc mixture. The insoluble portion (K/I/a/2-B) was purified by PLC F and afforded in the isolation of ED-105 (**37**) (9.3 mg R_f 0.5).

Crystallization was also applied on K/I/c by checking for its solubility in *n*-hexane–EtOAc mixture. Purification of the insoluble portion (K/I/c/A) by PLC G afforded ED-134 (**29**) (9.0 mg, R_f = 0.37). Purification of the soluble portion K/I/c/B by NP-HPLC 20 led to the isolation of ED-119 (**34**) (1.4 mg), ED-120 (**35**) (1.0 mg), and ED-121 (**36**) (0.9 mg). Crystallization was conducted on K/II/f using MeOH. The MeOH-insoluble portion (K/II/f/A) was soluble only in DMSO. NMR analysis confirmed its purity and was named ED-86 (**38**) (4.3 mg).

4.4. Isolation of compounds from *C. pauciflorus*

Extraction, solvent-solvent partitioning, and polyamide OCC were made as described in section **3.3**. (**Figure 4a**). The pharmacologically active fraction, MeOH–H_2O (3:2) (14 g) was separated by NP-VLC 7 yielding 109 fractions (109 x 55 ml). Fractions with similar profiles were combined, thus affording nine bulk fractions namely A-I. Among these bulk fractions, A–C displayed significant and well separated spots on TLC plates and were chosen for further chromatographic purification.

Bulk fraction A was subjected to NP-VLC 8 and yielded A/I–II (**Figure 4b**). Two step purification of A/I by RP-HPLC 27 and NP-HPLC 36 resulted in the isolation of VP-137 (**60**) (1.2 mg) and VP-138 (**61**) (1.1 mg). On the other hand, A/II was chromatographed by RP-HPLC 12 and afforded VP-140 (**63**) (6.9 mg) and A/II/1–3 and 5. Further purification of A/II/3 by NP-HPLC 37 resulted in the isolation of VP-145 (**62**) (1.1 mg). Similarly, purification of A/II/5 by NP-HPLC 21 resulted in the isolation of VP-146 (**39**) (1.8 mg) and VP-147 (**40**) (1.3 mg). Bulk fraction B was subjected to RP-VLC 9 which gave B/I–III. Separation of B/II and B/III were conducted by NP-VLC 9 and NP-VLC 10, respectively and afforded B/II/1–2, B/III/1–2 accordingly. B/II/2 was chromatographed by NP-VLC 13 and produced B/II/2/A–B. Purification of B/II/2/A was made by NP-HPLC 22 and RP-HPLC 13, respectively, and yielded the isolation of VP-153 (**55**) (2.4 mg). Similarly, B/III/2 was fractionated by NP-HPLC 23 and B/III/2-A–D were collected. RP-HPLC 14 and NP-HPLC 24 were consecutively applied on B/III/2-A and resulted in the isolation of VP-122 (**58**) (4.2 mg).

The largest bulk fraction C was subjected to RP-FLC 1 and yielded fractions C/I–V. Additionally, some white crystals were observed in three test tube fractions. They were carefully taken into a beaker. TLC analysis of solved crystals turned out to be mixture of two compounds with slightly different R_f values. They were subsequently purified by NP-HPLC 25 and led to the isolation of VP-5 (**48**) (20.6 mg) and VP-6 (**49**) (15.6 mg).

C/III was separated by NP-VLC 11 and afforded C/III/1–5 (**Figure 4c**). C/III/1 was separated by NP-VLC 14 and afforded C/III/1/A–G. Subsequently, C/III/1/B, C/III/1/C, C/III/1/E, C/III/1/F, and C/III/1/G fractions were purified by NP-HPLC 26, NP-HPLC 27, NP-HPLC 28, NP-HPLC 29 and NP-HPLC 30, respectively and afforded C/III/1/B/1–2, C/III/1/C/1–2, C/III/1/E/1–2, C/III/1/F/1–3, and C/III/1/G/1–

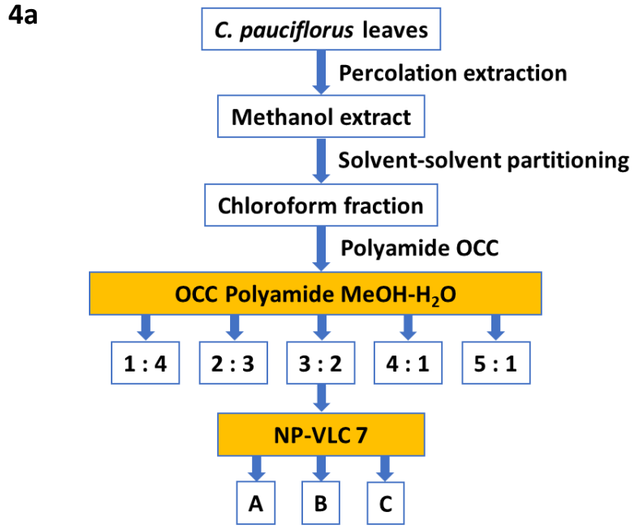

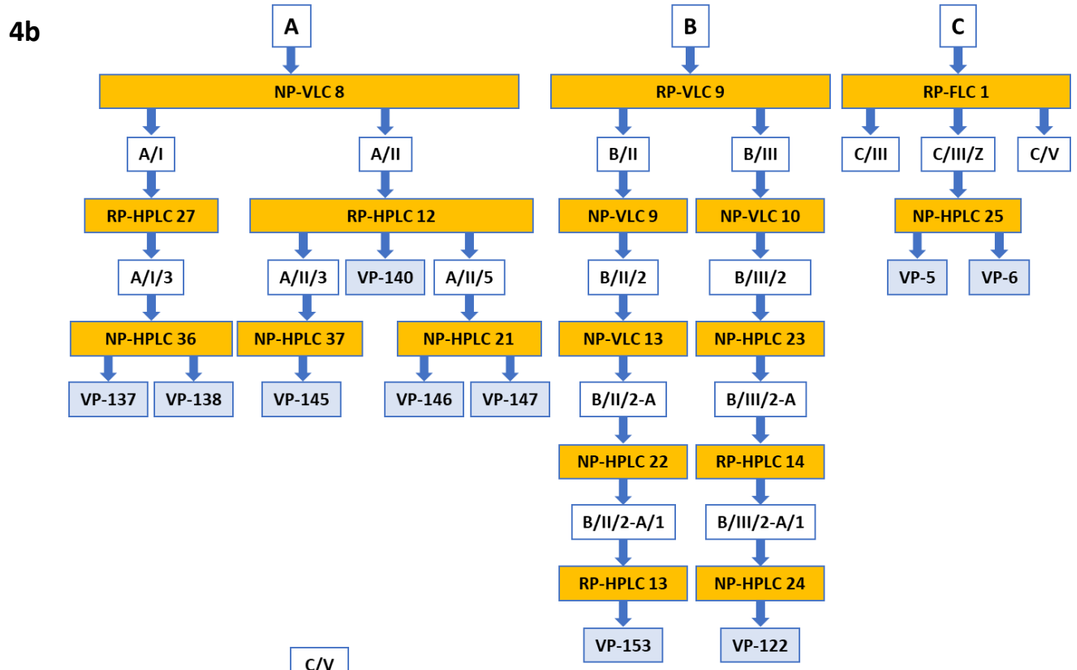

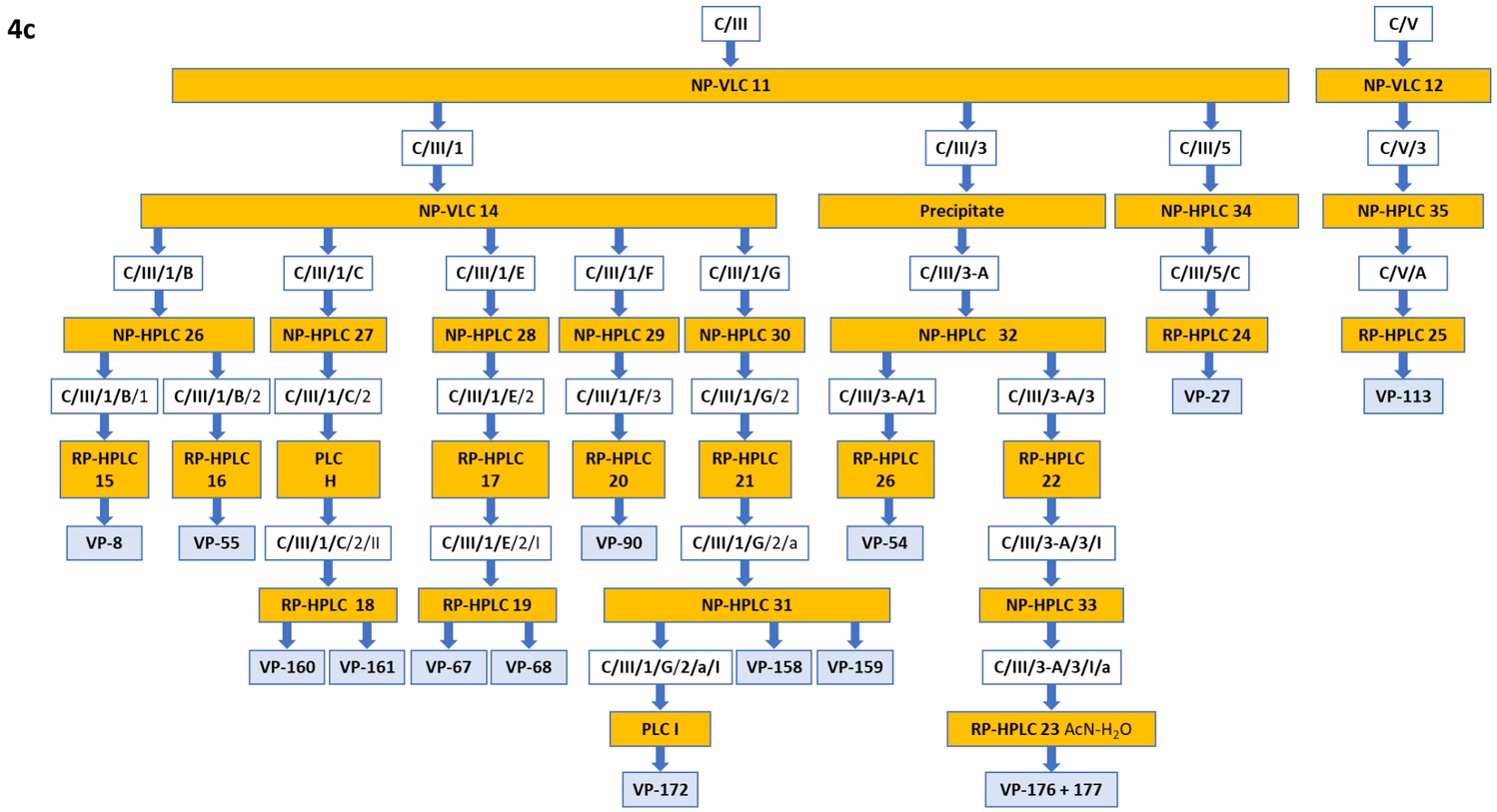

Figure 4. Isolation of compounds *C. pauciflorus.* **4a**: Extraction, solvent–solvent partition, OCC, and VLC 1; **4b**: Isolation of compounds from bulk fractions A–C; **4c**: Isolation of compounds from subfractions C/III and CV.

2, respectively. Further purification of C/III/1/B/1 and C/III/1/B/2 by RP-HPLC 15 and RP-HPLC 16, respectively, afforded VP-8 (**56**) (1.1 mg) and VP-55 (**43**) (156.7 mg), respectively. C/III/1/C/2 was purified on PLC H which gave C/III/1/C/2/I–II. Further purification of C/III/1/C/2/II by RP-HPLC 18 resulted in the isolation of VP-160 (**53**) (15.2 mg) and VP-161 (**54**) (9.6 mg). C/III/1/E/2 was purified by RP-HPLC 17 and gave C/III/1/E/2/I. Further purification of this fraction by RP-HPLC 19 led to the isolation of a pair of inseparable stereoisomers VP-67 (**44**) and VP-68 (**45**) (44.8 mg). Efforts were made to separate **44** and **45** by HPLC using chiral column, but after separation both compounds transformed to a mixture of the stereoisomers again. RP-HPLC 20 on C/III/1/F/3 led to the isolation of VP-90 (**57**) (17.4 mg) while RP-HPLC 21 on C/III/1/G/2 yielded C/III/1/G/2/a. Further purification of C/III/1/G/2/a by NP-HPLC 31 afforded a pair of inseparable isomers VP-158+VP-159 (**51**+**52**) (1.6 mg) and C/III/1/G/2/a/I. PLC I on C/III/1/G/2/A/I resulted in the isolation of VP-172 (**50**) (5.2 mg).

After storage in the refrigerator, in C/III/2, C/III/3 and C/III/4, white crystals were formed. Recrystallization resulted C/III/2-A and C/III/2-B, C/III/3-A and C/III/3-B, C/III/4-A and C/III/4-B, those with suffix -B formed crystals and were MeOH insoluble, while those with suffice -A were MeOH soluble. The purification of C/III/3-A by NP-HPLC 32 gave C/III/3-A/1–3. Purification of C/III/3-A/1 by RP-HPLC 26 resulted in the isolation of VP-54 (**59**) (6.1 mg). Purification of C/III/3-A/3 followed three steps process namely, RP-HPLC 22, NP-HPLC 33 and RP-HPLC 23, respectively, and resulted in the isolation of VP-176 (**46**) (39.9 mg) and VP-177 (**47**) (10.5 mg), a pair of isomers that even though well separated on HPLC, are unstable and easily converts to the mixture of both isomers again as indicated by the NMR results, in the ratio of 2:1. Meanwhile, C/III/5 was purified by NP-HPLC 34 which gave C/III/5-A–C. Further purification of C/III/5-C by RP-HPLC 24 afforded the isolation of VP-27 (**42**) (0.7 mg). Purification of C/V followed three steps process namely, NP-VLC 12, NP-HPLC 35 and RP-HPLC 25 and resulted in the isolation of VP-113 (**41**) (4.8 mg).

4.5. Structure determination of the isolated compounds

4.5.1. Structure determination of compounds from *E. deightonii*

ED-29 (**1**) was isolated as a white amorphous powder with an optical rotation of $[\alpha]_D$ +9 (*c* 0.2, $CHCl_3$). The molecular formula of ED-29 (**1**) was shown to be $C_{29}H_{40}O_9$ based on the high-resolution electrospray ionization mass spectrometry (HRESIMS) peak at *m/z* 555.2571 $[M+Na]^+$ (calcd for 555.2565, $C_{29}H_{40}O_9Na$). The ^1H and ^{13}C *J*-modulation nuclear magnetic resonance (JMOD NMR) spectra contained characteristic resonances of a macrocyclic diterpenoid core esterified with two acetyls (δ_H 2.07 s and 2.02 s; δ_C 170.8, 170.7, 21.2, and 20.6) and a tigloyl group (δ_H 6.88 q, 1.87 s, and 1.84 d; δ_C 166.8, 138.0, 128.8, 14.6, and 12.3) (**Annex 3** and **4**). The ^1H–^1H correlation spectroscopy (COSY) spectrum afforded two sequences of correlated skeletal protons, namely a $–CH_2–CH(CH_3)–CH(OR)–$ (δ_H

2.72 m, 1.71 d, 2.48 m, 0.94 d, 5.25 d) [A] and –CH(OR)–CH(OR)–CH–CH–CH(OR)–CH(CH_3)– (δ_H 5.12 br s, 4.51 br d, 1.23 m, 0.76 t, 3.24 dd, 2.71 m, 1.25 d) [B] structural fragments. Furthermore, a weak *W*-type ($^4J_{H,H}$) COSY cross-peak between a methyl resonating at δ_H 2.10 and a lone olefinic methine at δ_H 5.59 indicated the presence of a trisubstituted double bond in ED-29 (**1**). The connections between the aforementioned structural fragments were determined using relevant heteronuclear multiple bond correlation (HMBC) interactions. Heteronuclear correlations of the oxygen-attached non-protonated carbons C-4 and C-15 (δ_C 74.1 and 71.1, respectively) to H-1 (δ_H 1.71 and 2.72) and H-2 (δ_H 2.48) established an epoxy cyclopentane ring that occurs mostly in the ingol-type class of Euphorbiaceae diterpenoids. The downfield shifted H_3-17 methyl (δ_H 2.10) yielded two- and three-bond correlations with the unsaturated methine carbon C-5 (δ_C 117.2), C-6 (δ_C 140.5), and the oxymethine carbon C-7 (δ_C 77.3), while additional HMBC interactions between H-5 (δ_H 5.59), C-4, C-6, and C-7 confirmed the attachment of subunits A and B through a $\Delta^{(5,6)}$ trisubstituted olefinic bond. A keto group was placed onto C-14 (δ_C 213.2) using its HMBC with H-12 (δ_H 3.24), H-13 (δ_H 2.71), and H_3-20 (δ_H 1.25); thereafter, the eleven-membered macrocycle containing the $\Delta^{(5,6)}$ bond and COSY spin system [B] was finally assembled using the H-13/C-15 correlation. The fourth ring within the scaffold, a cyclopropane moiety, was determined by the HMBC of geminal methyl groups H_3-18 (δ_H 1.17) and H_3-19 (δ_H 0.98) with C-9 (δ_C 25.3), the quaternary C-10 (δ_C 19.0), and C-11 (δ_C 34.3). The positions of the ester groups were unambiguously shown by the $^3J_{C,H}$ heteronuclear correlations of skeletal oxymethines H-3 (δ_H 5.25), H-7 (δ_H 5.12), and H-8 (δ_H 4.51) with respective carbonyl carbons at δ_C 170.7 (acetoxy), δ_C 166.8 (tigloyloxy), and δ_C 170.8 (acetoxy). The upfield-shifted H-12 (δ_H 3.24), with the molecular formula, implied that the diterpenoid was substituted with a C-12 hydroxy group.

The relative configuration of the chiral centers was investigated through diagnostic nuclear Overhauser effect spectroscopy (NOESY) cross-peaks. The Overhauser effects H-1β (δ_H 1.71)/H_3-16 (δ_H 0.94), H-7/H-8, H-8/H-12, H-8/H-13, and H-12/H-13 dictated the H_3-16 methyl to be β-oriented, and the 7-*O*-tigloyl, 8-*O*-acetyl, 12-OH, and H_3-20 groups were α-oriented. A strong NOESY cross-peak between vicinal hydrogens H-2 and H-3 revealed the β-orientation of the 3-*O*-acetyl substituent. NOESY cross-peaks H-3/H-5, H-5/H-9, H-7/H_3-17, and H-8/H_3-17 suggested that the sp^2 methine H-5 and H_3-17 were located on the opposite side of the mean plane of the 11-membered macrocycle; thus, the $\Delta^{(5,6)}$ double bond had an *E*-configuration. Considering the H-9/H-11 cross-peak, it was observed that these adjacent protons had a *cis*-relationship. According to the NOESY correlations H-11/H_3-18, H-8/H_3-19, as well as H-12/H_3-19, the H_3-18 methyl group must be α and H_3-19 β. The above findings were consistent with the proposed structure of **1**.

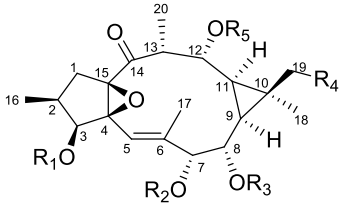

		R^1	R^2	R^3	R^4	R^5			R^1	R^2	R^3	R^4	R^5
1	(ED-29)	Ac	Tig	Ac	H	H	**14**	(ED-16)	Ac	Ac	Tig	H	Ac
2	(ED-58)	Ac	*i*-Bu	Ac	H	Ac	**15**	(ED-17)	Ac	2-MeBu	Ac	H	Ac
3	(ED-71)	Ac	Ac	Sal	H	Ac	**16**	(ED-27)	Ac	Ac	Ac	H	Ac
4	(ED-79)	Ac	Ang	Ac	Ac	Ac	**17**	(ED-42)	Ac	Tig	Ac	H	Ac
5	(ED-91)	H	Tig	Ac	H	Ac	**18**	(ED-46)	Ac	Bz	Me	H	Ac
6	(ED-93)	Ac	Bz	H	H	Ac	**19**	(ED-48)	Ac	Bz	Ac	H	Ac
7	(ED-98)	Ac	Ac	Bz	Ac	Ac	**20**	(ED-52)	Ac	Ang	Me	H	Ac
8	(ED-109)	Ac	Tig	Tig	Ac	H	**21**	(ED-54)	Ac	*i*-Val	Ac	H	Ac
9	(ED-112)	Ac	Ang	Bz	OH	Ac	**22**	(ED-89)	H	Tig	Me	H	Ac
10	(ED-7)	Ac	Ac	2-MeBu	H	Ac	**23**	(ED-92)	Ac	Tig	H	H	Ac
11	(ED-8)	Ac	Ac	Bz	H	Ac	**24**	(ED-94)	Ac	Ang	H	H	Ac
12	(ED-9)	Ac	Ang	Ac	H	Ac	**25**	(ED-102)	Ac	H	Tig	H	Ac
13	(ED-12)	Ac	Ang	Me	H	Ac	**26**	(ED-110)	Ac	Tig	Tig	OH	Ac

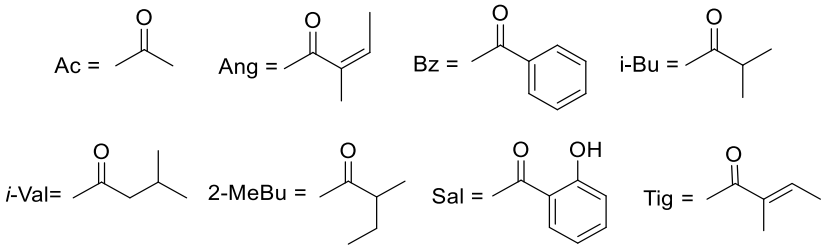

ED-58 (**2**) was isolated as a white amorphous powder with an optical rotation of $[\alpha]_D^{28}$ −6 (*c* 0.1, $CHCl_3$). The molecular formula of ED-58 (**2**) was calculated as $C_{30}H_{42}O_{10}$ by its sodium adduct ion at *m/z* 585.2676 $[M+Na]^+$ (calcd for 585.2670, $C_{30}H_{42}O_{10}Na$) in the HRESIMS. Comparing the ^1H NMR and JMOD ^{13}C NMR spectral data of ED-58 (**2**) with those of ED-29 (**1**) revealed that both compounds comprised the same ingol diterpene polyol structure. However, two differences were observed; one is the replacement of the tigloyl group with isobutyryl group (δ_H 2.66 m, 2 × 1.20 d; δ_C 175.9, 34.1, 18.6, 18.9) at C-7, as shown by the HMBC between H-7 (δ_H 5.12) and isobutyryl carbonyl (δ_C 175.9). The second difference is the replacement of the hydroxyl group at C-12 with an acetyl group (δ_H 2.10; δ_c 170.6, 21.1) in ED-58 (**2**), as indicated by the HMBC of H-12 (δ_H 4.87) with AcCO (δ_c 170.6). The structure of ED-58 was established as **2**. The 2-*epi* derivative of ED-58 (**2**) was described by Morgenstern et al.[63]. The presence of a 2α-CH_3 group resulted in the appearance of H_2-1 methylene as a doublet at δ_H 2.09 (2H) (**Annex 3** and **4**).

ED-71 (**3**) was isolated as a white amorphous powder with an optical rotation of $[\alpha]_D^{28}$ −31 (*c* 0.1, $CHCl_3$). The HRESIMS ion at *m/z* 635.2475 $[M+Na]^+$ (calcd for 635.2463, $C_{33}H_{41}O_{11}Na$) showed a molecular formula of $C_{33}H_{40}O_{11}$ for ED-71 (**3**). Its ^1H NMR spectrum was similar to that of ED-58 (**2**); however, an acetyl signal was replaced in a cluster of aromatic hydrogen resonances (δ_H 7.78, 7.47, 6.98, and 6.88) (**Annex 3** and **4**) The splitting pattern, mutual ^1H–^1H COSY interactions, and appearance of a sharp singlet peak at δ_H 10.51 (3′–OH), forming an H bond with the nonbonding electron pair belonging to one of the nearby carbonyl moieties, are characteristic features of a salicylic acid moiety. The HMBC from that particular hydroxy proton to C-2′ (δ_C 112.2), C-3′ (δ_C 162.1), and C-4′ (δ_C 118.0) and from H-7′ (δ_H 7.78) to C-1′ (δ_C 169.4) and C-3′ corroborated this conclusion. The HMBC from C-1′ to H-8 (δ_H 4.84) puts the salicylic acid onto C-8 (δ_C 72.7), and the presence of the salicylic acid in a *Euphorbia* diterpenoid is considerably unique. The three acetyl groups were placed onto C-3, C-7, and C-12 using the heteronuclear correlations of H-3 (δ_H 5.37), H-7 (δ_H 5.18), and H-12 (δ_H 4.92) with the corresponding carbonyl atoms at δ_C 170.9, 169.9, and 170.6. The NOE experiment permitted the assignment of the same configurations of stereogenic centers as for ED-29 (**1**) and ED-58 (**2**).

ED-79 (**4**) was isolated as a white amorphous powder with an optical rotation of $[\alpha]_D^{28}$ −10 (*c* 0.1, $CHCl_3$). It has the molecular formula of $C_{33}H_{44}O_{12}$ derived from the HRESIMS molecular ion at *m/z* 655.2741 $[M+Na]^+$ (calcd for 655.2725, $C_{33}H_{45}O_{12}Na$). Its 1D NMR spectra displayed the resonances of five ester functionalities, including four acetyls (δ_H 2.12, 2.07, 2.05, and 1.99; δ_C 170.8, 170.7, 2 × 170.4, 2 × 21.2, 20.9, and 20.7) and one angeloyl (δ_H 6.12, 1.98, 1.93; δ_C 166.5, 139.1, 127.6, 20.7, and 15.9) (**Annex 3** and **4**). The absence of a methyl group in the diterpenoid backbone, as well as an oxymethylene (δ_H 4.27 and 3.53; δ_C 64.5), affording HMBC with one of the carbonyls (δ_C 170.7), dictated that compound ED-79 (**4**) bears an acyl side chain at position C-19 instead of a 19-methyl. The downfield shifted C-10 (δ_C 22.3) and H-11 (δ_H 1.35) in ED-79 (**4**) compared to those in ED-71 (**3**) (δ_{C10} 19.8 and δ_{H11} 1.19) were in line with the above-discussed structural difference. The diterpenoid scaffold of ED-79 (**4**) further contained acetoxy groups on C-3, C-8, and C-12 according to the HMBC interactions of H-3 (δ_H 5.25), H-8 (δ_H 4.60), and H-12 (δ_H 4.94) with acetyl carbonyls. The HMBC of H-7 (δ_H 5.27) with the carbonyl carbon at δ_C 166.5 revealed the location of the angeloyloxy residue on C-7 (δ_C 76.2). The relative configuration of ED-79 (**4**) was evaluated using a set of NOE cross-peaks and was found to be identical to that of ED-29 (**1**) and ED-58 (**2**) and ED-71 (**3**).

ED-91 (**5**) was isolated as a white amorphous powder with an optical rotation of $[\alpha]_D^{28}$ +14 (*c* 0.2, $CHCl_3$). The molecular formula of $C_{29}H_{40}O_9$ was assigned to compound ED-91 (**5**) by its HRESIMS peak at *m/z* 555.2570 $[M+Na]^+$ (calcd for 555.2565, $C_{29}H_{40}O_9Na$). Although no hydroxy proton was observed in the ^1H NMR and heteronuclear single quantum coherence (HSQC) spectra, the markedly upfield-shifted H-3 (δ_H 4.28) with no HMBC with any of the carbonyl carbons suggested that ED-91 (**5**) possessed an –OH group at C-3 (δ_C 76.3) (**Annex 3** and **4**). The positions of the two acetyloxy and one

tigloyloxy groups, which were evident from the NMR spectra, were deduced from the HMBCs on C-8, C-12, and C-7, respectively.

ED-93 (**6**) was isolated as a white amorphous powder with an optical rotation of $[\alpha]_D^{28}$ +15 (*c* 0.1, $CHCl_3$). The molecular formula of $C_{31}H_{38}O_9$ was determined for ED-93 (**6**) using an HRESIMS peak at *m/z* 577.2419 $[M+Na]^+$ (calcd for 577.2408, $C_{31}H_{38}O_9Na$). Its ^1H NMR spectrum contained the distinctive signals of one benzoyl (δ_H 8.03, 7.60, and 7.47) and two acetyl groups (δ_H 2.13 and 2.05). The HMBCs of acyl carbonyls with H-3 (δ_H 5.19), H-7 (δ_H 5.31), and H-12 (δ_H 4.94) (**Annex 3** and **4**) revealed the locations of the ester residues on C-3 (acetoxy), C-7 (benzoyloxy), and C-12 (acetoxy). Moreover, the shielded nature of H-8 [δ_H 3.63 in ED-93 (**6**) vs. δ_H 4.61 in ED-91 (**5**)] indicated that C-8 was attached to a hydroxy group instead of an acyl moiety.

ED-98 (**7**) was isolated as a white amorphous powder with an optical rotation of $[\alpha]_D^{28}$ −20 (*c* 0.1, $CHCl_3$). The molecular formula of ED-98 (**7**) was identified as $C_{35}H_{42}O_{12}$ *via* its HRESIMS peak displayed at *m/z* 677.2589 $[M+Na]^+$ (calcd for 677.2569, $C_{35}H_{42}O_{12}Na$). Its ^1H NMR data showed similarities to those of ED-79 (**4**), such as the presence of five esters, including four acetyls (δ_H 2.14, 2.11, 2.08, and 1.68) and an oxymethylene H_2-19 (δ_H 4.09 and 3.72) (**Annex 3** and **4**). The lack of signals of an angeloyl moiety and the additional protons at δ_H 8.00, 7.56, and 7.44 attributed to a benzene ring demonstrated that these diterpenoids differ in one acyl substituent. After constructing the planar structure of ED-98 (**7**), the four acetyls were placed onto C-3 (δ_C 76.4), C-7 (δ_C 76.9), C-12 (δ_C 69.4), and C-19 (δ_C 64.4) using $^3J_{C,H}$ correlations between respective skeletal oxymethines and carbonyl carbons. The HMBCs recorded between H-8 (δ_H 4.89), sp^2 methines at δ_H 8.00, and the remaining ester carbonyl at δ_C 165.7 led to the conclusion that a benzoyloxy unit resides on C-8 (δ_C 70.9).

ED-109 (**8**) was isolated as a white amorphous powder with an optical rotation of $[\alpha]_D^{28}$ −13 (*c* 0.075, $CHCl_3$). Its molecular composition, $C_{34}H_{46}O_{11}$, was determined using the HRESIMS peak at *m/z* 653.2938 $[M+Na]^+$ (calcd for 653.2932, $C_{34}H_{46}O_{11}Na$). This compound was esterified with two acetic and two tiglic acids, as shown by its 1D NMR spectra. Based on relevant heteronuclear correlations, acetoxy groups were assigned to C-3 (δ_C 76.7) and C-19 (δ_C 65.1), while the two tigloyloxy groups were attached to C-7 (δ_C 76.8) and C-8 (δ_C 70.6) (**Annex 3** and **4**) Like ED-29 (**1**), the oxymethine H-12 of ED-109 (**8**) resonated upfield at δ_H 3.35, which indicated the presence of a hydroxy substituent at that position.

ED-112 (**9**) has an optical rotation of $[\alpha]_D^{28}$ −40 (*c* 0.1, $CHCl_3$) and molecular formula of $C_{36}H_{44}O_{11}$ [HRESIMS *m/z* 675.2795 $[M+H]^+$ (calcd for 675.2776, $C_{36}H_{44}O_{11}Na$)] contained two acetoxy, an angeloyloxy, and one benzoyloxy functions. The acetoxy groups were connected to C-3 (δ_C 76.7) and C-12 (δ_C 70.6) by the HMBC correlations of the acetyl carbonyls at δ_C 170.7 and 172.4 with H-3 (δ_H 5.28) and H-12 (δ_H 5.08) (**Annex 3** and **4**), respectively. The HMBC correlations between H-7 (δ_H 5.33) and δ_C 166.5, as well as between H-8 (δ_H 4.94) and δ_C 165.6, guided the placements of angeloyloxy and

benzoyloxy units onto C-7 and C-8. Additionally, the upfield-shifted H_2-19 (δ_H 3.57 and 3.41) substantiated the presence of an oxymethylene moiety in the cyclopropane ring of ED-112 (**9**).

Furthermore, eighteen ingol diterpenoids previously known were isolated from the extract of *E. deightonii* for the first time. The ingol esters which were previously isolated from *E. antiquorum* [(**10**), (**11**), (**13**), (**14**), (**17**), (**18**), (**20**), (**23**), (**27**)],[41,49,114–116] *E. cornigera* [(**10**), (**15**)],[47] *E. tirucalli* [(**10**), (**16**)],[36] *E. royleana* [(**11**), (**16**), (**19**)],[117–119] *E. nivulia* [(**11**), (**13**), (**20**), (**24**)],[33,120] *E. hermentiana* [(**11**), (**13**), (**14**), (**18**), (**20**), (**22**), (**23**)],[43] *E. kamerunica* [(**11**), (**12**), (**14**), (**18**), (**20**), (**22**), (**23**)],[35,46,121] *E. acrurensis* [(**12**), (**17**), (**21**), (**26**)],[42] *E. ingens* [(**14**), (**16**)],[21] *E. portulacoides* [(**15**), (**16**), (**19**)],[63] *E. canariensis* (**27**),[122] *E. neriifolia* [(**17**), (**19**)][123], and *E. lactea* (**25**).[124]

Based on their NMR data, ED-1 (**28**) and ED-134 (**29**) were proven to be *ent*-atisane diterpenoids known metabolites of Euphorbiaceae species. ED-1 (**28**) was isolated from *E. pilosa*,[125] *E. ebracteolate*,[126] *E. fischeriana*,[127] *E. yinshanica*,[128] *E. characias*,[129] *Stillingia sanguinolenta*,[130] and *E. fidjiana*. Previously, ED-134 (**29**) was isolated from *E. fidjiana*.[131] The stachane diterpenoid derivative ED-141 (**30**) was isolated from *Ptychopetalum olacoides.*[132]

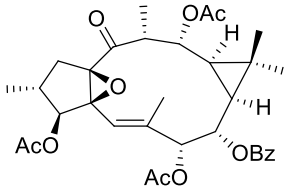

27 (ED-45)

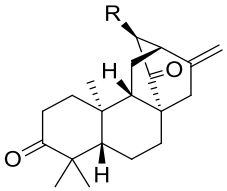

28 (ED-1) R= H

29 (ED-134) R = OH

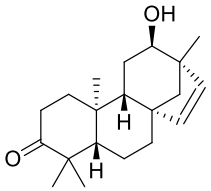

30 (ED-141)

ED-116 (**31**) was isolated as a white amorphous powder. The protonated molecular ion at *m/z* 471.3844 $[M + H]^+$ (calcd for 471.3833, $C_{31}H_{51}O_3$) in the HRESIMS spectrum provided the molecular formula $C_{31}H_{50}O_3$. The ^{1}H NMR spectrum displayed the resonances of five tertiary (δ_H 0.85, 0.92, 1.01, 1.05, and 1.17, each 3H, s) and three secondary (δ_H 0.92, d, J = 6.5 Hz; δ_H 1.02 and 1.03, each d, J = 6.7 Hz, 3H) methyl groups, two oxymethines (δ_H 3.32, dd, J = 11.2 and 5.0 Hz; δ_H 4.27, br s), and an exomethylene (δ_H 4.73, br s; δ_H 4.66, d, J = 1.2 Hz). The presence of a tetrasubstituted olefin bond was apparent from the nonprotonated sp^2 carbon signals at δ_C 141.6 and 157.3. The 1D NMR data suggested that ED-116 (**31**) is a tetracyclic triterpene with an exomethylene-containing side chain, similar to that of euphorbol-7-one **33** (ED-36) and its derivatives previously isolated from *Polyalthia oblique.* [133] The planar structure of ED-116 (**31**) was assembled with the aid of HSQC, ^{1}H–^{1}H COSY, and HMBC data. It was found that two hydroxy-groups are located at C-3 (δ_H 3.32, δ_C 78.8) and C-7 (δ_H 4.27, δ_C 65.6), while a keto substituent was placed onto C-11 (δ_C 200.4), which formed a conjugated enone with a $\Delta^{(8,9)}$ double bond. The relative configuration of ED-116 (**31**) was established based on relevant NOE correlations and coupling constant values. The large J value of H-3 (11.2 Hz) dictated that 3-OH is

oriented equatorially, thus occupying a *β*-position [134]. This conclusion agreed with NOE correlations between H-3, H-5, and H_3-29. Considering a strong NOE between H-7 and H_3-30, the 7-hydroxy group must be in an *β*-position. Furthermore, in the H-17*α*/H_3-21, H-20/H_3-18, and H-12*α*/H_3-21 NOESY correlations, the chemical shift of H_3-21 (δ_H 0.92, d, J = 6.5 Hz) (**Annex 5a**) was consistent with literature data reported for lanostane-type triterpenes[133]. Accordingly, ED-116 (**31**) was identified as 3*β*,7*β*-dihydroxy-24-methylenelanosta-8-ene-11-one.

Two further triterpenes, ED-33 (**32**) (kansenone) and ED-36 (**33**) (euphorbol-7-one) were isolated from *E. deightonii*. Kansenone (**32**) was reported from *Euphorbia kansui,*[134] (euphorbol-7-one) (**33**) was isolated from *E. sapinii*[135] and *Polyalthia oblique*.[133]

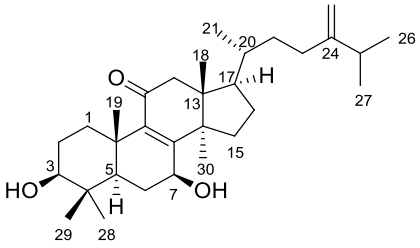

31 (ED-116)

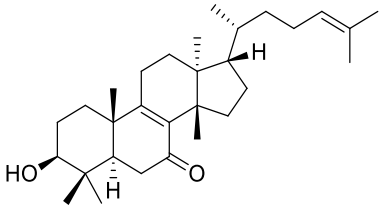

32 (ED-33)

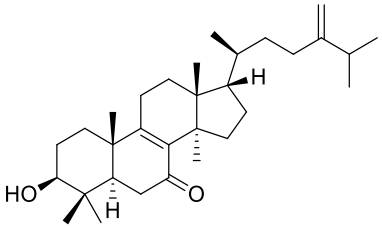

33 (ED-36)

ED-119 (**34**) was obtained as a colorless oil. The molecular formula $C_{23}H_{26}O_7$ was assigned for ED-119 (**34**) based on its molecular ion peak at *m/z* 415.1757 $[M+H]^+$ (calcd for 415.1751, $C_{23}H_{27}O_7$) in the HRESIMS spectrum. Its ^{1}H NMR spectrum showed characteristic signals of a neolignane, including a 1,3,4-trisubstituted benzene and a dihydrobenzofurane ring. Comparison of the 1D NMR data with literature data revealed that ED-119 (**34**) is similar to dihydrocarinatinol previously reported from *Virola carinata.* [136] However, unlike in dihydrocarinatinol, the allyl side chain of ED-119 (**34**) is substituted with a methoxy group, as shown by the HMBC correlations of C-7' (δ_C 84.8) with H-9' (δ_H 5.23 and 5.29) and 7'-OCH_3 (δ_H 3.34), while the hydroxymethyl moiety is acetylated, as suggested by heteronuclear correlations between the acetyl carbonyl (δ_C 170.9) and H_2-9 oxymethylene protons (δ_H 4.29 and 4.47) (**Annex 5b**). The vicinal coupling constant value of 7.6 Hz between H-7 and H-8 dictated their *trans* relationship.[137] Trivial name deightonin was given to ED-119 (**34**); its chemical name is *trans*-(2-(4-hydroxy-3-methoxyphenyl)-7-methoxy-5-(1-methoxyallyl)-2,3-dihydrobenzofuran-3-yl) methyl acetate. Although the absolute configuration has not been determined, ED-119 (**34**) is most likely a mixture of C-7' epimers, as indicated by the duplicated proton and carbon signals at and around C-7'. Chromatography of ED-119 (**34**) on chiral HPLC column afforded 4 peaks in an approximately 1:1:5:5 area % ratio, indicating four stereoisomers. 7*S*,8*R* or 7*R*,8*S* of trans-oriented H-7/H-8, and *R/S* configuration of C-7'.

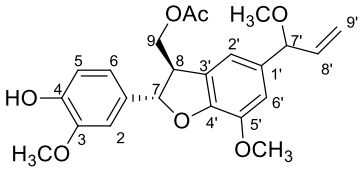

34 (ED-119)

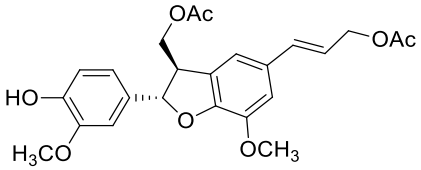

35 (ED-120)

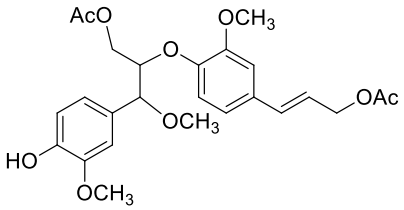

36 (ED-121)

ED-120 (**35**) and ED-121 (**36**) were identified as dehydrodiconiferyl-diacetate and marylaurencinol based on the literature data. Dehydrodiconiferyl-diacetate (**35**) was isolated from Chilean propolis,[138] marylaurencinol (**36**) was reported from cultivated plant, *Cymbidium* Great Flower 'Marylaurencin'.[139] Structures of two further phenolic compounds were established; ED-105 (**37**) was identified as scoparon (syn. esculetin) 6,7-dimethoxycoumarin isolated from *Skimmia laureola*[140] and the structure of ED-85 (**38**) was identified as that of 3,4,3'-tri-*O*-methylellagic acid isolated from many other plants, e.g. in *Lagerstroemia speciosa.*[141]

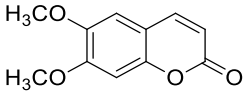

37 (ED-105)

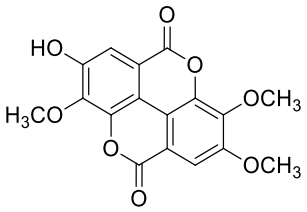

38 (ED-85)

In summary, thirty eight compounds were isolated from *E. deightonii*. These included thirty diterpenoids [ingol derivatives (**1**–**27**), *ent*-atisane (**28**–**29**), and stachane types (**30**)], three triterpenes (**31**–**33**), two lignans (**34**–**35**), one neolignan (**36**), coumarin (**37**) and ellagic acid derivative (**38**).

4.5.2 Structure determination compounds isolated from *C. pauciflorus*

VP-146 (**39**), named as centrapalus coumarin A, was isolated as a colorless oily material with optical rotation of $[\alpha]_D^{28}$ +68.0 (*c* 0.1, $CHCl_3$). The molecular formula of VP-146 (**39**) was found to be $C_{20}H_{22}O_3$ based on the HRESIMS peak at *m/z* 311.1634 $[M+H]^+$ (calcd for $C_{20}H_{23}O_3$ 311.1642). The ^1H NMR and ^{13}C JMOD spectra of VP-146 (**39**) indicated the presence of one vinyl [δ_H 4.95 d (17.2 Hz), 5.18 d (11.3 Hz), 6.00 dd (17.2, 11.3 Hz); δ_C 114.3, 144.6], one 2-methyl-1-propenyl [δ_H 5.36 d (8.1 Hz), 1.82 s, 1.71 s; δ_C 122.7, 138.5, 25.8, 18.6, 26.1], two methyl groups (δ_H 2.64 s, 1.58 s; δ_C 23.8, 26.1], and a skeleton consisted of 7 quaternary carbons (δ_C 164.2, 160.8, 154.1, 137.2, 114.8, 105.1, and 38.0), 4 methins (δ_H 7.32 t (8.1 Hz), 7.14 d (8.1 Hz), 7.00 d (8.1 Hz), and 4.83 br t (10.2 Hz); δ_C 127.4, 130.8, 114.9, 72.0), and 1 methylene group (δ_H 1.78 dd (14.2, 2.1 Hz), 1.88 dd (14.2, 2.1 Hz); δ_C 42.4). The NMR spectroscopic data were very similar to those of VP-147 (**40**) (preethulia coumarin)[61,142], and clearly showed that

compound VP-146 (**39**) is a 5-methylcoumarin derivative connecting with a monoterpene unit. The monoterpene part was elucidated by means of ^{1}H-^{1}H COSY and HMBC correlations. The ^{1}H–^{1}H COSY spectrum afforded sequences of correlated protons: –CH_2–CH(OR)–CH= (δ_H 1.78 dd, 1.88 dd, 4.83 br t and 5.36 d), and a vinyl group CH_2=CH– (δ_H 4.95 d, 5.18, d and 6.00 dd). The connections of these structural fragments were determined based on the HMBC correlations of C-3' (δ_C 38.0) with H-10' (δ_H 1.58), H-2' (δ_H 6.00), and H-4' (δ_H 1.78, 1.88); and C-7' (δ_C 138.5) with H-6' (δ_H 5.36), H-8' (δ_H 1.82), and H-9' (δ_H 1.71) (**Annex 6** and **7**). From these data it could be concluded that VP-146 (**39**) and VP-147 (**40**) are stereoisomers. The configuration of the compounds was solved using the NOESY spectra. Key NOESY correlations of VP-146 (**39**) were observed between H-6' and H-4' at δ_H 1.78 (α), and between H-4' at δ_H 1.88 (β) and H-5', confirming the opposite orientation of the vinyl and the 2-methyl-1-propenyl groups. In the NOESY spectrum of VP-147 (**40**) Overhauser effect between H-5' and H_3-10' was detected which indicates that these protons have the same orientation, most probably axial position on the ring with chair conformation.

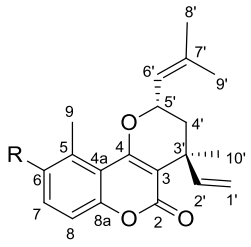

39 (VP-146) R = H

41 (VP-113) R = OH

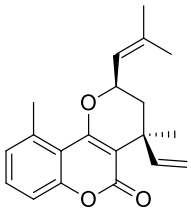

40 (VP-147)

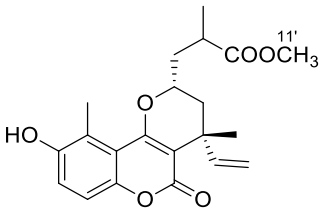

42 (VP-27)

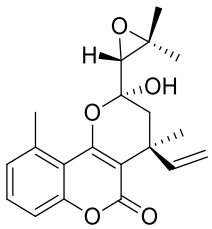

43 (VP-55)

VP-113 (**41**) named as centrapalus coumarin B, was isolated as colorless oily compound with optical rotation of $[\alpha]_D^{28}$ +160.7 (*c* 0.1, $CHCl_3$). The molecular formula of VP-113 (**41**) was shown to be $C_{20}H_{22}O_4$ based on the HRESIMS peak at *m/z* 327.1592 $[M+H]^+$ (calcd for $C_{20}H_{23}O_4$ 327.1591). Comparing ^{1}H NMR and ^{13}C NMR JMOD spectral data of VP-113 (**41**) with those of VP-149 (**39**) reveal that both compounds are based on 5-methylcoumarin structure substituted with a monoterpene unit. The monoterpene part of VP-149 (**39**) and VP-113 (**41**) is the same as indicated by the good agreement of the ^{1}H and ^{13}C NMR data, the difference between the two compounds lies in the aromatic ring, which in case VP-113 (**41**) contains an additional hydroxyl group at C-6, and NOE correlations of 6-OH with protons at δ_H 2.55 (H_3-9) and 6.99 (H-7). This was demonstrated by the *ortho* coupled doublet protons at δ_H 6.99 d (8.8) (H-7), 7.03 d (8.8) (H-8), carbon resonance of C-6 at δ_C 150.3 [for VP-149 (**39**) δ_C 127.4], and OH singlet at δ_H 5.05 (6–OH) (**Annex 6** and **7**). which showed HMBC correlation with C-6. The stereochemistry of VP-113 (**41**) was analyzed by NOESY spectroscopy and found that the configuration of C-3' and C-5' is identical with those of VP-149 (**39**) regarding the H-2'/H-4'β, H-4'α/H-6' and H-5'/H-4'β correlations. VP-147 (**40**) was previously reported from *Vernonia cinarescens*.[61]

VP-27 (**42**), named as centrapalus coumarin C, was isolated as a colorless oily compound with optical rotation of $[\alpha]_D^{25}$ +29.6 (*c* 0.05, $CHCl_3$). It was shown by HRESIMS to have the molecular formula of $C_{21}H_{24}O_6$ according to the quasi-molecular ion peak at *m/z* 373.1642 $[M+H]^+$ (calcd for $C_{21}H_{25}O_6$ 373.1646). ^1H NMR and ^{13}C JMOD NMR spectral data of VP-27 (**42**) showed similar 6-hydroxy-5-methylcoumarin core as compound VP-113 (**41**). For the monoterpene part the ^1H-^1H COSY spectrum suggested structural fragments with correlated protons: $-CH_2$-CH(OR)-CH_2–CH(CH_3)- (δ_H 1.83 d, 1.68 d, 4.38 m, 2.26 m, 1.74 m, and 1.28 d) (C4'–C8') and –CH=CH_2 (δ_H 6.15 dd, 5.11 d, 5.08 d) (vinyl group) (**Annex 6** and **7**). These structural parts, together with a quaternary carbon connecting methyl (δ_H 1.56 s), quaternary carbons (δ_C 36.6, 176.7) were connected by inspection of the long-range C–H correlations observed in the HMBC spectrum between C3' and H-1', H-2', and H-10'; C-10' and H-4'α, and H-2', and C-9' and H-6', H-7', H-8', and OCH_3 group. These data established the planar structure of this compound as depicted in structural formula **42**. The relative configurations of the chiral carbons C3' and C-5' were defined by NOESY correlation between H-5' and H-10'.

Spectral data of VP-55 (**43**), VP-67 (**44**), and VP-68 (**45**) confirmed that the structure of these compounds is identical to three known 5-methylcoumarins. VP-55 (**43**) was previously isolated from *Ethulia conyzoides*,[68] *Bothriocline ripensis,*[70] *Bothriocline amplifolia*,[69] *Conyza bovei,*[143] and *Vernonia brachycalyx*.[144] VP-67 (**44**) and VP-68 (**45**) were previously reported as a mixture of two inseparable isomers in *Ethulia conyzoides*.[58]

VP-176 (**46**), (centrapalus coumarin D) and VP-177 (**47**) (centrapalus coumarin E) were isolated as a mixture of two stereoisomers in ratio 2:1 whose components quickly transform into each other when separated on HPLC. Fortunately, it was possible to solve the structure of both compounds as a mixture. The protonated molecular ion of VP-176 (**46**) and VP-177 (**47**) at *m/z* 357.1329 $[M+H]^+$ (calcd for $C_{20}H_{21}O_6$ 357.1333) in the HRESIMS spectrum offered the molecular formula $C_{36}H_{56}O_8$. ^1H NMR and ^{13}C NMR JMOD spectral data indicated similar 3'-methly-3'-vinyl substituted A/B/C ring system as that of

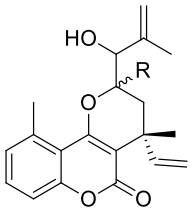

44 (VP-67) R = βOH
45 (VP-68) R = αOH

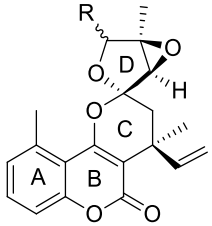

46 (VP-176) R = βOH
47 (VP-177) R = αOH

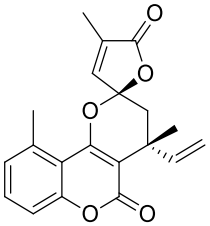

48 (VP-5)

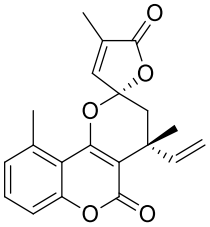

49 (VP-6)

VP-146 (**39**) with only difference of C-5' which is a quaternary carbon in case of VP-176 (**46**) and VP-177 (**47**) (δ_C 105.1 and 103.6), while a methine in case of VP-146 (**39**) (δ_C 72.0, δ_H 4.83). The HMBC correlations between C-5' and proton signals at δ_H 5.39 [VP-176 (**46**)] and 5.31 [VP-177 (**47**)] (H-8') suggested that the C-6'–C-9' part of the molecule is cyclized in VP-176 (**46**) and VP-177 (**47**) by

connecting to C-5′ through an oxygen linkage, thus forming ring D and resulting a tetracyclic coumarin structure. Ring D is substituted with a hydroxy and an epoxy group as proved by the HMBC correlations of C-6′ (VP-176: δ_C 62.7; VP-177: δ_C 63.6), C-7′ (VP-176: δ_C 64.0; VP-177: δ_C 63.5), and C-8′ (VP-176: δ_C 98.4; VP-177: δ_C 98.3) with 8′-OH (VP-176: δ_H 3.19 d; VP-177: δ_H 3.02 d), C-6′ with H-9′ (VP-176: δ_H 1.65 s; VP-177: δ_H 1.63 s), and C-5′ and C-7′ with H-8′ (VP-176: δ_H 5.39 d; VP-177: δ_H 5.31 d). The coupling constant of H-8′/8′-OH is different for VP-176 (**46**) and VP-177 (**47**) (VP-176: J = 4.4 Hz; VP-177: J = 11.6) (**Annex 6** and **7**)., which demonstrate the opposite configuration of VP-176 (**46**) and VP-177 (**47**) in this position. NOESY correlations provided further evidence for the stereochemistry of the compounds. The key Overhauser effect of VP-176 (**46**) was observed between 8′-OH group and H-9, which was possible only when spiro structure and 8′*β*-OH exists as depicted structure **46**. For all other isomers, the distance between the H-9 and the hydroxyl group is greater than 3 Å. NOE correlation of H-8′ with H-9′ indicated their *α* orientations. Overhauser effect between H-6′ and H-2′ indicate that the vinyl group is *β*-oriented, and 10′-methyl group occupies the *α* orientation. Accordingly, NOESY cross-peaks between 10′-methyl/H-4′*α* and H-4′*β*/H-6′ were detected. In case of compound VP-177 (**47**), strong NOESY correlation was found between H-9 and H-8′ which confirmed that the C-8′ configuration is reversed in this compound. Other NOE correlations correspond to the NOE correlations of the major isomer.

VP-5 (**48**) and VP-6 (**49**) could be separated, even though they are also stereoisomers. The difference between them is only in the stereochemistry of C-5′. VP-5 (**48**) and VP-6 (**49**) were previously reported in *Ethulia conyzoides*.[58,59]

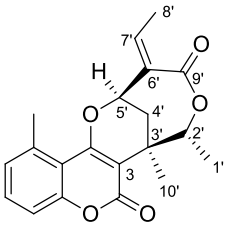

50 (VP-172)

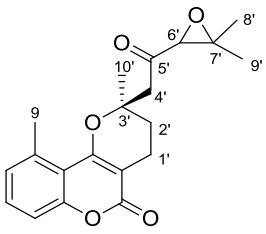

51 (VP-158) H-6′*α*

52 (VP-159) H-6′*β*

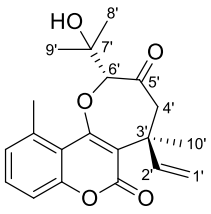

53 (VP-160)

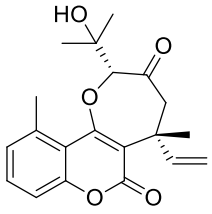

54 (VP-161)

VP-172 (**50**), named as centrapalus coumarin F, was obtained as a white amorphous powder with optical rotation of $[\alpha]_D^{27}$ −70.1 (*c* 0.1, $CHCl_3$). Its molecular formula was deduced to be $C_{20}H_{20}O_5$ from the protonated molecular ion at *m/z* 341.1381 $[M+H]^+$ (calcd for $C_{20}H_{21}O_5$ 341.1384) detected in the HRESIMS spectrum. ^{1}H NMR and ^{13}C NMR JMOD spectral data of VP-172 (**50**) showed similar A, B, and C rings as those of VP-146 (**39**). The linkage of C-10′ methyl group at C-3′ in VP-172 (**50**) was also evident regarding its cross-peaks with C-3, C-3′ and C-4′ in the HMBC spectrum. However, further parts of the monoterpene unit were found to be different. The connected structural parts were CH_3–CH< (δ_H 1.43 d, and 4.80 q; δ_C 15.6, and 93.0) (C-1′–C-2′) and CH_3–CH=C–C(O)– (δ_H 1.84 s, 7.00 brs; δ_C 10.5, 149.3,

129.6, and 174.0) (C-8′–C-7′–C-6′–C-9′) (**Annex 6** and **7**). The first one is linked to C-3′ because the proton at δ_H 4.80 (H-2′) gave HMBC correlations with C-3, C-4′ and C-10′, while the second one bound to C-5′ according to the HMBC cross-peak between H-7′ (δ_H 7.00) and C-5′. The chemical shift value of C-9′ (δ_C 174.0) indicated the presence of a lactone ring, and thus the elucidated structure VP-172 (**50**) corresponds to the molecular composition. NOESY correlations between H-1′/H-10′ and H-10′/H-4′ revealed the *α* orientation of 10′- and 1′-methyl groups, and H-5′.

VP-158 (**51**) (centrapalus coumarin G) and VP-159 (**52**) (centrapalus coumarin H) were isolated as mixture of two isomers. The molecular formulas of VP-158 (**51**) and VP-159 (**52**) were shown to be $C_{20}H_{22}O_5$ based on the HRESIMS peak at *m/z* 343.1537 $[M+H]^+$ (calcd for $C_{20}H_{23}O_5$ 343.1540). ^{1}H NMR and ^{13}C NMR JMOD spectra of VP-158 (**51**) and VP-159 (**52**) showed two very close set of ^{1}H and ^{13}C signals suggesting the presence of a stereoisomer pair in about 1:1 ratio. The aromatic range of the spectra allowed to assign a 5-methylcoumarin structure for VP-158 (**51**) and VP-159 (**52**). However, it was found to have an interesting arrangement of the monoterpene component that differs substantially to those described before. The vinyl group and methyl group previously seen to attach to ring C at C-3′ was absent, but the ^{1}H–^{1}H COSY spectrum of the monoterpene part showed structural fragment of $–CH_2–CH_2–$ (δ_H 2.60 m, 1.98 dd/2.03 dd and 2.10 dd/2.13 dd; δ_C 17.4, 29.7/29.8). HMBC correlation of the monoterpene component revealed the $–CH_2–CH_2–C(CH_3)(OR)–CH_2–CO–CH(O)C(CH_3)_2$ structure (δ_H 2.60 m, 1.98 dd/2.03 dd, 2.10 dd/2.13 dd, 2.91 d/2.94 d, 3.05 d/2.99 d, 3.36 s/3.38 s, 1.41 s/1.43 s, 1.27 s and 1.60/1.57, s; $C_{20}H_{22}O_5$ 7.4, 29.7/29.8, 78.8/78.9, 48.3/48.5, 203.2/203.0, 65.9/66.0, 61.6/61.7, 24.8/24.9, 18.5/18.7 and 24.7/25.0) (C-1′–C-9′) (**Annex 8** and **9**). This unusual monoterpene segment was corroborated by HMBC correlations observed between H-1′/C-3, C-4, C-3′, H-10′/C-2′, C-3′, C-4′, H-4′/C-5′, H-6′/C-5′, C-7′, C-8′, and H-8′/C-9′. The stereochemistry of the two stereoisomers was investigated by NOESY spectroscopy. H-10′ showed correlations with H-9, H-2′a, H-2′b in case of both compounds, which suggested that they have the same configuration at C-3′ and the difference lies in the configuration of C-6′.

VP-160 (**53**), named as centrapalus coumarin I, was isolated as a white amorphous powder with optical rotation of $[\alpha]_D^{27}$ +111.8 (*c* 0.05, $CHCl_3$). The molecular formula of VP-160 (**53**) was determined as $C_{20}H_{22}O_5$ by analyzing the prominent ion peak at *m/z* 343.1540 $[M+H]^+$ (calcd for $C_{20}H_{23}O_5$ 343.1540) in the HRESIMS. ^{1}H NMR and ^{13}C NMR JMOD spectral data of VP-160 (**53**) showed similar pattern characteristic to 5-methylcoumarin derivatives like compounds discussed previously. The same methyl and vinyl groups were identified at position C-3′ as in case of **39**–**49**, which was displayed by the NMR signals at δ_H 1.66 s and δ_C 30.2 (C-10′), and δ_H 5.22 d, 5.10 d (H-1′), and 6.19 dd (H-2′) and δ_C 115.1 (C-1′), and 141.0 (C-2′), and HMBC cross-peaks between C-3′/H-1′, H-2′ and H-10′ (**Annex 8** and **9**). However, substantial difference was found in its ring C which contains a seven membered ring in contrast to six membered ring C seen in compounds **39**–**52**. The C-4–C-9 part of the molecule was

composed of a keto group (δ_C 208.4), an O-substituted quaternary carbon (δ_C 72.0), an O-substituted methine (δ_H 4.30 s; δ_C 93.7), a methylene (δ_H 3.45 d, 2.68 d; δ_C 53.4), and two tertiary methyls (δ_H 1.41 s, and 1.27 s; δ_C 24.9, and 26.9). The long-range heteronuclear correlations between C-3′/H_2-4′, C-5′/H_2-4′, H-6′, C-6′/H_2-4′, H-7′, H-8′ and C-7′/H-6′, H_3-8′ and H_3-9′ enabled to elucidate an oxepane ring C substituted with keto group at C-5′ and 1-hydroxyisopropyl group at C-6′). The stereochemical assignment was determined by a set of NOESY cross peaks between H-9/H-8′, OH/H-10′, H-10′/H-4′α, H-4′β/H-2′, H-4′β/H-1′, H2′/H-6′, indicating α-orientation of 1-hydroxyisopropyl group, H_3-10′, and H-4′α (δ_H 3.45 d), and β-orientation of H-4′β (δ_H 2.68 d), H-1′ (δ_H 5.10 d), H-2′, and H-6′.

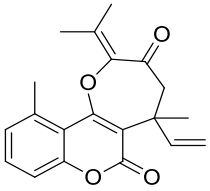

55 (VP-153)

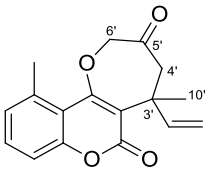

56 (VP-8)

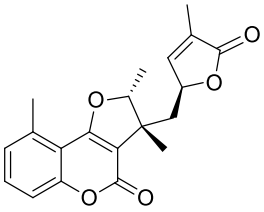

57 (VP-90)

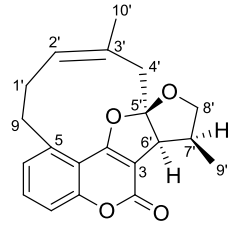

58 (VP-122)

VP-161 (**54**), named as centrapalus coumarin J, was obtained as a white amorphous powder with optical rotation of $[\alpha]_D^{27}$ −186.0 (*c* 0.05, $CHCl_3$). The molecular formula of VP-161 (**54**) was calculated as $C_{20}H_{22}O_5$ by its quasi-molecular ion peak appeared at *m/z* 343.1540 $[M+H]^+$ (calcd for $C_{20}H_{23}O_5$ 343.1540) in the HRESIMS. Evaluation of its ^{1}H NMR and ^{13}C NMR JMOD spectral data allowed the elucidation of the same planar structure as VP-160 (**53**). Difference was found in chemical shift values of C-1′–C-3′, C-10′ and H-1′ and H-4′, and NOESY correlations suggesting their opposite stereochemistry at C-3′ (**Annex 8** and **9**). In the case of VP-161 (**54**), H-6′ and H_3-10′ showed NOESY cross-peaks, from which the β position of 10′-methyl group was concluded.

VP-153 (**55**), with trivial name of centrapalus coumarin K, was isolated as a colorless oily compound with optical rotation of $[\alpha]_D^{27}$ +31.7 (*c* 0.05, $CHCl_3$). The molecular formula of VP-153 (**55**) was shown to be $C_{20}H_{20}O_4$ based on the HRESIMS peak at *m/z* 325.1434 $[M+H]^+$ (calcd for $C_{20}H_{21}O_4$ 343.1440). ^{1}H and ^{13}C NMR JMOD spectroscopic data of compound VP-153 (**55**) showed similar structural pattern as VP-160 (**53**). The main difference was observed in chemical shifts of C-6′ and C-7′. The deshielded signals of C-6′ (VP-153 (**55**): δ_C 147.8; VP-160 (**53**): δ_C 93.7) and C-7′ (VP-153 (**55**): δ_C 137.5; VP-160 (**53**): δ_C 72.0) (δ_C) suggested the presence of C-6′/C-7′ olefin bond in VP-153 (**55**) instead of H-6′ and 7′-OH in **53** (**Annex 8** and **9**). HMBC correlations of H-8′ and H-9′ with C-5′ (weak J_4), C-6′, and C-7′ also support the isopropylidene group at C-6′. The configuration of the chiral carbon, C-3′, could not be determined. Interestingly, the 4′-methylene protons were not visible as two doublets in the ^{1}H NMR spectrum similar to **51**–**54**, and and subsequently, VP-8 (**56**). The signals of this methylene group were located in the ^{1}H NMR spectrum in in the range of 2.80 to 3.25 ppm. On the other hand, the 4′-methylene carbon (δ_C 53.5) was clearly visible in the JMOD spectrum. ^{1}H NMR spectra were recorded under

different conditions to detect the missing protons. ^{1}H NMR spectrum was measured in benzene-d_6 at 328 K affording the appearance of doublet pairs with J = 13.7 Hz coupling constant at 2.91 and 2.74 ppm. These protons show mutual coupling in the ^{1}H-^{1}H COSY spectrum recorded at 328 K, and therefore these signals were assigned to H_2-4′. Another unexpected observation during determination of the structure of VP-153 (**55**) was defining C-10′. Protons of this methyl group in the HSQC spectrum don't show the HSQC correlation with the corresponding carbon. This behavior is probably related to the presence of a double bond in C-6′–C-7′ position, which is in conjugation with the keto group C-5′, causing anisotropy around carbons C-4′ and C-10′.

VP-8 (**56**), named as centrapalus coumarin L, was isolated as a white amorphous powder with optical rotation of $[\alpha]_D^{27}$ +45.4 (*c* 0.05, $CHCl_3$). Its molecular formula $C_{17}H_{16}O_4$ was obtained from the quasi-molecular peak at *m/z* 285.1114 $[M+H]^+$ (calcd for $C_{17}H_{17}O_4$ 285.1121) in the HRESIMS. ^{1}H and ^{13}C NMR signals of VP-8 (**56**) showed similar 5-methylcoumarin structure substituted with seven membered ring C as seen in compounds **53**–**55**. However, the monoterpene component of VP-8 (**56**) is composed only of seven carbons in contrast to ten in **53**–**55**. The seven-membered ring was substituted with methyl and vinyl groups at C-3′ as proved by the long-range heteronuclear correlations of C-3 and C-3′ with H_2-1′, H-2′ and H_3-10′. The presence of a 5′-keto group (δ_C 207.4) was suggested by the isolated 4′- and 6′-methylenes ($\delta_{H\text{-}4'}$ 3.19 d, 3.03 d, each 13.2 Hz; $\delta_{H\text{-}6'}$ 4.55 d, 4.51 d, each 17.3 Hz), and further confirmed by the HMBC correlations between C-5′ and H_2-4′, H_2-6′ (**Annex 8** and **9**).

Based on the NMR data, it was revealed that the monoterpene part of VP-90 (**57**) forms a lactone ring. This compound has the name Hoehnelia coumarin and it was isolated from *Ethulia vernonioides*.[62]

VP-122 (**58**), with trivial name of centrapalus coumarin M, was isolated as a white crystalline powder with optical rotation of $[\alpha]_D$ +76.6 (*c* 0.05, $CHCl_3$). Its molecular formula of was shown to be $C_{20}H_{20}O_4$ based on the HRESIMS peak at *m/z* 325.1431 $[M+H]^+$ (calcd for $C_{20}H_{21}O_5$ 325.1434). ^{1}H and ^{13}C NMR data of VP-122 (**58**) displayed an unusual complex pentacyclic coumarin structure. Although rings A and B are similar to those of previously described compounds, the methyl group at C-5 is replaced by a methylene (δ_H 2.82 m, 3.31 dd; δ_C 34.2). Ring C and D were elucidated as 5-membered rings while ring E formed a 10-membered macrocycle. The ^{1}H–^{1}H COSY spectrum revealed the presence of structural parts A >CH–CH(CH_3)–CH_2– (δ_H 3.50 d, 2.68 m, 3.54 d, 4.27 d and 1.14 d; δ_C 51.1, 37.3, 76.3 and 12.2) [C-6′–C-7′(C-9′)–C-8′] and B –CH_2–CH_2–CH= (δ_H 2.82 m, 3.31 dd, 1.77 m, 2.33 m, 5.70 dd; δ_C 34.2, 33.1, 128.8) (C-9–C-1′–C-2′) (**Annex 10**). HMBC correlations between H-6′ (δ_H 3.50 d) and C-3 (δ_C 103.8) and C-4 (δ_C 167.6), and H-8′ (δ_H 4.27 d) and C-5′ (δ_C 129.9) revealed the existence of five-membered rings C and D. The macrocyclic ring is formed between C-5 and C-5′ with participation of structural part B and quaternary carbon C-3′ (δ_C 130.4), a methylene C-4′ (δ_H 2.17 m, 3.03 d, δ_C 37.6) and methyl group C-10′ (δ_H 1.98 s, δ_C 26.9). Their connection was verified by HMBC correlations of C-5/H-9, C-4′/H-2′, C-4′/H-10′, C-5′/H-4′, and C-10′/H-2′. Information obtained from NOESY spectrum

showed that H-6′, H-7′ and C-4′ are in *α*-orientation while C-9′ is *β*-oriented. This was proved by Overhauser effects observed between H-4′/H-6′, H-6′/H-8′*α*, H-8′*β*/H-9′, H-8′*α*/H-7′. In VP-122 (**58**) the 5-methylcoumarin part is condensed with a head-to-tail coupled monoterpene unit in an unusual way. Instead of C-3/C-3′ connection, C-3/C-6′ and C-9/C-1′ was formed, resulting a new macrocyclic carbon skeleton.

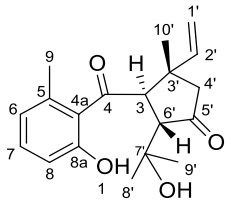

59 (VP-54)

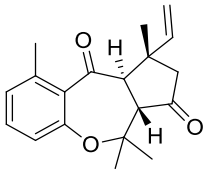

60 (VP-137)

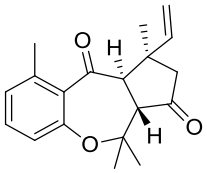

61 (VP-138)

VP-54 (**59**) named pauciflorin A, was isolated as a colorless oily material with optical rotation of $[\alpha]_D$ −157.8 (*c* 0.1, $CHCl_3$). The molecular formula of VP-54 (**59**) was shown to be $C_{19}H_{24}O_4$ based on the positive-ion HRESIMS peak at *m/z* 339.1567 $[M+Na]^+$ (calcd for $C_{19}H_{24}O_4Na^+$ 339.1567). The ^1H and ^{13}C NMR JMOD spectra showed characteristic resonances of a 4 methyl, 2 methylene, 6 methine and 7 quaternary carbon containing compound. The aromatic ^1H resonances at δ_H 6.71 d (8.0 Hz), 7.20 t (8.0 Hz), and 6.78 d (8.0 Hz) indicated an 1,2,3-trisubstituted aromatic ring, which was substituted with a methyl (δ_H 2.39 s, δ_C 21.5), a hydroxyl, and a keto group (δ_C 205.9). The position the methyl group at C-5 was showed by the HMBC correlations between H-9 (δ_H 2.39) and C-5 (δ_C 137.5), C-4a (δ_C 127.3), and C-6 (δ_C 123.4). The connection of the keto group at C-4a was proved by the weak $^4J_{C\text{-}H}$ correlation between H-9 and C-4 (δ_C 205.9) detected in the HMBC spectrum of VP-54 (**59**). A monoterpene part was elucidated as 2-(1-hydroxyisopropyl)-4-methyl-4-vinyl-1-cyclopentanone coupled with the aromatic part in position C-3. The monoterpene fragment was displayed by ^1H-^1H COSY correlations of H-3 [δ_H 4.15 d (11.3 Hz)] with H-6′ (δ_C 59.7), and H_2-1′ [δ_H 4.89 d (17.2 Hz), 4.78 d (10.6 Hz)] with H-2′ [δ_H 5.65 dd (17.2, 10.6 Hz)], and by HMBC correlations of H-10 (δ_H 1.04 s) with C-3 (δ_C 59.2), C-2′ (δ_C 143.1), C-3′ (δ_C 43.9), C-4′ (δ_C 55.7); C-6′ (δ_C 59.7) and C-7′ (δ_C 73.1) with H-3, H-8′ (δ_H 1.56 s) and H-9′ (δ_H 1.23 s). The C-4 keto group (δ_C 205.9) connected the aromatic ring and monoterpene unit, this was confirmed by the long-range heteronuclear correlations of C-4 with H-3 (δ_H 4.15 d), H-6′ (δ_H 3.43 d) and H-6 (δ_H 6.71 d) (**Annex 11a** and **12**). The stereochemistry of VP-54 (**59**) was investigated by NOESY spectroscopy. Overhauser effects were observed between H-3/H-8′, H-3/H-9′, H-2′/H-4′*α* and H-6′/H-10′, which were indicative for *α*-oriented H-3, and vinyl group and *β* position of H-10′ and H-6′. The absolute configuration was determined by X-ray crystallography (**Figure 6**). The colorless, chunk single crystals grown from a mixture of methanol and ethyl acetate at −5°C are light and thermally sensitive. They crystallize in the trigonal system, space group $P3_12_1$. The absolute configuration of the chiral atoms was C-3 (*R*), C-3′ (*S*) and C-6′ (*S*), Flack x= 0.11(5), Parsons z = 0.09(5). Details on molecular

conformation, intra- and intermolecular interactions and packing arrangement can be found in the Supplementary Information. The carbon skeleton of VP-54 (**59**) has a 2-norchromone monoterpene origin, it was not described previously.

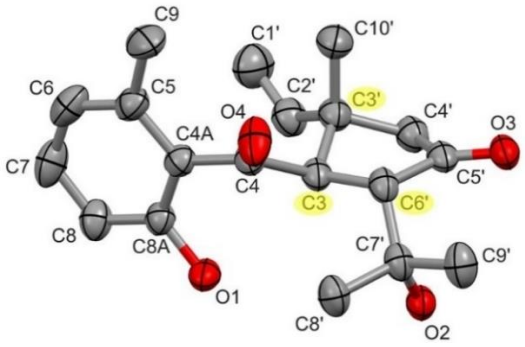

Figure 6. Molecular structure ORTEP presentation of VP-54 (**59**) showing atom labelling. The chiral centres are highlighted by yellow. Hydrogen atoms are omitted for clarity.

VP-137 (**60**) named as pauciflorin B, was obtained as a white amorphous powder with optical rotation of $[\alpha]_D^{27}$ –270.8 (*c* 0.1, $CHCl_3$). The molecular formula of VP-137 (**60**) was assigned as $C_{19}H_{22}O_3$ from the protonated molecular ion at *m/z* 299.1641 $[M+H]^+$ (calcd for $C_{19}H_{23}O_3$ 299.1642) observed in the positive-ion HRESIMS spectrum. ^{1}H NMR and ^{13}C NMR JMOD spectroscopic data of VP-137 (**60**) revealed the presence of a 1,2,3-trisubstituted aromatic ring [δ_H 6.71 d (8.0 Hz), 7.20 t (8.0 Hz), and 6.78 d (8.0 Hz); δ_C 123.5, 128.5, 2×132.2, 140.0, 154.4], four tertiary methyls (δ_H 1.12 s, 1.34 s, 1.51 s, 2.43 s, δ_C 20.6, 20.7, 22.4, 26.1), and a vinyl group [δ_H 5.12 d (17.5 Hz), 5.17 d (11.0 Hz), 6.51 dd (17.5, 11.0 Hz); δ_C 112.1, 145.7]. Two carbonyl functionalities were evident from carbon resonances at δ_C 204.5, and 213.4. These structural parts were built together with two quaternary carbons (δ_C 43.7, 80.5), two methines [δ_H 3.21 d (11.6Hz), 2.73 d (11.6 Hz); δ_C 58.4, 56.3] and one methylene [δ_H 2.27 d (18.0 Hz), 2.51 d (18.0 Hz); δ_C 54.4] yielding a tricyclic compound, that can be originated from VP-54 (**59**) by loss of H_2O. The HMBC correlations that verified the structure of VP-137 (**60**) were observed between C-4/H-3, and H-6′; C-8a/H-7, H-8, H_3-8′; C-7′/H-3, H-6′, H_3-8, and H_3-9; C-5′/H-6′, and H_2-4; C-3′/H-3, H-1′, H-2′, H-10′ and H_2-4′. After determination of the planar structure, the relative configuration was analyzed by the NOESY spectroscopy. Starting from *β*-oriented H-6′, the position of H_3-10′, H_3-9′, and H-4′*β* was found to be in *β,* and H-3, H_3-8′ and H-4*α* in *α*-position according to the NOESY cross-peaks detected between H-6′/H_3-8′, H-6′/H_3-10′, H_3-10′/H-4′*β*, H-3/H_3-9′, H-3/H-4*α*. The absolute configuration of C-3, C-3′ and C-6′ were proposed as (*R*), (*S*) and (*S*), respectively, after considering the structural similarity of VP-137 (**60**) with VP-54 (**59**).

VP-138 (**61**) trivial name pauciflorin C, was a white amorphous powder with optical rotation of $[\alpha]_D^{27}$ +67.6 (*c* 0.05, $CHCl_3$). It had the molecular formula of $C_{19}H_{22}O_3$ based on the positive-ion HRESIMS peak at *m/z* 299.1646 $[M+H]^+$ (calcd for $C_{19}H_{23}O_3$ 299.1642). 1D (^{1}H NMR and JMOD) and 2D NMR (^{1}H-^{1}H COSY, HSQC, HMBC) data showed that VP-138 (**61**) is a diastereomer of VP-137 (**60**). Different ^{1}H and

^{13}C NMR chemical shift of H-3, H-1′, H_2-2′, H_3-10′, C-4, C-1′, C-2′, C-10′ suggested that VP-137 (**60**) and VP-138 (**61**) differ in the stereochemistry of C-3′ (**Annex 11a** and **12**). This was corroborated by the key NOESY correlations between H-3/H_3-10′, H-3/H_3-9′, and H-6′/H_3-8′. The absolute configuration of 3*R*, 3′*R* and 6′*S* can be accordingly proposed for VP-138 (**61**).

VP-145 (**62**), named pauciflorin D, was a colorless oily material with optical rotation of $[\alpha]_D^{26}$ +6.9 (*c* 0.05, $CHCl_3$). Its molecular formula was identified as $C_{20}H_{22}O_5$ by the positive ion HRESIMS spectrum with an molecular ion peak at *m/z* 343.1539 $[M+H]^+$ (calcd for $C_{20}H_{23}O_5$ 345.1540) indicating 10 degrees of unsaturation. NMR data showed the clear chromone-monoterpene hybrid motif of VP-145 (**62**). The 5-methylchromone part of VP-145 (**62**) is the same with the (C-3–C-9) part of **59**–**61**, in addition, VP-145 (**62**) contains a further quaternary carbon (C-2, δ_C 123.8). The C-1′–C-5′ monoterpene part of VP-145 (**62**) was also similar to those of **59**–**61**, the difference lies in the C-2, C-6′–C-9′ parts of the molecules. This structural part of VP-145 (**62**) was elucidated from the presence of two additional oxygen atoms related to VP-137 (**60**) and VP-138 (**61**) (as shown by the HRESIMS), HMBC correlations between C-2/H-3, C-2/H-6′, C-6′/H-4′b, C-6′/H_3-8′, C-6′/H_3-9′, C-7′/H_3-8′, and C-7′/H_3-9′, and O-bearing quaternary carbons at δ_C 158.3 (C-8a), 123.8 (C-2), 87.0 (C-6′), 85.1 (C-7′) were considered. With regard to the two keto groups (δ_C 191.7, 211.0), one vinyl group [δ_H 5.17 d (18.0 Hz), 5.11 d (11.0 Hz), 6.26 dd (18.0, 11.0 Hz); δ_C 114.3, 142.3] and the aromatic ring [δ_H 6.88 d (7.8 Hz), 7.35 t (7.8 Hz), and 6.90 d (7.8 Hz); δ_C 119.0, 142.4, 126.1, 134.8, 115.8, 158.3] (**Annex 11b** and **12**), a tetracyclic ring system was required to satisfy the remaining four degrees of unsaturation. Analysis of ^{1}H-^{1}H COSY, HSQC, and HMBC spectra afforded the elucidation of the planar structure of VP-145 (**62**). A NOESY experiment was performed to assign the relative configuration of VP-145 (**62**). NOESY cross-peaks were observed between H-3/H_3-10′, H_3-10′/H-4′*α* pointing to *α*-oriented 10′-methyl group and H-3, and on the other hand *β*-oriented vinyl group, and *gem*-dimethyl substituted –C-7′–O– bridge was shown byNOESY correlationsbetween H-4′*β*/H-2′, H-2′/H-9′. The other O-bridge between C-2–C-6′ must have accordingly *α*-orientation. Consequently, VP-145 (**62**) was identified to have an unprecedented tetracyclic heterocyclic ring system.

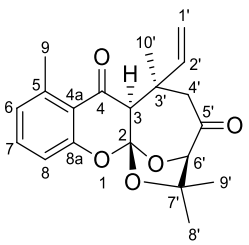

62 (VP-145)

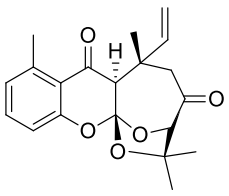

63 (VP-140)

VP-140 (**63**), named as pauciflorin E, was isolated as a colorless oily material with optical rotation of $[\alpha]_D^{27}$ +21.9 (*c* 0.1, $CHCl_3$). The molecular formula was established as $C_{20}H_{22}O_5$ based on the positive ion HRESIMS peak at *m/z* 343.1546 $[M+H]^+$ (calcd for $C_{20}H_{23}O_5$ 345.1540). The 1D NMR data of VP-140 (**63**) showed striking similarities to those of VP-145 (**63**) except for the chemical shifts of C-10' (VP-140 (**62**): δ_H 1.37, δ_C 20.0; VP-145 (**62**): δ_H 1.60, δ_C 32.2) and C-2' (VP-140 (**63**): δ_C 148.6; VP-145 (**62**): δ_C 142.3) (**Annex 11b** and **12**). The stereochemical differences were studied by NOESY experiment. Key Overhauser effects between H-3/H-2', H-3/H-1'a, H-3/H-4'α indicated H-3 and the vinyl group in α position, and NOESY cross-peaks between H-4'β/H_3-10' implied the β-orientation of the 10'-methyl group. Therefore, VP-140 (**63**) was identified as a diastereomer of VP-145 (**62**) differing in positions C-3'.

5. Discussion

All through human history, natural products (from plants and animals) have been recognized and used as a source of remedies and treatments for various diseases.[145–147] It was natural products that provided the source and raw materials for the first conventional drugs. Despite great scientific and technological advances in combinatorial chemistry, drugs derived from natural product still make an enormous contribution to drug discovery today.[148–151] Natural products of plant origin will continue to play significant roles in discovery and development of drugs for the foreseeable future. Tropical Africa is home to some important species-rich biodiversity regions in the world.[152] Our investigations aimed to find new bioactive compounds from two African plant species, and contribute to recognise the value of the African flora to drug discovery.

For quality research outcome and to enhance maximum yield quantity of *E. deightonii* and *C. pauciflorus* extracts, each of the freshly collected plant materials were washed with water to remove unwanted soil particles, thus, preventing adulteration. Drying of plant samples were done in the absence of sunlight because sunlight can denature the bioactive compounds present in the plant. Lastly, the dried plant materials were grinded into powdered form to increase its surface area, thereby enhancing maximum extraction. The importance of quality control of plant sample has been emphasized to prevent adulteration and is also critical to the quality and quantity of the targeted result.[153–156]

Research on *E. deightonii* was chemistry-guided. It was done with the goal of isolating diterpenoid compounds. Diterpenes have been isolated from most parts of plants belonging to Euphorbiaceae; these parts include, the seeds,[157] latex,[158] roots,[159] and aerial parts.[160] In this research, we collected only aerial parts of the plant since it is the most abundant part of the plant. Diterpenes are usually occuring in low quantity in plant materials, and this makes it impossible to detect them directly from an extract. Compounds easily detectable from an extract like phenols, triterpenes, alkaloids, sugars are often present in large amounts in the plants, this makes it easier to develop their detection methods. In order to detect diterpenes, the plant materials needed to be extracted, partitioned and subjected to OCC with polyamide as stationary phase. The plant material was extracted by an amphipolar solvent (e.g. methanol) which has the capacity for extraction of lipophilic and polar components from the plant. The concentrated extract was partitioned with $CHCl_3$ using liquid–liquid partitioning. The resulting $CHCl_3$ soluble phase was subjected to polyamide OCC and various mixtures of methanol–water as eluents (1:4, 3:2, 4:1 and 5:0) were used. Previous studies as well as TLC analysis of the polyamide fractions from this research showed that fractions from methanol–water 3:2 are rich in diterpenoids. These three steps were necessary to remove polysaccharides, proteins, chlorophyll, and other substances present in large quantities in the extract and therefore, with each step, the diterpenes becomes increasingly visible in the fraction, thus, enabling its detection. Literature have

shown that fractions eluted with methanol–water 2:3 and 3:2 from polyamide OCC are rich in diterpenoids rich in *E. taurinensis*,[161] *E. dulcis*,[162] *E. guyoniana*.[163]

Study conducted on *C. pauciflorus* followed partly bioassay-guided, i.e., pharmacologically guided. After extraction, partitioning and polyamide OCC, the resulting polyamide fractions were evaluated for their antiproliferative effect on cervical, ovarian and breast cancer cell lines. Fraction obtained from methanol–water 3:2 elution showed potent and better antiproliferative effect than the other four polyamide fractions and it also displayed significant cytotoxic effect on all cancer cell lines evaluated. Chromatographic purification of the most potent fraction (methanol–water 3:2) led to the isolation of a rare group of compounds called 5-methylcoumarin– and chromone–monoterpene-derived meroterpenoids. Only few compounds beloonging to these groups have been reported in the literature, mainly from *Ethulia conyzoides,*[58,59] *E. vernonioides,*[62] *Bothriocline ripensis,*[70] *B. amplifolia,*[69] *Conyza bovei,*[143] and *Vernonia brachycalyx,*[144] *V. cinarescens,*[61] *Gerbera hybrida*[53] and a few others.

Isolation of natural products are usually tedious task and requires well thought procedure. This is so because many compounds may have very similar chemical structure and physical properties, thus, forming complex mixtures. For instance, in this research, ingol-type diterpenes from *E. deightonii* had the same skeletal core and differ only in the ester groups attached to the skeleton. The extent of the complexity was even greater in *C. pauciflora* where some compounds had same planar structure but differ only in stereochemistry. Therefore, isolation of compounds required a well thought, carefully planned, multi-step chromatographic methods with maneuvering tactics that involved the use of various stationary and mobile phases.

In both experiments, the chosen polyamide fraction were separated first by VLC. Fractions collected were monitored on TLC and similar fractions were combined to form bulk fractions. These bulk fractions were then monitored on TLC using different solvent systems on different stationary phases (NP and RP). In each case, the solvent system along with the stationary phase that showed better selectivity of the constituents guided the choice of the next method to be used. In every case, after exhausting the options of VLC, FLC and PLC, we used HPLC (NP, RP, and chiral columns) to purify compounds. As a consequence, 38 compounds were isolated from *E. deightonii*, and 25 compounds were isolated from *C. pauciflorus*.

5.1 Structural characteristics of the isolated compounds

The structures of isolated compounds were established using advanced spectroscopic analysis; 1D and 2D NMR and HRESIMS. Furthermore, compounds isolated from *E. deightonii* can be grouped into; diterpenoids (compounds **1**–**30**), triterpenoids (**31**–**33**), lignans (**34** and **35**), neolignan (**36**), coumarin (**37**) and ellagic acid derivative (**38**). Compounds **1**–**27** are lathyrane type diterpenoids. They have the

same ingol parent core, however, differ in the type and position of the ester moieties. The compounds are esterified with acetic, benzoic, tiglic, angeolic, 2-methyl butyric, isobutyric, isovaleric and salicylic acids. Four compounds (**13**, **18**, **20**, **22**) have a methoxy group on C-8. (**Annex 1**). These ester groups form the bulk of esters in macrocyclic diterpenoids as seen in ingols,[164] jatrophanes,[163,165,166] segetanes,[161] and ingenanes.[164] The frequency of the ester groups varies, the acetyl group is by far the most prevalence ester group, it appeared sixty-six times; tigloyl appeared eleven times ; benzoyl, seven times; angeloyl, six times; 2-methyl butyl, two, times while *i*-valeryl, *i*-butyryl and salicylyl appeared one times. The positions of these ester moieties are usually at C-3, C-7, C-8, C-12, and C-19. The angeloyl, isobutyryl, isovaleryl groups were found exclusively attached to C-7, while methoxy group and salicylic acid were found exclusively attached at C-8. Tigloyl, 2-methyl butyl and benzoyl were found exclusively attached to C-7 and C-8. The acetyl group was more versatile and could be found attached to all position of ester linkage at C-3, C-7, C-8, C-12 and C-19. Unlike other ingols isolated, compound **26** have a *β*-oriented methyl group at C-2 and by virtue of that, compound **26** is a stereoisomer of compound **11** which have *α*-oriented methyl group at same position. Compounds **31**–**33** are triterpenoids. Triterpenoids with similar skeletal core have been reported in several *Euphorbia* species like *E. lathyris,*[167] *E. rigida*,[168] *E. hirta*,[169] *E. resinifera*,[170] *E. maculata*,[171] and many other *Euphorbia* species.[172]

Compounds isolated from *C. pauciflorus* included twenty of 5-methylcoumarin meroterpenoids (**39**–**58**) and five chromone meroterpenoids (**59**–**63**). The 5-methylcoumarins are a rare type of coumarines and are formed via polyketide synthases.[173]. 5-methylcoumarin meroterpenoids are constructed of two main components: the parent 5-methylcoumarin core and the terpene part. While all have same 5-methylcoumarin core, the terpene component is primarily responsible for most of the variation. The terpene component varied in the number of carbons, the number of ring system, ester moieties, epoxy formation and the configuration of its stereocenters. The same is true for the isolated chromones. The terpene component in the isolated compounds from this research are mainly C_{10} monoterpene in all the coumarins except compound **57** which contains a modified dinormonoterpene unit with 8 carbons. Isolated 5-methylcoumarins varied in the number of ring system formed namely, 6-6-6 (**39**–**52**) and 6-6-7 (**53**–**56**) tricyclic, 6-6-5-5 (**57**) tetracyclic, 6-6-5-5-10 pentacyclic (**58**) ring systems. 5-methylcoumarins have been reported in Vernonieae, Mutiseae, Nasauvieae, and Onoserideae tribes of Asteraceae family.[51] The number of carbons in ring C varies as well. Compound **42** was esterified with methanol at C-9′. Compounds **43**, **46**, **47**, **51** and **52** have an epoxy group at C-6′ and C-7′. 5-methylcoumarins from *C. pauciflorus* showed high occurrence of stereoisomeric compounds. Their configuration differs due to stereochemistry of carbons C-3′ and C-5′. In this regard, compounds **39** and **40**, compounds **48** and **49**, and compounds **53** and **54** are diastereomeric pairs. Furthermore, some stereoisomers were unstable in individual form and readily converts to a mixture of both

stereoisomers, for example, compounds **44** and **45**, compounds **46** and **47**, and compounds **51** and **52** are inseparable and interconvertible diastereomers. The complex pentacyclic structure of compound **58** is particularly interesting and unprecedented. Concerninging chromones, compounds **60** and **61** and compounds **62** and **63** are diastereomers.

5.2 Chemotaxonomy of investigated species

The occurrence of macrocyclic diterpenoids are restricted to Euphorbiaceae and Thymeleaceae families in the plant kingdom and are the major diterpenoid constituents of *Euphorbia* genus. This makes them a significant chemotaxonomic marker in delimiting *Euphorbia* species. Ingols have been isolated from *E. trigona*,[164] *E. antiquorum*,[41,49,116] *E. lactea*,[45,124] *E. royleana*,[117,118,155] *E. kamerunica,*[35,46] *E. ingens*,[21] *E. hermentiana*[43] and others. This isolated compounds evidenced chemotaxonomically that the *E. deightonii* was rightly placed in the taxonomic order.

5-methylcoumarins and 5-methylchromones derived meroterpeoids have restricted occurrence in few tribes of Asteraceae family namely, Vernonieae, Nassauvieae, Onoserideae and Mutisieae and this makes them a vital chemotaxonomic marker. In Onoserideae and Nassauvieae tribes mainly sesquiterpenes occur. Mutisieae and Vernonieae tribes have monoterpenes as their terpene components.[51,58–62] Furthermore, based on available data on 5-methylcoumarins, the presence of the vinyl group in the monoterpene part is common among Vernonieae and Nassauvieae tribes. Since all 5-methylcoumarins and 5-methylchromones derived meroterpeoids isolated have monoterpene component and fifteen of them have a vinyl group, we have thus established that *C. pauciflorus* is well placed in the Vernonieae tribe of Asteraceae family.

5.3 MDR-reversing and cytotoxic activities of diterpenoids isolated from *E. deightonii*

MDR proteins are member of the ATP-binding membrane transporter superfamily and are present in a majority of human tumors.[174] Rise of MDR is a serious challenge to human health globally and has increased morbidity, mortality and healthcare cost.[175–177] Any compound that can inhibit the function of MDR protein may likely possess anti-MDR properties.[174] *Euphorbia* diterpenoids have been reported to inhibit the P-glycoprotein (P-gp) in different tumor cell lines, thereby increasing the intracellular accumulation of antitumor agents.[166,174,178] The first documented diterpenoids with MDR reversal effect was described by our research team in 2002.[179] Many macrocyclic diterpenoids such as ingenane, segetane and jatrophane have shown significant anti-MDR effects.[161,180,181]

Thirteen diterpenes (**5**, **7**, **10**–**15**, **17**, **23**, **24**, **28**, and **29**) were evaluated for their cytotoxicity and anti-MDR effects to establish their structure activity relationship. Inhibition of the efflux pump was evaluated by flow cytometry measurement of the retention of rhodamine 123 in drug-resistant mouse T-lymphoma cells. The cytotoxicity of the thirteen purified diterpenoids were tested on parental and

human MDR1-gene transfected mice T-cell lymphoma cells, and the obtained experimental results are summarized in **Table 8**. The activity was presented as a fluorescence activity ratio (FAR), and the P-gp modulator, tariquidar, was used as a positive control at a concentration of 0.2 μM. In the cytotoxicity assay, MDR cell line proved to be more sensitive than the parental cells. Ingol esters **11**–**13** and **15** exhibited moderate cytotoxic activity with IC_{50} values of 27.8–85.7 μM against MDR cells, and only compound **13** was toxic to the parental cells (IC_{50} 41.9 μM).

Table 8. P-gp efflux pump inhibitory activity of compounds **5**, **7**, **10**–**15**, **17**, **23**, **24**, **28**, and **29** against L5178Y mouse T-cell lymphoma cells

	Concentration (μM)	FSC	SSC	FL-1	FAR
Tariquidar	0.2	2136	1332	165.0	73.7
5	20	2312	1471	17.7	7.9
7	20	2266	1494	74.7	33.4
10	20	2287	1486	122.0	54.5
11	2	2224	1463	157.0	70.1
	20	2211	1864	157.0	70.1
12	2	2271	1535	44.7	20.0
	20	2262	1592	178.0	79.5
13	2	2167	1431	8.6	3.9
	20	2233	1411	136.0	60.7
14	20	2273	1536	159.0	71.0
15	20	2315	1524	147.0	65.6
17	20	2311	1544	22.2	9.9
23	20	2372	1477	27.0	12.1
24	20	2197	1661	47.0	21.0
28	20	2231	1550	19.4	8.7
29	20	2253	1494	6.80	3.0

FSC: forward scatter count; SSC: side scatter count; FL-1: mean fluorescence intensity of the cells; FAR: fluorescence activity ratio

As indicated by FAR values, ingol esters **11**–**15** demonstrated high P-gp inhibitory effect at concentration of 20 μM, while the *ent*-atisane diterpenoids (**28**, **29**) showed considerably low activity at the same concentration. Regarding the preliminary structure–activity relationships, a decrease in esterification degree of ingol derivatives can cause a decrease in efflux pump inhibition, as demonstrated by compounds **5** (3-OH), **23**, and **24** (8-OH). The presence of a 19-CH_2OR group instead of a 19-methyl group seemed to decrease the P-gp inhibitory activity, as observed for compounds **7** and **11**. The influence of the aromatic ester group (benzoyloxy) instead of aliphatic esters (tigloyl or 2-methylbutyrate) can be evaluated by comparing the activities of **11** vs. **14** and **11** vs. **10**, whose esterification was different at C-8. The MDR modulating activity of compound **11** was slightly enhanced with an aromatic ester function. For the ingol esters **14** and **17**, differing in the position of tigloyl and acetyl groups at C-7 and C-8, the FAR values (**14**: 71.0 vs. **17**: 9.9 at 20 μM) suggested that C-8 tigloyl

and C-7 acetyl moieties (**14**) can lead to a drastic increase in activity, in relation to 8-acetyl and 7-tigloyl (**17**). Additionally, the comparison of the P-gp inhibitory activity of compounds **15** and **17** suggested that the presence of a C-7 tigloyl ester was undesirable for the anti-MDR effect of ingol polyesters (FAR in 20 μM **15**: 65.6 versus **17**: 9.9).

5.4 Cytotoxicity and anti-HSV-2 activity of the compounds isolated from *E. deightonii*

Herpes simplex virus (HSV) causes one of the most common viral infections in humans. It is estimated that more than two-thirds of population under the age of 50 are infected with either HSV-1 or HSV-2. Two different types of HSV are distinguished: HSV-1 and HSV-2; the former is primarily responsible for oral herpes cases, while the latter causes genital herpes. Our research focused on the latter.

Table 9. Cytotoxic (CC_{50}) and antiviral activity (IC_{50}) of compounds **31**–**38**.
For determination of CC_{50} concentration, Vero cells were seeded at a density of 4 × 104/well.

Compound	Cytotoxicyty C_{50} (μM)	Anti-HSV-2 IC_{50}) (μM)	IC_{50} Selectivity Index
31	35.49 ± 1.62	7.05 ± 0.25	5.03
32	52.14 ± 2.21	inactive	–
33	7.84 ± 0.96	2.42 ± 0.06	3.23
34	39.76 ± 4.73	11.73 ± 0.79	3.389
35	82.533 ± 8.94	inactive	–
36	71.64 ± 5.83	inactive	–
37	0.35 ± 0.016	0.032 ± 0.0021	10.923
38	25.74 ± 1.84	inactive	–
Acyclovir	100 ± 6.15	0.77 ± 0.032	129.87

First, the CC_{50} concentration of the compounds (**31**–**38**) (**Table 9**) was determined by MTT assay on Vero cells; then the possible antiviral effects of the substances were measured. 3*α*,7*β*-dihydroxy-24-methylenelanosta-8-ene-11-one (**31**), euphorbol-7-one (**33**) deightonin (**34**), and scoparon (**37**) exhibited an anti-HSV-2 effect. Furthermore, IC_{50} values of compounds **31**, **33**, **34**, and **37** were 7.05, 2.42, 11.73, and 0.032 μM, respectively. Among the tested triterpenes, the lanostane (**31**) and 24-methylenelanostane (**33**) proved to be effective, while among the neolignans, only deightonin (**34**) with the methoxylated allyl group showed an antiviral effect. The most pronounced activity was exerted by the coumarin scoparon (**37**); its effect (IC_{50} 0.032 μM) was better in comparison to that of acyclovir (IC_{50} 0.77 μM). However, selectivity index (SI) of **37** (SI 10.923) was lower than that of acyclovir (SI 129.87).

5.5 Anti-proliferative effects of compounds isolated from *C. pauciflorus*

Cancer is the second largest cause of death after cardiovascular disease, it accounts for nearly 10 million deaths annually i.e. one in every six deaths is caused by cancer.[182,183] Top among the most prevalence cancer are breast cancer, cervical cancer and ovarian cancer.[184] The effects of the isolated compounds on the growth of a panel of human adherent cancer cell lines were determined by MTT [3-(4,5-dimethylthiazol-2-yl)-2,5-diphenyltetrazolium bromide] assay.[185]

Twenty one of the twenty-five isolated compounds from *C. pauciflorus* were investigated to describe their antiproliferative properties against a panel of human adherent cell lines of gynecological origin. Generally, HeLa cells (cervical cancer) seems the most sensitive, while MDA-MB-231 cells (triple-negative breast cancer) show the least sensitivity. 5-methylcoumarin derivatives with 2-methyl-1-propenyl group on ring C (**39**–**41**) exhibited similar antiproliferative effects; their activity against HeLa cells was comparable to that of cisplatin, but the other cell lines were less sensitive. The structurally closely related **44**+**45** was ineffective, which may be the consequence of the changed orientation of the substituents of ring C at C-3'. The presence of a five-membered ring D (**46**+**47**, **44**, and **45**) is not advantageous, especially when it bears an epoxy group (**46** and **47**). The 5-methylcoumarin derivatives with a seven-membered ring (**50**) proved to be the most potent compound; its action on MCF-7 cells was similar to that of cisplatin, while it was substantially more effective against HeLa cells. The cancer selectivity of this compound was additionally determined using the same assay against intact murine fibroblasts (NIH-3T3) cells. Treatment with **50** resulted in an inhibition of 30.72 ± 1.29% and 52.59 ± 0.92% at 10 and 30 µM, respectively, while the reference agent cisplatin caused 73.88 ± 1.63% and 97.10 ± 0.15% inhibition, at the same concentrations. The calculated IC_{50} values against NIH-3T3 cells were 25.42 µM and 5.19 µM for **50** and cisplatin, respectively, indicating an improved cancer selectivity of **50**. Selectivity index (SI) is the ratio of the toxic concentration of a drug to its bioactive concentration. An ideal drug should have high SI value i.e. a high toxic concentration and a lower bioactive concentration.[186–188] Pena-Moran et al. suggested that a potential anti-cancer sample should have an SI of ≥ 10.[186] Weerapreeyakul et. al. suggested a lesser SI of ≥ 3.[189] The effect of the mixture of **51** and **52** was the most pronounced against SiHa cervical cancer cells, but the growth inhibition was less than 50% at 30 µM. Compounds with seven-membered ring C (**53** and **54**) elicited no relevant actions, and the molecules containing five-membered ring C (**57** and **58**) exhibited only modest activities. All five chromones (dihydro chromones and 2-nor chromones) (**59–63**) exhibited low activity.

Table 10. Calculated IC_{50} values (µM of antiproliferative properties of some isolated compounds

Compound	Breast cancer cell lines		Cervical cancer cell lines		Ovarian cancer cell lines	Intact murine fibroblast
	MCF-7	MDA-MB-231	HeLa	SiHa	A2780	NIH-3T3
39	–	–	9.21	–	19.65	
40	–	–	9.58	–	26.50	
41	–	–	8.44	–	27.29	
43	–	–	–	–	–	
44+45	–	–	–	–	–	
46+47	–	–	–	–	–	
48	15.30	–	14.59	18.94	26.94	
49	–	–	–	–	–	
50	6.59		2.28		15.41	25.42
51+52	–	–	–	–	–	
53	–	–	–	–	–	
54	–	–	–	–	–	
57	–	–	–	–	–	
58	–	–	–	–	–	
59	–	–	–	–	–	
60	–	–	–	–	–	
61	–	–	–	–	–	
62	–	–	–	–	–	
63	–	–	–	–	–	
Cisplatin	5.78	19.13	12.43	7.84	1.30	5.19

– : Cell growth inhibition values less than 20% were considered negligible and are not given numerically

6. Summary

The scope of this study covered the phytochemical and pharmacological investigations of two African plant species, namely, *E. deightonii* and *C. pauciflorus*. The isolation procedure involved multi-step chromatographic methods that included polyamide OCC, NP and RP VLC, NP and RP FCC, NP and RP HPLC, PLC and crystallization techniques. Structural elucidation were done by use of advanced spectroscopic methods: 1D (^{1}H, JMOD) and 2D (HSQC, HMBC, ^{1}H-^{1}H COSY, NOESY) NMR, and HRESIMS. Interpretation of the spectral data allowed the complete and unambiguous ^{1}H- and ^{13}C assignments of the novel compounds which were then confirmed by means of HRESIMS. In addition, the absolute configuration of compound **59** was determined by single-crystal X-ray diffraction.

Phytochemical investigation of MeOH extract of *E. deightonii* yielded thirty-eight compounds (**1**–**38**); of which thirty are diterpenes **1**–**30** (**1**–**9** are novel), three triterpenes **31**–**33** (**31** is novel), three lignans or neolignans **34**–**36** (**34** is novel), one coumarin (**37**) and one ellagic acid derivative (**38**). **1**–**27** are ingol type diterpenoids, all of which possess $\Delta^{(5,6)}$ double bond, and are highly esterified with acetic, benzoic, angeloic, tiglic, *i*-valeric, isobutyric, and salicylic acids. Particularly interesting is the presence of salicylic acid ester in compound **3**. Only compound **27** has *β*-orientation of methyl at C–16. **28** and **29** are *ent*-atisane diterpenoids while **30** belongs to the rare stachane diterpenoid group. The pharmacological investigation on MDR-reversing activities in an L5178 mouse lymphoma cell line of thirteen diterpenoids (**5**, **7**, **10**–**15**, **17**, **23**, **24**, **28**, and **29**) revealed that ingols derivatives **11**–**13** and **15** exhibited moderate cytotoxic activity with IC_{50} values of 27.8–85.7 µM against MDR cells, and only compound **13** was toxic to the parental cells (IC_{50} 41.9 µM). *Ent*-atisane diterpenoids were ineffective in the cytotoxicity assay. Ingol diterpenoid esters **11**–**15** demonstrated a high P-gp inhibitory effect at a concentration of 20 µM, while the *ent*-atisane diterpenoids (**28**, **29**) showed considerably lower activity at the same concentration when compared to the positive control tariquidar. Anti-HSV-2 studies of compounds **31**–**38** showed that **31**, **33**, **34** and **37** exhibited antiviral activities.

Phytochemical investigation of the MeOH extract of *C. pauciflorus* yielded twenty 5-methylcoumarin based meroterpenoids **39**–**58** (thirteen **39**, **41**, **42**, **46**+**47**, **50**–**56** and **58** are previously undescribed compounds) and five 5-methylchromone based meroterpenoids **59**–**63** (all five are previously undescribed compounds). The monoterpene component is responsible for the structural variability of the compounds. Additionally, the monoterpene part contained chiral carbons C-3', C–5' and C–6' and, eight pairs of diastereomers were isolated including three inseparable pairs. Anti-proliferative activities of twenty-one compounds were tested on cervical (HeLa and SiHa), breast (MCF-7 and MDA-MB-231) and ovarian (A2780) cancer cell lines. Among the cell lines, HeLa were the most sensitive. Compounds **39**–**41** showed comparable antiproliferative effects with the positive control cisplatin on HeLa cells. However, **50** was the most potent, its activity on MCF-7 was comparable with that of

cisplatin, while its effect on HeLa cells was much higher than those of cisplatin. Testing on normal cell line murine fibroblast (NIH-3T3) revealed that it has better cancer selectivity than cisplatin.

In summary from the two plant species, sixty-three compounds were isolated, of which twenty nine are novel compounds. Our work on *C. pauciflorus* indicated that pauciflorins A–E (**59**–**63**) are the first examples of hybrid molecules of chromone–monoterpene origin with unprecedented carbon skeletons. Pauciflorins A–C (**59**–**61**) can be derived by the connection of a 2-nor-chromone and a monoterpene unit, while pauciflorin D (**63**) and E (**62**) are dihydrochromone-monoterpene adducts with a rarely occurring ortho ester functionality. Pauciflorin A (**59**) can be a precursor of pauciflorin B (**60**). Additionally, our findings indicated that *C. pauciflorus* is an excellent source of structurally diverse meroterpenoids; the discovery of their pharmacological potential will be needed in the future.

7. References

1. Global Energy Interconnection Development and Cooperation Organization. Hydropower resources and development planning of the Congo river. in *Research on hydropower development and delivery in Congo river* 11–39 (Springer Singapore, 2020). doi:10.1007/978-981-15-3428-7_2.
2. Molua, E. L. Global warming and carbon sequestration in Africa's forests: potential rewards for new policy directions in the Congo basin. in *New frontiers in natural resources management in Africa* (eds. Ayuk, E. T. & Unuigbe, N. F.) **53**, 59–77 (Springer International Publishing, 2019).
3. Klopper, R. R., Gautier, L., Chatelain, C., Smith, G. F. & Spichiger, R. Floristics of the angiosperm flora of Sub-saharan Africa: An analysis of the African plant checklist and database. *Taxon* **56**, 201–208 (2007).
4. Linder, H. P. The evolution of African plant diversity. *Front. Ecol. Evol.* **2**, 38 (2014).
5. Baishya, R. A., Sarma, J. & Begum, A. Forest-based medicinal plants rendering their services to the rural community of Assam, India. *Int. J. Med. Plants Res.* **4**, 314–323 (2015).
6. Teklay, A., Abera, B. & Giday, M. An ethnobotanical study of medicinal plants used in Kilte Awulaelo District, Tigray Region of Ethiopia. *J. Ethnobiol. Ethnomed.* **9**, 1–23 (2013).
7. Ekor, M. The growing use of herbal medicines: issues relating to adverse reactions and challenges in monitoring safety. *Front. Pharmacol.* **4**, 177 (2014).
8. Oyebode, O., Kandala, N.-B., Chilton, P. J. & Lilford, R. J. Use of traditional medicine in middle-income countries: a WHO-SAGE study. *Health Policy Plan.* **31**, 984–991 (2016).
9. Birhan, W., Giday, M. & Teklehaymanot, T. The contribution of traditional healers' clinics to public health care system in Addis Ababa, Ethiopia: a cross-sectional study. *J. Ethnobiol. Ethnomedicine* **7**, 39 (2011).
10. Fowler, M. W. Plants, medicines and man. *J. Sci. Food Agric.* **86**, 1797–1804 (2006).
11. Farnsworth, N. R. & Morris, R. W. Higher plants--the sleeping giant of drug development. *Am. J. Pharm.* **225**, 46–52 (1976).
12. Proudfoot, A. The early toxicology of physostigmine: a tale of beans, great men and egos. *Toxicol. Rev.* **25**, 99–138 (2006).
13. Keglevich, P., Hazai, L., Kalaus, G. & Szántay, C. Modifications on the basic skeletons of vinblastine and vincristine. *Mol. Basel Switz.* **17**, 5893–5914 (2012).
14. Popik, P. & Skolnick, P. Pharmacology of ibogaine and ibogaine-related alkaloids. in *The alkaloids: chemistry and biology* **52**, 197–231 (Elsevier, 1999).
15. Jesus, M., Martins, A. P. J., Gallardo, E. & Silvestre, S. Diosgenin: recent highlights on pharmacology and analytical methodology. *J. Anal. Methods Chem.* **2016**, 4156293 (2016).
16. Togola, A., Diallo, D., Dembélé, S., Barsett, H. & Paulsen, B. S. Ethnopharmacological survey of different uses of seven medicinal plants from Mali, (West Africa) in the regions Doila, Kolokani and Siby. *J. Ethnobiol. Ethnomed.* **1**, 1–9 (2005).

17. Vasas, A., Sulyok, E., Martins, A., Rédei, D., Forgo, P., Kele, Z., Zupkó, I., Molnár, J., Pinke, G. & Hohmann, J, A. Cyclomyrsinane and premyrsinane diterpenes from *Euphorbia falcata* modulate resistance of cancer cells to doxorubicin. *Tetrahedron* **68**, 1280–1285 (2012).

18. Vasas, A. & Hohmann, J. *Euphorbia* diterpenes: isolation, structure, biological activity, and synthesis (2008–2012). *Chem. Rev.* **114**, 8579–8612 (2014).

19. Kemboi, D., Siwe-Noundou, X., Krause, R. W. M., Langat, M. K. & Tembu, V. J. Euphorbia diterpenes: an update of isolation, structure, pharmacological activities and structure–activity relationship. *Molecules* **26**, 5055 (2021).

20. Schmidt, R. J. The biosynthesis of tigliane and related diterpenoids; an intriguing problem. *Bot. J. Linn. Soc.* **94**, 221–230 (1987).

21. Opferkuch, H. J. & Hecker, E. Ingol - a new macrocyclic diterpene alcohol from *Euphorbia ingens*. *Tetrahedron Lett.* **14**, 3611–3614 (1973).

22. Rinner, U. Progress in the preparation of jatrophane diterpenes: progress in the preparation of jatrophane diterpenes. *Eur. J. Org. Chem.* **2015**, 3197–3219 (2015).

23. Bruneton, J. *Pharmacognosy, phytochemistry, medicinal plants*. **1**, 915 (Lavoisier Tec & Doc publishing, 1995).

24. Bathe, U. & Tissier, A. Cytochrome P450 enzymes: A driving force of plant diterpene diversity. *Phytochemistry* **161**, 149–162 (2019).

25. Evans, F. J. & Taylor, S. E. Pro-inflammatory, tumour-promoting and anti-tumour diterpenes of the plant families Euphorbiaceae and Thymelaeaceae. in *Fortschritte der Chemie organischer Naturstoffe / Progr. Chem. of Org. Nat. Prod.* **44**, 1–99 (Springer Vienna, 1983).

26. Xu, Z.-H., Sun, J., Xu, R.-S. & Qin, G.-W. Casbane diterpenoids from Euphorbia ebracteolata fn2fn2Part 3 in the series chemical studies of Lang-Du, a traditional chinese medicine. *Phytochemistry* **49**, 149–151 (1998).

27. Moura, V. L. A., Monte, F. J. O. & Filho, R. B. A new casbane-type diterpenoid from *Croton nepetaefolius*. *J. Nat. Prod.* **53**, 1566–1571 (1990).

28. Ghisalberti, E. L., Jefferies, P. R., Mori, T. A., Skelton, B. W. & White, A. H. A new class of macrocyclic diterpenes from *Bertya dimerostigma* (Euphorbiaceae). *Tetrahedron* **41**, 2517–2526 (1985).

29. Choi, Y. H., Kim, J., Pezzuto, J. M., Kinghorn, A. D., Farnsworth, N. R., Letter, H., & Wagner, H. Agrostistachin, a novel cytotoxic macrocyclic diterpene from *Agrognstachys hookeri*. *Tetrahedron Lett.* **27**, 5795–5798 (1986).

30. Choi, Y.-H., Pezzuto, J. M., Kinghorn, A. D. & Farnsworth, N. F. Plant anticancer agents, XLVI. cytotoxic casbane-type constituents of *Agrostistachys hookeri*. *J. Nat. Prod.* **51**, 110–116 (1988).

31. Erich, H. Cocarcinogenic principles from the seed oil of *Croton tiglium* and from other Euphorbiaceae. *Cancer Res* **28**, 2338–2348 (1968).

32. Adolf, W., Hecker, E., Balmain, A., Lhomme, M. F., Nakatani, Y., Ourisson, G., Ponsinet, G., Pryce, R.J., Santhanakrishnan, T.S., Matyukhina, L.G. & Saltikova, I. A. “Euphorbiasteroid” (epoxy-lathyrol) A new tricyclic diterpene from *Euphorbia lathyris* L. *Tetrahedron Lett.* **11**, 2241–2244 (1970).

33. Ravikanth, V., Reddy, V. N., Rao, T. P., Diwan, P. V., Ramakrishna, S., & Venkateswarlu, Y. Macrocyclic diterpenes from *Euphorbia nivulia*. *Phytochemistry* **59**, 331–335 (2002).

34. Hickey, T. A., Worobec, S. M., West, D. P. & Kinghorn, A. D. Irritant contact dermatitis in humans from phorbol and related esters. *Toxicon* **19**, 841–850 (1981).

35. Abo, K. & Evans, F. J. Macrocyclic diterpene esters of the cytotoxic fraction from *Euphorbia kamerunica*. *Phytochemistry* **20**, 2535–2537 (1981).

36. Abdul, Q. K. & Abdul, M. A new macrocyclic diterpene ester from the latex of *Euphorbia tirucalli*. *J. Nat. Prod.* **53**, 728–731 (1990).

37. Lotter, H., Opferkuch, H. J. & Hecker, E. Crystal structure and stereochemistry of ingol-3,7,8,12-tetraacetate. *Tetrahedron Lett.* **20**, 77–78 (1979).

38. Kong, L.-Y., Li, Y., Wu, X.-L. & Min, Z.-D. Cytotoxic diterpenoids from *Euphorbia pekinensis*. *Planta Med.* **68**, 249–252 (2002).

39. Tran, C. L., Dao, T. B. N., Tran, T. N., Mai, D. T., Tran, T. M. D., Tran, N. M. A., Dang, V.S., Vo, T.X., Duong, T.H. & Sichaem, J. Alpha-glucosidase inhibitory diterpenes from *Euphorbia antiquorum* growing in Vietnam. *Molecules* **26**, 2257 (2021).

40. Zhao, N. D., Ding, X., Song, Y., Yang, D. Q., Yu, H. L., Adelakun, T. A., Qian, W.D., Zhang, Y., Di, Y.T., Gao, F., Hao, X.J., & Li, S. L. Identification of ingol and rhamnofolane diterpenoids from *Euphorbia resinifera* and their abilities to induce lysosomal biosynthesis. *J. Nat. Prod.* **81**, 1209–1218 (2018).

41. Qi, W. Y., Zhang, W. Y., Shen, Y., Leng, Y., Gao, K., & Yue, J. M. Ingol-type diterpenes from *Euphorbia antiquorum* with mouse 11β - hydroxysteroid dehydrogenase type 1 inhibition activity. *J. Nat. Prod.* **77**, 1452–1458 (2014).

42. Marco, J. A., Sanz-Cervera, J. F., Ropero, F. J., Checa, J. & Fraga, B. M. Ingenane and lathyrane diterpenes from the latex of *Euphorbia acrurensis*. *Phytochemistry* **49**, 1095–1099 (1998).

43. Lin, L.-J. & Kinghorn, A. D. 8-Methoxyingol esters from the latex of *Euphorbia hermentiana*. *Phytochemistry* **22**, 2795–2799 (1983).

44. Sosath, S., Ott, H. H. & Hecker, E. Irritant principles of the spurge family (Euphorbiaceae) XIII. oligocyclic and macrocyclic diterpene esters from latices of some *Euphorbia* species utilized as source plants of honey. *J. Nat. Prod.* **51**, 1062–1074 (1988).

45. Upadhyay, R. R. & Hecker, E. Diterpene esters of the irritant and cocarcinogenic latex of *Euphorbia lactea*. *Phytochemistry* **14**, 2514–2516 (1975).

46. Abo, K. & Evans, F. The composition of a mixture of ingol esters from *Euphorbia kamerunica*. *Planta Med.* **43**, 392–395 (1981).

47. Baloch, I., Baloch, M. & Saqib, Q. Cytotoxic macrocyclic diterpenoid esters from *Euphorbia cornigera*. *Planta Med.* **72**, 830–834 (2006).

48. Miranda, F. J., Alabadí, J. A., Pérez, P., Ortí, M., Centeno, J. M., Yuste, A., A., Sanz-Cervera, J.F., Marco, J.A. & Alborch, E. Analysis of rabbit vascular responses to DBI, an ingol derivative isolated from *Euphorbia canariensis*. *J. Pharm. Pharmacol.* **49**, 573–576 (2011).

49. Yin, Z. Y., Dai, Y., Hua, P., Sun, Z. J., Cheng, Y. F., Yuan, S. H., Chen, Z.Y. & Gu, Q. Discovery of diverse diterpenoid scaffolds from *Euphorbia antiquorum* and their activity against RANKL-induced osteoclastogenesis. *Bioorg. Chem.* **92**, 103292 (2019).

50. Murray, R. D. H. Naturally occurring plant coumarins. in *Fortschritte der chemie organischer naturstoffe / Progr. Chem. of Org. Nat. Prod.* (eds. Herz, W., Grisebach, H. & Kirby, G. W.) **35**, 199–429 (Springer Vienna, 1978).

51. Vestena, A. S., Meirelles, G. de C., Zuanazzi, J. A. & von Poser, G. L. Taxonomic significance of coumarins in species from the subfamily Mutisioideae, Asteraceae. *Phytochem. Rev.* **22**, 85–112 (2022).

52. Inoue, T., Toyonaga, T., Nagumo, S. & Nagai, M. Biosynthesis of 4-hydroxy-5-methylcoumarin in a *Gerbera jamesonii* hybrid. *Phytochemistry* **28**, 2329–2330 (1989).

53. Pietiäinen, M., Kontturi, J., Paasela, T., Deng, X., Ainasoja, M., Nyberg, P., Hotti, H. & Teeri, T. H. Two polyketide synthases are necessary for 4-hydroxy-5-methylcoumarin biosynthesis in *Gerbera hybrida*. *Plant J.* **87**, 548–558 (2016).

54. Austin, M. B. & Noel, J. P. The chalcone synthase superfamily of type III polyketide synthases. *Nat. Prod. Rep.* **20**, 79–110 (2003).

55. Abe, I. & Morita, H. Structure and function of the chalcone synthase superfamily of plant type III polyketide synthases. *Nat. Prod. Rep.* **27**, 809 (2010).

56. Gliszczyńska, A. & Brodelius, P. E. Sesquiterpene coumarins. *Phytochem. Rev.* **11**, 77–96 (2012).

57. Catalán, C. A. N., Borkosky, S. A. & Joseph-Nathan, P. The secondary metabolite chemistry of the subtribe Gochnatiinae (tribe Mutisieae, family Compositae). *Biochem. Syst. Ecol.* **24**, 659–718 (1996).

58. Mahmoud, A. A., Ahmed, A. A., Iinuma, M. & Tanaka, T. Further monoterpene 5-methylcoumarins and an acetophenone derivative from *Ethulia conyzoides*. *Phytochemistry* **48**, 543–546 (1998).

59. Shukla, V. S., Dutta, S. C., Baruah, R. N., Sharma, R. P., Thyagarajan, G., Herz, W., Kumar, N., Watanabe, K. and Blount, J. F. New 5-methylcoumarins from *Ethulia conyzoides*. *Phytochemistry* **21**, 1725–1731 (1982).

60. Mahmoud, Z. F., Sarg, T. M., Amer, M. E. & Khafagy, S. M. Anthelmintic coumarin from *Ethulia conyzoides var. gracilis* Asch. and Schweinf. *Pharm.* **38**, 486–487 (1983).

61. Bohlmann, F. & Zdero, C. Glaucolides and other constituents from South African *Vernonia* species. *Phytochemistry* **21**, 2263–2267 (1982).

62. Schuster, N., Christiansen, C., Jakupovic, J. & Mungai, M. An unusual [2+2] cycloadduct of terpenoid coumarin from *Ethulia vernonioides*. *Phytochemistry* **34**, 1179–1181 (1993).

63. Morgenstern, T., Bittner, M., Silva, M., Aqueveque, P. & Jakupovic, J. Diterpenes and phloracetophenones from *Euphorbia portulacoides*. *Phytochemistry* **41**, 1149–1153 (1996).

64. Hoeneisen, M., Hernandez, V., Becerra, J., Silva, M., Bittner, M., & Jakupovic, J. 5-Methyl coumarins and a new phenol from *Nassauvia pyramidalis* & *N. digitata*. *Phytochemistry* **52**, 1667–1669 (1999).

65. Zdero, C., Bohlmann, F., King, R. M. & Robinson, H. Further 5-methyl coumarins and other constituents from the subtribe Mutisiinae. *Phytochemistry* **25**, 509–516 (1986).

66. Hoeneisen, M., Silva, M. & Jakupovic, J. Coumarins from *Nassauvia cumingii*. *Phytochemistry* **46**, 1393–1395 (1997).

67. Bittner, M., Jakupovic, J., Bohlmann, F., Grenz, M. & Silva, M. 5-methyl coumarins and chromones from *Triptilion* species. *Phytochemistry* **27**, 3263–3266 (1988).

68. Kady, M. M., Brimer, L., Furu, P., Lemmich, E., Nielsen, H. M., Thiilborg, S. T., Thastrup, O. & Christensen, S. B. The molluscicidal activity of coumarins from *Ethulia conyzoides* and of dicumarol. *Planta Med.* **58**, 334–337 (1992).

69. Ahmed, M., Jakupovic, J., Bohlmann, F. & Mungai, M. G. A 5-methylcoumarin and glaucolides from *Bothriocline amplifolia*. *Phytochemistry* **30**, 2807–2808 (1991).

70. Jakupovic, J., Boeker, R., Schuster, A., Bohlmann, F. & Jones, S. B. Further guaianolides and 5-alkylcoumarins from *Gutenbergia* and *Bothriocline species*. *Phytochemistry* **26**, 1069–1075 (1987).

71. He, F., Wang, M., Gao, M., Zhao, M., Bai, Y., & Zhao, C. Chemical composition and biological activities of *Gerbera anandria*. *Molecules* **19**, 4046–4057 (2014).

72. Simirgiotis, M. J., Bórquez, J., Neves-Vieira, M., Brito, I., Alfaro-Lira, S., Winterhalter, P., Echiburú-Chau, C., Jerz, G. and Cárdenas, A. Fast isolation of cytotoxic compounds from the native Chilean species *Gypothamnium pinifolium* Phil. collected in the Atacama Desert, northern Chile. *Ind. Crops Prod.* **76**, 69–76 (2015).

73. Monks, N. R., Bordignon, S. A., Ferraz, A., Machado, K. R., Faria, D. H., Lopes, R. M., Mondin, C.A., Souza, I.C., Lima, M.F., da Rocha, A.B. & Schwartsmann, G. Anti-tumour screening of Brazilian plants. *Pharm. Biol.* **40**, 603–616 (2002).

74. Viturro, C. I., Fuente, J. R. de la & Maier, M. S. Antifungal methylphenone derivatives and 5-methylcoumarins from *Mutisia friesiana*. *Z. Naturforsch. C* **58**, 533–540 (2003).

75. Sales Junior, P. A., Zani, C. L., de Siqueira, E. P., Kohlhoff, M., Marques, F. R., Caldeira, A. S. P., Cota, B.B., Maia, D.N.B., Tunes, L.G., Murta, S.M.F. & Alves, T. M. A. Trypanocidal trixikingolides from *Trixis vauthieri*. *Nat. Prod. Res.* **35**, 2691–2699 (2021).

76. Coelho de Souza, G., Haas, A. P. S., von Poser, G. L., Schapoval, E. E. S. & Elisabetsky, E. Ethnopharmacological studies of antimicrobial remedies in the south of Brazil. *J. Ethnopharmacol.* **90**, 135–143 (2004).

77. Truiti, M. D. C. T. & Sarragiotto, M. H. Three 5-methylcoumarins from *Chaptalia nutans*. *Phytochemistry* **47**, 97–99 (1998).

78. Celaya, L., Viturro, C. & Silva, L. R. Chemical composition and biological prospects of essential oils and extracts of *Aphyllocladus spartioides* growing in northwest Argentina. *Chem. Biodivers.* **14**, e1600227 (2017).

79. Wang, J., Petrova, V., Wu, S. B., Zhu, M., Kennelly, E. J., & Long, C. Antioxidants from *Gerbera piloselloides* : an ethnomedicinal plant from southwestern China. *Nat. Prod. Res.* **28**, 2072–2075 (2014).

80. Vicente, G., Moon, Y. J. K., Rosa, D. W., Lima, L. A., Saleh, N. A., da Rosa, J. S., Creczynski-Pasa, T.B., Biavatti, M.W., Dalmarco, E.M. & Fröde, T.S. Anti-inflammatory profile of *Jungia sellowii* Less. by

downregulation of proinflammatory mediators and inhibition of NF- *κ* B and p38 pathways. *Mediators Inflamm.* **2020**, 1–12 (2020).

81. Nader, M., Vicente, G., da Rosa, J. S., Lima, T. C., Barbosa, A. M., Santos, A. D. C., Barison, A., Dalmarco, E.M., Biavatti, M.W. & Fröde, T. S. *Jungia sellowii* suppresses the carrageenan-induced inflammatory response in the mouse model of pleurisy. *Inflammopharmacology* **22**, 351–365 (2014).
82. Martínez, A., Madariaga-Mazón, A., Rivero-Cruz, I., Bye, R. & Mata, R. Antidiabetic and antihyperalgesic effects of a decoction and compounds from *Acourtia thurberi*. *Planta Med.* **83**, 534–544 (2016).
83. Nazir, M., Saleem, M., Tousif, M. I., Anwar, M. A., Surup, F., Ali, I., Wang, D., Mamadalieva, N.Z., Alshammari, E., Ashour, M.L. & Hussain, H. Meroterpenoids: A comprehensive update insight on structural diversity and biology. *Biomolecules* **11**, 957 (2021).
84. Matsuda, Y. & Abe, I. Biosynthesis of fungal meroterpenoids. *Nat. Prod. Rep.* **33**, 26–53 (2016).
85. Matsuda, Y., Awakawa, T. & Abe, I. Reconstituted biosynthesis of fungal meroterpenoid andrastin A. *Tetrahedron* **69**, 8199–8204 (2013).
86. El-Elimat, T., Raja, H. A., Ayers, S., Kurina, S. J., Burdette, J. E., Mattes, Z., Sabatelle, R. & Oberlies, N. H. Meroterpenoids from *Neosetophoma* sp.: A dioxa[4.3.3]propellane ring system, potent cytotoxicity, and prolific expression. *Org. Lett.* **21**, 529–534 (2019).
87. Cornforth, J. W. Terpenoid biosynthesis. *Chem. Br.* **4**, 102–106 (1968).
88. Geris, R. & Simpson, T. J. Meroterpenoids produced by fungi. *Nat. Prod. Rep.* **26**, 1063 (2009).
89. Peng, X. & Qiu, M. Meroterpenoids from *Ganoderma* species: A review of last five years. *Nat. Prod. Bioprospec.* **8**, 137–149 (2018).
90. Britannica, The Editors of Encyclopaedia. ''spurge''. *Encyclopedia Britannica* (2021). https://www.britannica.com/plant/spurge. Accessed 11 May 2023.
91. Bruyns, P. V., Mapaya, R. J. & Hedderson, T. J. A new subgeneric classification for *Euphorbia* (Euphorbiaceae) in southern Africa based on ITS and *psbA-trnH* sequence data. *Taxon* **55**, 397–420 (2006).
92. Pascal, O. A., Bertrand, A. E. V., Esaïe, T., Sylvie, H. A. M. & Eloi, A. Y. A review of the ethnomedical uses, phytochemistry and pharmacology of the *Euphorbia genus*. *Pharma Innov.* **6**, 34 (2017).
93. Horn, J. W., van Ee, B. W., Morawetz, J. J., Riina, R., Steinmann, V. W., Berry, P. E., & Wurdack, K. J. Phylogenetics and the evolution of major structural characters in the giant genus *Euphorbia* L. (Euphorbiaceae). *Mol. Phylogenet. Evol.* **63**, 305–326 (2012).
94. Ernst, M., Grace, O. M., Saslis-Lagoudakis, C. H., Nilsson, N., Simonsen, H. T., & Rønsted, N. Global medicinal uses of *Euphorbia* L. (Euphorbiaceae). *J. Ethnopharmacol.* **176**, 90–101 (2015).
95. Govaerts, R., Frodin, D. G. & Radcliffe-Smith, A. *World checklist and bibliography of Euphorbiaceae (with Pandaceae)*. **2**, 320–328 (Royal Botanic Gardens, Kew, 2000).
96. Burkill, H. M. *The useful plants of West Africa.* **1**, 190 (Royal Botanical Gardens, Kew, 1985).

97. Croizat, L. *Euphorbia* (diacanthium) *deightonii*, a new succulent from West Africa, with brief notes on some allied species. *Bulletin of Miscellaneous Information (Royal Botanic Gardens, Kew),* 53–59 (1938).

98. Nikolić, M. & Stevović, S. Family Asteraceae as a sustainable planning tool in phytoremediation and its relevance in urban areas. *Urban For. Urban Green.* **14**, 782–789 (2015).

99. Britannica, The Editors of Encyclopaedia. Asteraceae. *Encyclopedia Britannica* (2015). https://www.britannica.com/plant/Asteraceae. Accessed 11 May 2023. Accessed 11 May 2023.

100. Robinson, H. "Tribe Vernonieae Cass (1819).–Pp. 149–174 in: Kadereit JW & Jeffrey C.(ed.), The families and genera of vascular plants 8." *Flowering plants. Eudicots. Asterales.–Berlin, Heidelberg & New York: Springer*, 149–174, (2007).

101. Isawumi, M. A. The status of generic revision in the African Vernonieae (Asteraceae). *Compos. Newsl.* **46**, 27–48 (2008).

102. Bohm, B. A. & Stuessy, T. F. Flavonoids of the sunflower family (Asteraceae). *Springer Sci. Bus. Media* (2001).

103. Zelaya, I. A., Owen, M. D. K. & VanGessel, M. J. Transfer of glyphosate resistance: evidence of hybridization in *Conyza* (Asteraceae). *Am. J. Bot.* **94**, 660–673 (2007).

104. Robinson, H. E. Generic and subtribal classification of American Vernonieae. *Smithson. Contrib. Bot.* 1–116 (1999).

105. *Royal Botanical Gardens, Kew*. (Wild plants for a sustainable future: 110 multipurpose species / edited by Tiziana Ulian [and eleven others], 2019).

106. POWO. *POWO (2022). "Plants of the World Online Vernonia galamensis''*. (Facilitated by the Royal Botanic Gardens, Kew. Published on the Internet;, 2022). https://powo.science.kew.org/results?q=Vernonia%20galamensis, accessed, 2023/05/11.

107. Jeffrey, C. The Vernonieae in east tropical Africa: notes on compositae: V. *Kew Bull.* **43**, 195 (1988).

108. Baye, T. & Becker, H. C. Exploration of *Vernonia galamensis* in Ethiopia, and variation in fatty acid composition of seed oil. *Genet. Resour. Crop Evol.* **52**, 805–811 (2005).

109. Thulin, M., *Flora of Somalia*. **3**: 226 (Royal Botanic Gardens, Kew, 1993).

110. Chakraborty, S., Cici, S. Z. H., Todd, J., Loucks, C. & Van Acker, R. C. Exploring the weed biology of two potentially novel oilseed crops: *Euphorbia lagascae* and *Centrapalus pauciflorus*. *Can. J. Plant Sci.* **96**, 677–688 (2016).

111. Favi, F., Cantrell, C. L., Mebrahtu, T. & Kraemer, M. E. Leaf peltate glandular trichomes of *Vernonia galamensis* ssp. *galamensis* var. *ethiopica* Gilbert: development, ultrastructure, and chemical composition. *Int. J. Plant Sci.* **169**, 605–614 (2008).

112. Chhabra, S. C., Mahunnah, R. L. A. & Mshiu, E. N. Plants used in traditional medicine in Eastern Tanzania. II. Angiosperms (Capparidaceae to Ebenaceae). *J. Ethnopharmacol.* **25**, 339–359 (1989).

113. Neuwinger, H. D. *African traditional medicine: a dictionary of plant use and applications with supplement: search system for diseases*. **1**, 1-547 (Medpharm Scientific Publishers, 2000).

114. Dong, M., Chen, X.-Q., Chen, C.-H. & Li, R.-T. Terpenes from *Euphorbia antiquorum* and their *in vitro* anti-HIV activity. *Chem. Biodivers.* **15**, e1700560 (2018).

115. An, L., Liang, Y., Yang, X., Wang, H., Zhang, J., Tuerhong, M., Li, D., Wang, C., Lee, D., Xu, J., Shuai, L., and Guo, Y. NO inhibitory diterpenoids as potential anti-inflammatory agents from *Euphorbia antiquorum*. *Bioorg. Chem.* **92**, 103237 (2019).

116. Gewali, M. B., Hattori, M., Tezuka, Y., Kikuchi, T. & Namba, T. Four ingol type diterpenes from *Euphorbia antiquorum* L. *Chem. Pharm. Bull. (Tokyo)* **37**, 1547-1549. (1989).

117. Li, X. L., Li, Y., Wang, S. F., Zhao, Y. L., Liu, K. C., Wang, X. M., & Yang, Y. P. Ingol and ingenol diterpenes from the aerial parts of *Euphorbia royleana* and their antiangiogenic activities. *J Nat Prod* **72**, 1001–1005 (2009).

118. Rizk, A. M., Hammouda, F. M., El-Missiry, M. M., Radwan, H. M. & Evans, F. J. Macrocyclic diterpene esters from *Euphorbia royleana*. *Phytochemistry* **33**, 2377–2379 (1984).

119. Wang, P., Xie, C., An, L., Yang, X., Xi, Y., Yuan, S., Zhang, C., Tuerhong, M., Jin, D.Q., Lee, D., Zhang, J. & Guo, Y. Bioactive diterpenoids from the stems of *Euphorbia royleana*. *J. Nat. Prod.* **82**, 183–193 (2019).

120. Ravikanth, V., Niranjan Reddy, V. L., Vijender Reddy, A., Diwan, P. V. & Venkateswarlu, Y. Diterpenes from the latex of *Euphorbia nivulia*. *Biochem. Syst. Ecol.* **31**, 447–449 (2003).

121. Connoly, J. D., Facunle, C. O. & Rycroft, D. S. Five ingol esters and a 17-hydroxyingenol ester from the latex of *Euphorbia kamerunica*. Assignment of esters using ^{13}C.N.M.R. methods. *Tetrahedron Lett.* **25**, 3773–3776 (1984).

122. Marco, J. A., Sanz-Cervera, J. F. & Yuste, A. Ingenane and lathyrane diterpenes from the latex of *Euphorbia canariensis*. *Phytochemistry* **45**, 563–570 (1997).

123. Yan, S. L., Li, Y. H., Chen, X. Q., Liu, D., Chen, C. H., & Li, R. T. Diterpenes from the stem bark of *Euphorbia neriifolia* and their in vitro anti-HIV activity. *Phytochemistry* **145**, 40–47 (2018).

124. Ahmed, A. A., Couladis, M., Mahmoud, A. A., de Adams, A. & Mabry, T. J. Ingol diterpene ester from the latex of *Euphorbia lactea*. *Fitoterapia* **70**, 140–143 (1999).

125. Zhang, X. D., Ni, W., Yan, H., Li, G. T., Zhong, H. M., Li, Y., & Liu, H. Y. Daphnane-type diterpenoid glucosides and further constituents of *Euphorbia pilosa*. *Chem. Biodivers.* **11**, 760–766 (2014).

126. Wang, B., Wei, Y., Zhao, X., Tian, X., Ning, J., Zhang, B., Deng, S., Li, D., Ma, X. & Wang, C. Unusual *ent*-atisane type diterpenoids with 2-oxopropyl skeleton from the roots of *Euphorbia ebracteolata* and their antiviral activity against human rhinovirus 3 and enterovirus 71. *Bioorg. Chem.* **81**, 234–240 (2018).

127. Yang, L., Liu, S., Zhang, B. & Suo, Y. Alboatisin A, A new diterpenoid from *Euphorbia fischeriana*. *J. Chem. Res.* **35**, 692–693 (2011).

128. Zhang, B. Y., Wang, H., Luo, X. D., Du, Z. Z., Shen, J. W., Wu, H. F., & Zhang, X. F. Bisyinshanic acids A and B, two novel diterpene dimers from the roots of *Euphorbia yinshanica*. *Helv. Chim. Acta* **95**, 1672–1679 (2012).

129. Appendino, G., Belloro, E., Cesare Tron, G., Jakupovic, J. & Ballero, M. Polycyclic diterpenoids from *Euphorbia characias*. *Fitoterapia* **71**, 134–142 (2000).

130. Dräger, G., Jeske, F., Kunst, E., Lopez, E. G., Sanchez, H. V., Tsichritzis, F., Kirschning, A. & Jakupovic, J. Tonantzitlolone and other diterpenes from *Stillingia sanguinolenta*. *Eur. J. Org. Chem.* **2007**, 5020–5026 (2007).

131. Lal, A. R., Cambie, R. C., Rutledge, P. S. & Woodgate, P. D. *Ent*-atisane diterpenes from *Euphorbia fidjiana*. *Phytochemistry* **29**, 1925–1935 (1990).

132. Tang, W.-X., Wang, Q.-B., Zhang, W.-Z., Zhang, S.-J. & Fukuyama, Y. Two new stachane diterpenoids from the bark of *Ptychopetalum olacoides*. *Chem. Nat. Compd.* **52**, 841–844 (2016).

133. Wang, L. K., Zheng, C. J., Li, X. B., Chen, G. Y., Han, C. R., Chen, W. H., & Song, X. P. Two new lanostane triterpenoids from the branches and leaves of *Polyalthia oblique*. *Molecules* **19**, 7621–7628 (2014).

134. Wang, L.-Y., Wang, N.-L., Yao, X.-S., Miyata, S. & Kitanaka, S. Euphane and tirucallane triterpenes from the roots of *Euphorbia kansui* and their in vitro effects on the cell division of *xenopus*. *J. Nat. Prod.* **66**, 630–633 (2003).

135. Tsopmo, A. & Kamnaing, P. Terpenoids constituents of *Euphorbia sapinii*. *Phytochem. Lett.* **4**, 218–221 (2011).

136. Kawanishi, K., Uhara, Y. & Hashimoto, Y. Neolignans of *Virola carinata* bark. *Phytochemistry* **21**, 2725–2728 (1982).

137. Wongsomboon, P., Rattanajak, R., Kamchonwongpaisan, S., Pyne, S. G. & Limtharakul, T. Unique polyacetylenic ester-neolignan derivatives from *Mitrephora tomentosa* and their antimalarial activities. *Phytochemistry* **183**, 112615 (2021).

138. Valcic, S., Montenegro, G. & Timmermann, B. N. Lignans from Chilean propolis. *J. Nat. Prod.* **61**, 771–775 (1998).

139. Yoshikawa, K., Baba, C., Iseki, K., Ito, T., Asakawa, Y., Kawano, S., & Hashimoto, T. Phenanthrene and phenylpropanoid constituents from the roots of *Cymbidium* great flower 'marylaurencin' and their antimicrobial activity. *J. Nat. Med.* **68**, 743–747 (2014).

140. Waight, E. S., Razdan, T. K., Qadri, B. & Harkar, S. Chromones and coumarins from *Skimmia laureola*. *Phytochemistry* **26**, 2063–2069 (1987).

141. Bai, N., He, K. A. N., Roller, M., Zheng, B., Chen, X., Shao, Z., Peng, T. & Zheng, Q. Active compounds from *Lagerstroemia speciosa* , insulin-like glucose uptake-stimulatory/inhibitory and adipocyte differentiation-inhibitory activities in 3T3-L1 cells. *J. Agric. Food Chem.* **56**, 11668–11674 (2008).

142. Appendino, G., Cravotto, G., Minassi, A. & Palmisano, G. Three-component tandem knoevenagel/hetero diels−alder reactions - Total synthesis of (±)-preethulia coumarin. *Eur. J. Org. Chem.* **2001**, 3711–3717 (2001).

143. Metwally, M. A. Coumarin derivative from *Conyza bovei*. *Boll. Chim.-Farm.* **135**, 223–224 (1996).

144. Keige, A., Maxwell, S. R. J., Vogler, B., Klaiber, I. & Kraus, W. Novel coumarins and sesquiterpene lactones from *Vernonia brachycalyx*. *Pharm. Pharmacol. Lett.* **8**, 43–45.

145. Farnsworth, N. R., Akerele, O., Bingel, A. S., Soejarto, D. D. & Guo, Z. Medicinal plants in therapy. *Bull. World Health Organ.* **63**, 965–981 (1985).

146. Cragg, G. M., Newman, D. J. & Snader, K. M. Natural products in drug discovery and development. *J. Nat. Prod.* **60**, 52–60 (1997).

147. Cragg, G. M. & Pezzuto, J. M. Natural products as a vital source for the discovery of cancer chemotherapeutic and chemopreventive agents. *Med. Princ. Pract.* **25**, 41–59 (2016).

148. Kinghorn A.D. and Balandrin, M.F. in *Human Medicinal Agents from Plants* (ed. Kinghorn A.D. and, B., M. F.) **534**, 1–25 (American Chemical Society, 1993).

149. Fabricant, D. S. & Farnsworth, N. R. The value of plants used in traditional medicine for drug discovery. *Environ. Health Perspect.* **109**, 69–75 (2001).

150. Da Rocha, A. Natural products in anticancer therapy. *Curr. Opin. Pharmacol.* **1**, 364–369 (2001).

151. Cragg, G. M. & Newman, D. J. Discovery and development of antineoplastic agents from natural sources. *Cancer Invest.* **17**, 153–163 (1999).

152. Linder, H. P. Plant diversity and endemism in Sub-Saharan tropical Africa: African phytogeography. *J. Biogeogr.* **28**, 169–182 (2001).

153. World Health OrganizationWHO. *Quality control methods for medicinal plant materials*. vol. 2 (World Health Organization, 1998) (No. WHO/PHARM/92.559/rev. 1) (accessed 01/09/2022, 1998).

154. Muyumba, N. W., Mutombo, S. C., Sheridan, H., Nachtergael, A. & Duez, P. Quality control of herbal drugs and preparations: The methods of analysis, their relevance and applications. *Talanta Open* **4**, 100070 (2021).

155. Li, S., Han, Q., Qiao, C., Song, J., Lung Cheng, C., & Xu, H. Chemical markers for the quality control of herbal medicines: an overview. *Chin. Med.* **3**, 7 (2008).

156. Abubakar, A. & Haque, M. Preparation of medicinal plants: Basic extraction and fractionation procedures for experimental purposes. *J. Pharm. Bioallied Sci.* **12**, 1 (2020).

157. Onwukaeme, N. D. & Rowan, M. G. Jatrophane and lathyrane diterpenoid esters from north american leafy spurge seed. *Phytochemistry* **31**, 3479–3482 (1992).

158. Betancur-Galvis, L., Checa, J., Marco, J. A. & Estornell, E. Jatrophane diterpenes from the latex of *Euphorbia obtusifolia* with inhibitory activity on the mammalian mitochondrial respiratory chain. *Planta Med.* **69**, 177–178 (2003).

159. Ferreira, A. M. V. D., Carvalho, L. H. M., Carvalho, M. J. M., Sequeira, M. M. & Silva, A. M. S. Jatrophane and lathyrane diterpenoids from *Euphorbia hyberna* L. *Phytochemistry* **61**, 373–377 (2002).

160. Appendino, G., Spagliardi, P., Ballero, M. & Seu, G. Macrocyclic diterpenoids from *Euphorbia hyberna* L. subsp. *insularis* and their reaction with oxyphilic reagents. *Fitoterapia* **73**, 576–582 (2002).

161. Rédei, D., Kúsz, N., Sátori, G., Kincses, A., Spengler, G., Burián, K., Barina, Z. & Hohmann, J. Bioactive segetane, ingenane, and jatrophane diterpenes from *Euphorbia taurinensis*. *Planta Med.* **84**, 729–735 (2018).

162. Kúsz, N., Orvos, P., Bereczki, L., Fertey, P., Bombicz, P., Csorba, A., Talosi, L., Jakab, G., Hohmann, J. & Rédei, D. Diterpenoids from *Euphorbia dulcis* with potassium ion channel inhibitory activity with selective G protein-activated inwardly rectifying ion channel (GIRK) blocking effect. *J. Nat. Prod.* **81**, 2483–2492 (2018).

163. Kúsz, N., Orvos, P., Csorba, A., Tálosi, L., Chaieb, M., Hohmann, J., & Rédei, D. Jatrophane diterpenes from *Euphorbia guyoniana* are new potent inhibitors of atrial GIRK channels. *Tetrahedron* **72**, 5724–5728 (2016).

164. Hammadi, R., Kúsz, N., Dávid, C. Z., Behány, Z., Papp, L., Kemény, L., Hohmann, J., Lakatos, L. & Vasas, A. Ingol and ingenol-type diterpenes from *Euphorbia trigona* Miller with keratinocyte inhibitory activity. *Plants* **10**, 1206 (2021).

165. Rédei, D., Hohmann, J., Evanics, F., Forgo, P., Szabo, P., & Mathe, I. & Máthé, I. Isolation and structural characterization of new, highly functionalized diterpenes from *Euphorbia serrulata*. *Helv. Chim. Acta* **86**, 280–289 (2003).

166. Hohmann, J., Rédei, D., Forgo, P., Molnár, J., Dombi, G., & Zorig, T. Jatrophane diterpenoids from *Euphorbia mongolica* as modulators of the multidrug resistance of L5128 mouse lymphoma cells. *J. Nat. Prod.* **66**, 976–979 (2003).

167. Forestier, E., Romero-Segura, C., Pateraki, I., Centeno, E., Compagnon, V., Preiss, M., Berna, A., Boronat, A., Bach, T.J., Darnet, S. & Schaller, H. Distinct triterpene synthases in the laticifers of *Euphorbia lathyris*. *Sci. Rep.* **9**, 4840 (2019).

168. Gherraf, N., Zellagui, A., Mohamed, N. S., Hussien, T. A., Mohamed, T. A., Hegazy, M. E. F., Rhouati, S., Moustafa, M.F., El-Sayed, M.A. & Mohamed, A. E. H. H. Triterpenes from *Euphorbia rigida*. *Pharmacogn. Res.* **2**, 159–162 (2010).

169. Ragasa, C. Y. & Cornelio, K. B. Triterpenes from *Euphorbia hirta* and their cytotoxicity. *Chin. J. Nat. Med.* **11**, 528–533 (2013).

170. Wang, S. Y., Huang, C., Sun, R. K., Lu, L. N., Liang, H. G., Gao, L., Huang, J., Wang, J.H. & Yang, B. F. New tirucallane triterpenoids from the dried latex of *Euphorbia resinifera*. *Phytochem. Lett.* **29**, 220–224 (2019).

171. Sun, Y., Gao, L. L., Tang, M. Y., Feng, B. M., Pei, Y. H., & Yasukawa, K. Triterpenoids from *Euphorbia maculata* and their anti-inflammatory effects. *Molecules* **23**, 2112 (2018).

172. Kemboi, D., Peter, X., Langat, M. & Tembu, J. A review of the ethnomedicinal uses, biological activities, and triterpenoids of *Euphorbia species*. *Molecules* **25**, 4019 (2020).

173. Mascellani, A., Leiss, K., Bac-Molenaar, J., Malanik, M., Marsik, P., Hernandez Olesinski, E., Tauchen, J., Kloucek, P., Smejkal, K. & Havlik, J. Polyketide derivatives in the resistance of *Gerbera hybrida* to powdery mildew. *Frontiers in Plant Science*, **12,** 3040 (2022).

174. Molnár, J., Gyémánt, N., Tanaka, M., Hohmann, J., Bergmann-Leitner, E., Molnár, P., Deli, J., Didiziapetris, R. & Ferreira, M. J. Inhibition of multidrug resistance of cancer cells by natural diterpenes, triterpenes and carotenoids. *Curr. Pharm. Des.* **12**, 287–311 (2006).

175. Van Duin, D. & Paterson, D. L. Multidrug-resistant bacteria in the community. *Infect. Dis. Clin. North Am.* **30**, 377–390 (2016).

176. Zahreddine, H. & Borden, K. L. B. Mechanisms and insights into drug resistance in cancer. *Front. Pharmacol.* **4**, 28 (2013).

177. Sampath, D. Pharmacodynamics of cytarabine alone and in combination with 7-hydroxystaurosporine (UCN-01) in AML blasts in vitro and during a clinical trial. *Blood* **107**, 2517–2524 (2006).

178. Engi, H., Hohmann, J., Gang, G., Pusztai, R., Rédei, D., Kovács, O., Schelz, Z. & Molnár, J. Chemoprevention and inhibition of P-glycoprotein in cancer cells by Chinese medicinal herbs. *Phytother. Res.* **22**, 1671–1676 (2008).

179. Hohmann, J., Molnár, J., Rédei, D., Evanics, F., Forgo, P., Kálmán, A., Argay, G. & Szabó, P. Discovery and biological evaluation of a new family of potent modulators of multidrug resistance: reversal of multidrug resistance of mouse lymphoma cells by new natural jatrophane diterpenoids isolated from *Euphorbia* species. *J. Med. Chem.* **45**, 2425–2431 (2002).

180. Vasas, A., Rédei, D., Csupor, D., Molnár, J. & Hohmann, J. Diterpenes from European *Euphorbia* species serving as prototypes for natural-product-based drug discovery. *Eur. J. Org. Chem.* **2012**, 5115–5130 (2012).

181. Barile, E., Corea, G. & Lanzotti, V. Diterpenes from *Euphorbia* as potential leads for drug design. *Nat. Prod. Commun.* **3**, 1003–1020 (2008).

182. Global Burden of Disease Collaborative Network. Global burden of disease study 2019 (GBD 2019) reference life table (2021) (accessed 2022-10-20).

183. Ferlay, J., Colombet, M., Soerjomataram, I., Parkin, D. M., Piñeros, M., Znaor, A., & Bray, F. Cancer statistics for the year 2020: An overview. *Int. J. Cancer* **149**, 778–789 (2021).

184. Fridlender, M., Kapulnik, Y. & Koltai, H. Plant derived substances with anti-cancer activity: from folklore to practice. *Front. Plant Sci.* **6**, 799 (2015).

185. Mosmann, T. Rapid colorimetric assay for cellular growth and survival: Application to proliferation and cytotoxicity assays. *J. Immunol. Methods* **65**, 55–63 (1983).

186. Peña-Morán, O., Villarreal, M., Álvarez-Berber, L., Meneses-Acosta, A. & Rodríguez-López, V. Cytotoxicity, post-treatment recovery, and selectivity analysis of naturally occurring podophyllotoxins from *Bursera fagaroides var. fagaroides* on breast cancer cell lines. *Molecules* **21**, 1013 (2016).

187. López-Lázaro, M. How many times should we screen a chemical library to discover an anticancer drug? *Drug Discov. Today* **20**, 167–169 (2015).

188. Indrayanto, G., Putra, G. S. & Suhud, F. Validation of in-vitro bioassay methods: Application in herbal drug research. in *Profiles of Drug Substances, Excipients and Related Methodology* **46**, 273–307 (Elsevier, 2021).

189. Weerapreeyakul, N., Nonpunya, A., Barusrux, S., Thitimetharoch, T. & Sripanidkulchai, B. Evaluation of the anticancer potential of six herbs against a hepatoma cell line. *Chin. Med.* **7**, 15 (2012).

Acknowledgements

I will want to use this medium to express my utmost and profound gratitude to my supervisor *Dr. Dóra Rédei Ph.D.* for providing me with conducive and enabling environment to conduct my research. Indeed, her guidance, experience, support, and contributions were vital to the success of this research. I will forever remain grateful to her.

I would like to express my immense and sincere gratitude and appreciation to the Head of our research group, *Univ. Professor Dr. Judit Hohmann D.Sc.* for her unwavering support (both technical and financial), guidance, contribution and kindness showered on me throughout the scope of this research. Indeed, we have gained a lot from her pool of knowledge and wealth of experience. Her contributions were critical to the achievements attained throughout the research. I will call her 'A living hero of pharmacognosy and science'. *Univ. Professor Dr. Judit Hohmann* and *Dr. Dóra Rédei* are embodiment of goodness and specimens of great scientist.

I also wish to thank *Dr. Norbert Kúsz Ph.D.* and *Dr. Anita Barta Pharm.D.* (Institute of Pharmacognosy, University of Szeged) for the NMR measurements; *Dr. Gordana Krystic Ph.D.* (Faculty of Chemistry, University of Belgrade) and *Dr. Norbert Kúsz Ph.D.* for NMR structure elucidation of compounds; *Dr. Róbert Berkecz Ph.D.* (Institute of Analytical Chemistry, University of Szeged) for the HRESIMS measurements; *Dr. Petra Bombicz Ph.D.* (Chemical Crystallography Research Laboratory, Research Centre for Natural Sciences, Hungarian Academy of Sciences) and *Dr. Pierre Fertey Ph.D.* (Synchrotron SOLEIL L'Orme des Merisiers – Saint Aubin, Gif-sur-Yvette Cedex, France) for the X-ray data; *Univ. Prof. Dr. Katalin Burián Ph.D.*, *Dr. Gabriella Spengler Ph.D.*, *Dr. Annamária Kincses Ph.D.*, and *Dr. Dávid Kókai Ph.D.* (Department of Medical Microbiology Educational and Research Center, University of Szeged) for testing the compounds for their MDR modulating, cytotoxic and antiviral activities; and *Univ. Prof. Dr. István Zupkó D.Sc.* and *Hazhmat Ali* (Department of Pharmacodynamics and Biopharmacy, University of Szeged) for measuring the antiproliferative activity of plant extracts and isolated compounds.

I would also like to thank Staff members of the Institute of Pharmacognosy, *Dr. Andrea Vasas Ph.D.* for her kindness, generosity and guidance. My appreciation also goes to *Dr. Katalin Veres Ph.D.*, who was always there whenever I needed extra hours for research after the official closing hours. My sincere appreciation also goes to *Attila Horváth*, who was always available to help with the repair of any laboratory equipment including HPLC.

My special thanks also go to the entire staff members and laboratory personnel, *Kornél Szemerédi* and *Tamara Sápi* for their help. *Tamara Sápi* was very helpful whenever as foreign students, we needed one in our day-to-day activities.

I would like to thank my parents; *Mr. S. M. Bello* and *Mrs. Fatima Ahmad*, my great uncle; *Mr. M. K Bello*, for their spiritual and moral support. My gratitude also goes to my siblings, relatives, and entire family members.

I would like to express my sincere thanks to *Professor Dr. Abubakar Ahmad* (Ahmadu Bello University, Zaria, Nigeria) for his mentorship. I will also want to thank *Umar Gallah* (National Research Institute for Chemical Technology, Zaria, Nigeria) for the identification, collection, and preparations of the plant materials.

I also want to thank *Stipendium Hungaricum* scholarship program for their financial support and the opportunity they offered me.

Finally, I would like to express my gratitude to the Nigerian government including her agencies like the Federal Ministry of Education, Federal Scholarship Board and Nigerian Embassy in Hungary for their support and coordination.

Annex 1

Structures of compounds **1**–**38** isolated from *E. deightonii*

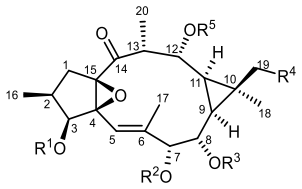

		R^1	R^2	R^3	R^4	R^5			R^1	R^2	R^3	R^4	R^5
1	(ED-29)	Ac	Tig	Ac	H	H	**14**	(ED-16)	Ac	Ac	Tig	H	Ac
2	(ED-58)	Ac	*i*-Bu	Ac	H	Ac	**15**	(ED-17)	Ac	2-MeBu	Ac	H	Ac
3	(ED-71)	Ac	Ac	Sal	H	Ac	**16**	(ED-27)	Ac	Ac	Ac	H	Ac
4	(ED-79)	Ac	Ang	Ac	Ac	Ac	**17**	(ED-42)	Ac	Tig	Ac	H	Ac
5	(ED-91)	H	Tig	Ac	H	Ac	**18**	(ED-46)	Ac	Bz	Me	H	Ac
6	(ED-93)	Ac	Bz	H	H	Ac	**19**	(ED-48)	Ac	Bz	Ac	H	Ac
7	(ED-98)	Ac	Ac	Bz	Ac	Ac	**20**	(ED-52)	Ac	Ang	Me	H	Ac
8	(ED-109)	Ac	Tig	Tig	Ac	H	**21**	(ED-54)	Ac	*i*-Val	Ac	H	Ac
9	(ED-112)	Ac	Ang	Bz	OH	Ac	**22**	(ED-89)	H	Tig	Me	H	Ac
10	(ED-7)	Ac	Ac	2-MeBu	H	Ac	**23**	(ED-92)	Ac	Tig	H	H	Ac
11	(ED-8)	Ac	Ac	Bz	H	Ac	**24**	(ED-94)	Ac	Ang	H	H	Ac
12	(ED-9)	Ac	Ang	Ac	H	Ac	**25**	(ED-102)	Ac	H	Tig	H	Ac
13	(ED-12)	Ac	Ang	Me	H	Ac	**26**	(ED-110)	Ac	Tig	Tig	OH	Ac

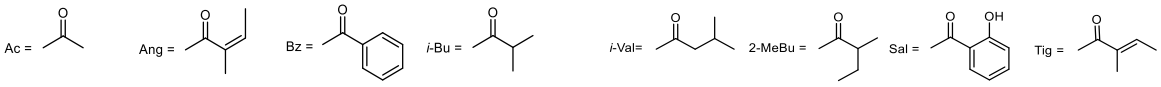

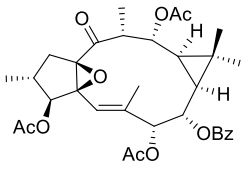

27 (ED-45)

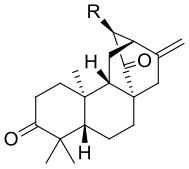

28 (ED-1) R= H
29 (ED-134) R = OH

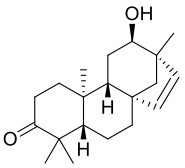

30 (ED-141)

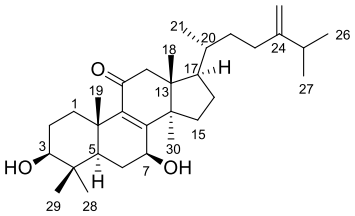

31 (ED-116)

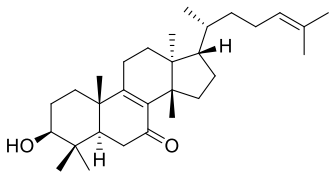

32 (ED-33)

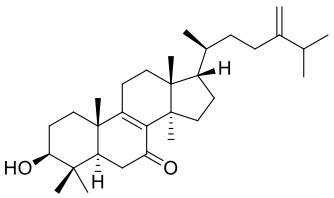

33 (ED-36)

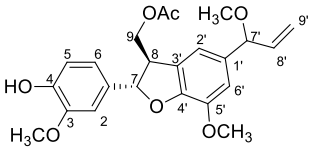

34 (ED-119)

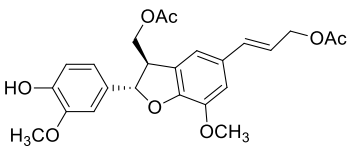

35 (ED-120)

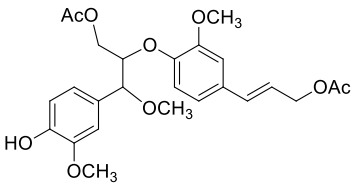

36 (ED-121)

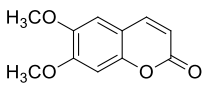

37 (ED-105)

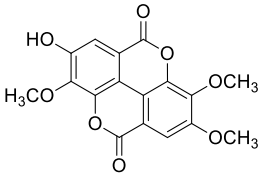

38 (ED-85)

Annex 2

Structures of compounds **39**–**63** isolated from *C. pauciflorus*

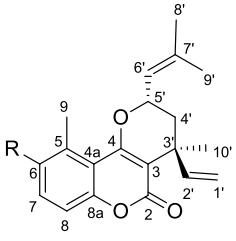

39 (VP-146) R = H
41 (VP-113) R = OH

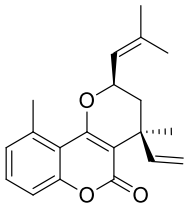

40 (VP-147)

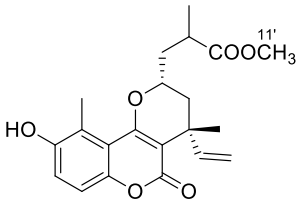

42 (VP-27)

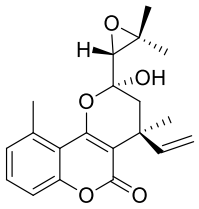

43 (VP-55)

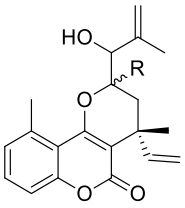

44 (VP-67) R = *β*OH
45 (VP-68) R = *α*OH

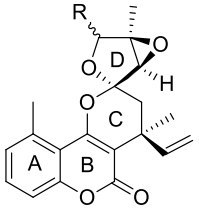

46 (VP-176) R = *β*OH
47 (VP-177) R = *α*OH

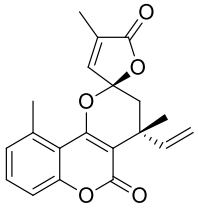

48 (VP-5)

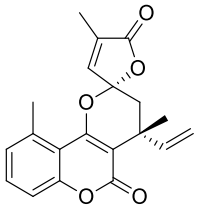

49 (VP-6)

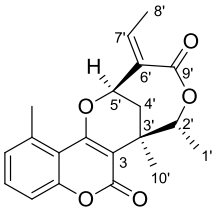

50 (VP-172)

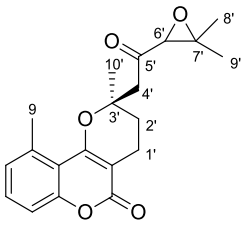

51 (VP-158) H-6′*α*
52 (VP-159) H-6′*β*

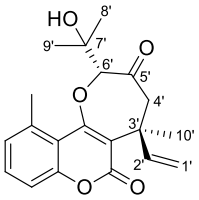

53 (VP-160)

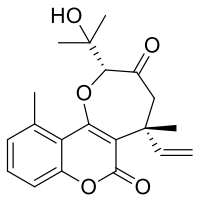

54 (VP-161)

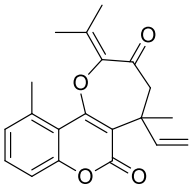

55 (VP-153)

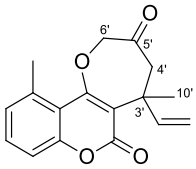

56 (VP-8)

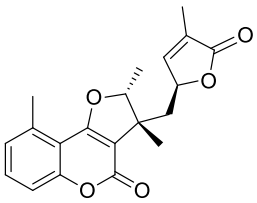

57 (VP-90)

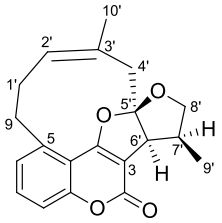

58 (VP-122)

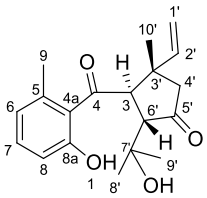

59 (VP-54)

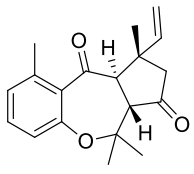

60 (VP-137)

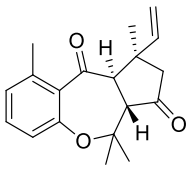

61 (VP-138)

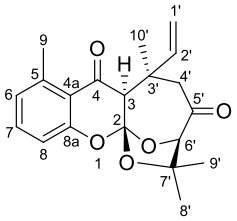

62 (VP-145)

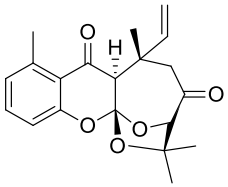

63 (VP-140)

Annex 3

^{1}H NMR spectroscopic data of compounds **1**–**9** [δ ppm (*J* =Hz), $CDCl_3$, 500 MHz (^{1}H)]

Position	1	2	3	4	5	6	7	8	9
1a	2.72 dd (overlap)	2.80 dd (9.05, 15.0)	2.80 dd (15.0; 9.0)	2.80 dd (15.0; 9.1)	2.78 dd (15.0; 9.3)	2.80 dd (15.0; 9.0)	2.79 dd (15.0; 9.0)	2.75 dd (15.0; 9.0)	2.82 dd (15.0; 9.0)
1b	1.71 d (15.0)	1.70 dd (0.9, 15)	1.72 d (15.0)	1.70 br d (15.0)	1.64 dd (15.0; 2.0)	1.68 dd (15.0; 0.6)	1.72 br d (15.0)	1.72 br d (15.0)	1.72 br d (15.0)
2	2.48 m	2.49 m	2.47 m	2.51 m	2.40 m	2.46 m	2.49 m	2.49 m	2.52 m
3	5.25 d (8.5)	5.28 d (8.6)	5.37 d (8.6)	5.25 d (8.6)	4.28 d (8.5)	5.19 d (8.6)	5.36 d (8.5)	5.25 d (8.6)	5.28 d (8.5)
5	5.59 br s	5.57 br s	5.64 br s	5.56 br s	5.66 br s	5.66 br s	5.63 br s	5.57 br s	5.63 br s
7	5.12 br s	5.15 br s	5.18 br d (1.6)	5.27 br d (1.2)	5.35 br s	5.31 br d (1.8)	5.23 br s	5.17 br d (1.3)	5.33 br s
8	4.51 br d (10.8)	4.58 dd (10.8, 1.9)	4.84 dd (10.9; 1.9)	4.60 dd (10.6; 1.7)	4.61 dd (10.6; 1.8)	3.63 dd (10.3; 2.1)	4.89 br dd (10.7; 0.8)	4.65 dd (10.7; 1.7)	4.94 dd (10.7; 1.8)
9	1.23 m	1.25 dd (8.65) overlap	1.44 dd (10.9; 9.1)	1.46 m	1.25 dd (10.6; 9.2)	1.31 dd (10.3; 9.3)	1.63 br dd (10.7; 9.4)	1.51 dd (10.7; 9.2)	1.58 dd (10.7; 9.2)
11	0.76 t (9.7)	1.12 dd (9.15; 3.4)	1.19 dd (11.1; 9.1)	1.35 dd (11.1; 9.2)	1.16 dd (10.9; 9.2)	1.11 dd (11.0; 9.3)	1.37 dd (11.0; 9.4)	1.09 m	1.36 dd (10.9; 9.2)
12	3.24 dd (10.6; 2.1)	4.87 dd (11.1, 4.0)	4.92 dd (11.1; 4.0)	4.94 dd (11.1; 3.9)	4.88 dd (10.9; 4.0)	4.94 dd (11.0; 4.0)	5.00 dd (11.0; 3.7)	3.35 ddd (11.1; 8.4; 3.2)	5.08 dd (10.9; 3.7)
13	2.71 m	2.93 m	2.97 m	2.93 m	2.94 m	2.98 m	2.99 m	2.78 m	3.00 m
16	0.94 d (7.4)	0.94 d (7.5)	0.99 d (7.4)	0.94 d (7.4)	1.03 d (7.5)	0.93 d (7.5)	0.99 d (7.4)	0.95 d (7.5)	0.96 d (7.4)
17	2.10 s	2.10 s	2.15 d (1.3)	2.13 d (1.2)	2.13 d (1.2)	2.14 d (1.2)	2.16 br s	2.13 d (1.3)	2.20 d (1.1)
18	1.17 s	1.18 s	1.16 s	1.12 s	1.09 s	1.15 s	1.19 s	1.23 s	1.23 s
19a	0.98 s	0.85 s	0.84 s	4.27 d (12.1)	0.86 s	1.11 s	4.09 d (12.2)	4.11 d (12.1)	3.57 dd (12.1; 5.8)
19b				3.53 d (12.1)			3.72 d (12.2)	3.92 d (12.1)	3.41 dd (12.1; 5.7)
20	1.25 d (7.3)	1.07 d (7.6)	1.09 d (7.3)	1.08 d (7.3)	1.08 d (7.3)	1.07 d	1.09 d (7.3)	1.28 d (7.4)	1.13 d (7.3)
Acetyl									
3-OAc	2.07 s	2.01 d (4.35)	2.08 s	2.07 s	–	2.05 s	2.08 s	2.07 s	2.08 s
7-OAc	–	–	2.13 s	–	–	–	2.14 s	–	–
8-OAc	2.02 s	2.08 s	–	2.05 s	2.00 s	–	–	–	–
12-OAc	–	2.10 s	2.10 s	2.12 s	2.10 s	2.13 s	2.11 s	–	2.12 s
19-OAc	–	–	–	1.99 s	–	–	1.68 s	2.00 s	–

[1] Compound **1**: 7-*O*-Tigloil 6.88 (1H, q, *J* = 7.0 Hz, H-3), 1.84 (3H, d, *J* = 7.0 Hz, H-4), 1.87 (3H, brs, H-5); Compound **2**: 7-*O*-*i*-Bu 2.66 (1H, m, H-2), 1.20 (6H, d, *J* = 6.7 Hz, H-3, H-4); compound **3**: 8-*O*-Sal 6.98 (1H, dd, *J* = 8.4; 0.9 Hz, H-4), 7.47 (1H, dd, *J* = 8.4; 1.7 Hz, H-5), 6.88 (1H, ddd, *J* = 8.4; 8.0; 1.7 Hz, H-6), 7.78 (1H, dd, J = 8.0; 1.7 Hz, H-7), 10.51 (1H, s, OH); Compound **4**: 7-*O*-Angeloyl 6.12 (1H, dq, *J* = 7.2; 1.4 Hz, H-3), 1.98 (3H, dd, *J* = 7.2; 2.9 Hz, H-4), 1.93 (3H, br t, *J* = 1.5 Hz, H-5); Compound **5**: 7-*O*-Tigloyl 6.91 (1H, dq, *J* = 7.1; 1.4 Hz, H-3), 1.83 (3H, dd, *J* = 7.1, 1.0 Hz, H-4), 1.87 (3H, br t, *J* = 1.1 Hz, H-5); Compound **6**: 7-OBz 8.03 (2H, dd, *J* = 8.4; 1.3 Hz, H-3, H-7), 7.47 (2H, br dd, *J* = 8.0; 7.4 Hz, H-4, H-6), 7.60 (1H, dt, *J* = 7.5; 1.3 Hz, H-5); Compound **7**: 8-OBz 8.00 (2H, d, *J* = 7.5 Hz, H-3, H-7), 7.44 (2H, t, *J* = 7.7 Hz, H-4, H-6), 7.56 (1H, t, *J* = 7.4 Hz, H-5); Compound **8**: 7-*O*-Tigloil 6.86 (1H, dq, *J* = 7.1; 1.3 Hz, H-3), 1.84 (3H, dd, *J* = 7.1; 1.1 Hz, H-4), 1.86 (3H, br t, *J* = 1.2 Hz, H-5), 8-*O*-Tigloyl 6.82 (1H, dq, *J* = 7.3; 1.6 Hz, H-3), 1.79 (6H, m, H-4, H-5), 12-OH 2.80 br s; Compound **9**: 7-*O*-Angeloyl 6.10 (1H, m, H-3), 1.95 (6H, m, H-4, H-5), 8-OBz 7.68 (2H, d, *J* = 8.1, 1.3 Hz, H-3, H-7), 7.44 (2H, dd, *J* = 8.1; 7.6 Hz, H-4, H-6), 7.57 (1H, dt, *J* = 7.6; 1.3 Hz, H-5) , 19-OH 1.9 (1H, br t, *J* = 5.8 Hz).

Annex 4

^{13}C NMR data of compounds **1**-**9** [δ ppm (*J* = Hz), $CDCl_3$ 125 MHz (^{13}C)]

Position	1	2	3	4	5	6	7	8	9
1a	31.1	31.6	31.5	31.7	32.0	31.6	31.6	31.4	31.7
2	29.4	29.6	29.6	29.7	32.2	29.6	29.6	29.4	29.7
3	76.7	76.7	76.3	76.7	76.3	76.8	76.4	76.7	76.7
4	74.1	73.5	73.6	73.6	75.9	73.6	73.6	73.9	73.6
5	117.2	117.1	117.5	117.1	117.5	117.0	117.2	116.9	117.0
6	140.5	140.0	139.6	140.1	139.7	140.1	140.0	140.5	140.3
7	77.3	76.4	77.1	76.2	76.5	80.7	76.9	76.8	76.8
8	71.7	71.7	72.7	71.0	72.0	70.1	70.9	70.6	71.9
9	25.3	25.0	25.0	25.5	25.0	29.0	25.6	26.3	25.4
10	19.0	19.0	19.8	22.3	19.4	19.2	22.5	22.1	25.6
11	34.3	30.8	31.2	31.3	30.8	31.2	31.4	34.9	31.5
12	71.6	70.8	70.7	69.3	70.8	71.0	69.4	70.4	70.6
13	43.4	43.2	43.2	43.5	43.3	43.2	43.5	43.3	43.6
14	213.2	207.8	207.6	207.6	208.0	207.8	207.5	211.8	207.3
15	71.1	71.3	71.3	71.4	73.1	71.3	71.3	71.2	71.3
16	17.1	17.1	17.1	17.1	16.3	17.1	17.1	17.1	17.1
17	17.8	17.6	17.5	17.7	17.7	18.0	17.6	17.7	17.6
18	29.6	29.6	29.3	24.6	29.3	29.7	24.7	25.2	24.6
19	15.7	16.2	16.3	64.5	16.3	16.8	64.4	65.1	62.6
20	14.7	13.5	13.6	13.5	13.4	13.5	13.5	14.5	13.6
Acetyl									
3-OAc	170.7	170.5	170.9	170.8	–	170.6	170.9	170.8	170.7
3-OAcMe	20.6	20.7	20.7	20.7	–	20.6	20.7	20.7	20.7
7-OAc	–	–	169.9	–	–	–	169.7	–	–
7-OAcMe	–	–	21.1	–	–	–	21.2	–	–
8-OAc	170.8	170.7	–	170.4	170.6	–	–	–	–
8-OAcMe	21.2	21.2	–	21.2	21.1	–	–	–	–
12-OAc	–	170.6	170.6	170.4	170.5	170.8	170.3	–	172.4
12-OAcMe	–	21.1	21.8	21.2	21.2	21.2	21.2	–	21.3
19-OAc	–	–	–	170.7	–	–	170.6	170.8	–
19-OAcMe	–	–	–	20.9	–	–	20.5	21.0	–

Compound **1**: 7-*O*-Tigloyl 166.83 (C-1), 128.77 (C-2), 137.96 (C-3), 14.64 (C-4), 12.29 (C-5); Compound **2**: 7-*O*-i-Bu 175.89 (C-1), 34.13 (C-2), 18.60 (C-3), 18.94 (C-4); Compound **3**: 8-*O*-Sal 169.4 (C-1), 112.2 (C-2), 162.1 (C-3), 118.0 (C-4), 136.2 (C-5), 119.4 (C-6), 129.8 (C-7), 162.1 (C-8); Compound **4**: 7-O-Angeloyl 166.45 (C-1), 127.60 (C-2), 139.07 (C-3), 15.94 (C-4), 20.71 (C-5); Compound **5**: Compound **6**: 7-OBz 165.95 (C-1), 130.06 (C-2), 129.73 (C-3, C-7), 128.72 (C-4, C-6), 133.51 (C-5); Compound **7**: 8-OBz 165.65 (C-1), 129.68 (C-2), 129.85 (C-3, C-7), 128.66 (C-4, C-6), 133.53 (C-5); Compound **8**: 7-*O*-Tigloyl 166.61 (C-1), 128.65 (C-2), 137.98 (C-3), 14.70 (C-4), 12.32 (C-5), 8-*O*-Tigloyl 167.10 (C-1), 128.30 (C-2), 138.60 (C-3), 14.63 (C-4), 12.09 (C-5); Compound **9**: 7-*O*-Angeloyl 166.47 (C-1), 127.66 (C-2), 138.70 (C-3), 15.89 (C-4), 20.69 (C-5), 8-OBz 165.62 (C-1), 129.62 (C-2), 129.73 (C-3, C-7), 128.74 (C-4, C-6), 133.58 (C-5).

Annex 5a

^{1}H (500 MHz) data of compound **31** in $CDCl_3$ (δ_H in ppm, *J* in Hz)

Position	^{1}H	^{13}C
1a	1.02, m	33.9
1b	2.56, m	
2	1.66–1.72, m (2H)	28.0
3	3.32, dd (11.2, 5.0)	78.8
4	–	38.5
5	1.42, m	45.5
6a	1.69, m	28.6
6b	1.83, d (13.8)	
7	4.27, br s	65.6
8	–	157.3
9	–	141.6
10	–	38.6
11	–	200.4
12a	2.42, d (16.7)	51.6
12b	2.58, d (16.7)	
13	–	44.3
14	–	50.9
15a	1.39, m	29.8*
15b	2.37, m	
16a	1.43, m	29.8*
16b	2.05, m	
17	1.69, m	50.7
18	0.92, s (3H)	18.11
19	1.1,7 s (3H)	18.12
20	1.43, m	36.4
21	0.92, d (6.5) (3H)	18.5
22a	1.16, m	34.7
22b	1.58, m	
23a	1.90, m	31.3
23b	2.12, m	
24	–	156.7
25	2.23 sept (6.7)	34.0
26	1.03*, d (6.7) (3H)	22.0
27	1.02*, d (6.7) (3H)	22.1
28	1.05, s (3H)	28.3
29	0.85, s (3H)	16.2
30	1.01, s (3H)	25.9
1'a	4.73, br s	106.3
1'b	4.66, d (1.2)	

* overlapping signals

Annex 5b

^{13}C NMR (125 MHz) data of compound **34** in $CDCl_3$ (δ_H in ppm, *J* in Hz)

Position	^{1}H	^{13}C
1	–	132.7
2	6.91, m	108.9
3	–	146.9
4	–	146.0
5	6.88*, m	114.5
6	6.88*, m	119.7
7	5.46, d (7.6)	88.9
8	3.78, m	50.7
9a	4.47, dd (11.2, 5.4)	65.7
9b	4.29, dt (11.2, 7.8)	
1'	–	134.93$^{\#}$, 134.96$^{\#}$
2'	6.79*, m	111.19$^{\#}$, 112.23$^{\#}$
3'	–	127.5
4'	–	147.8
5'	–	144.6
6'	6.79*, m	115.27$^{\#}$, 115.35$^{\#}$
7'	4.56, br d (7.0)	84.76$^{\#}$, 84.87$^{\#}$
8'	5.93*, ddd (17.1, 10.3, 7.0) 5.92*, ddd (17.1, 10.3, 7.0)	138.90$^{\#}$, 138.95$^{\#}$
9'a	5.29, dd (17.1, 1.2)	116.5
9'b	5.23, dd (10.3, 1.6)	
4-OH	5.61, s	-
3-OCH_3	3.87, s (3H)	56.2
5'-OCH_3	3.90, s (3H)	56.3
7'-OCH_3	3.34, s (3H)	56.5
9-Ac Me	2.01, s (3H)	20.9
9-Ac CO	–	170.9

* overlapping signals; $^{\#}$ interchangeable signals

Annex 6

^{1}H NMR spectroscopic data of compounds **39, 41, 42, 46, 47** and **50** [δ ppm (*J* =Hz), $CDCl_3$, 500 MHz (^{1}H)]

Position	39	41	42	46	47	50
6	7.00, d (8.1)	-	-	7.02, d (7.6)	7.03, d (7.6)	7.04, d (8.0)
7	7.32, t (8.1)	6.99, d (8.8)	7.07, d (8.7)	7.34, t (7.6)	7.36, t (7.6)	7.40, t (8.0)
8	7.14, d (8.1)	7.03, d (8.8)	7.05, d (8.7)	7.13, d (7.6)	7.16, d (7.6)	7.20, d (8.0)
9	2.64, s	2.55, s	2.77, s	2.73, s	2.64, s	2.66, s
1'a	4.95, d (17.2)	4.94, d (17.4)	5.11, d (16.9)	5.16, d (9.5)	5.16, d (9.5)	1.43, d (6.5)
1'b	5.18, d (11.3)	5.18, d (10.5)	5.08, d (10.1)	5.11, d (17.7)	5.11, d (17.7)	
2'	6.00, dd (17.2, 11.3)	6.02, dd (10.5, 17.4)	6.15, dd (16.9, 10.1)	6.16, dd (17.7, 9.5)	6.16, dd (17.7, 9.5)	4.80, q (6.5)
4'α	1.78, dd (14.1, 11.5)	1.78, dd (14.1, 10.6)	1.83, dd (14.1, 12.2)	2.08, d (14.0)	2.14, d (14.2)	2.54[a] dd (15.2, 2.5)
4'β	1.88, dd (14.1, 1.7)	1.89, dd (14.1, 1.6)	1.68, br d (14.1)	2.31, d (14.0)	2.37, d (14.2)	1.78 [a] dd (15.2, 9.2)
5'	4.83, ddd (11.5, 8.3, 1.7)	4.83, ddd (10.6, 8.2, 1.6)	4.38, m	-	-	5.27, br d (9.2)
6'	5.36, d (8.3)	5.38, br d (8.2)	1.74, m, 2.26, m	3.69, s	3.68, s	-
7'	-	-	2.81 m			7.00, br s
8'	1.82, s	1.82, s	1.28, d (7.1)	5.39, d (4.5)	5.31, d (12.2)	1.84, s
9'	1.71, s	1.72, d (0.6)	-	1.65, s	1.63, s	-
10'	1.58, s	1.58, s	1.56, s	1.62, s	1.61, s	1.58, s
11'	-	-	3.74, s	-	-	
6(OH)	-	5.05, s	4.85, s	-	-	
8'(OH)	-		-	3.19, d (4.5)	3.02, d (12.2)	

[a] Signals may be reversed.

Annex 7

^{13}C NMR data of compounds **39**, **41, 42**, **46**, **47**, and **50** (125 MHz, $CDCl_3$, δ ppm)

Position	39	41	42	46	47	50
2	160.8	164.2	162.4	160.5	160.3	160.9
3	105.1	105.1	103.4	107.2	106.9	108.9
4	164.2	161.1	167.4	160.1	160.0	167.4
4a	114.8	115.6	115.4	114.3	114.2	112.1
5	137.2	121.4	123.8	137.3	136.5	136.7
6	127.4	150.3	150.7	127.7	127.8	126.4
7	130.8	115.0	115.4	131.2	131.3	131.9
8	114.9	119.2	120.2	115.0	115.3	114.8
8a	154.1	148.5	148.7	154.1	154.2	156.1
9	23.8	13.8	12.6	24.0	23.8	21.3
1'	114.3	114.2	111.6	113.1	113.3	15.6
2'	144.6	144.7	145.8	144.5	144.1	93.0
3'	38.0	38.1	36.6	36.3	36.6	45.4
4'	42.4	42.5	43.5	39.3	39.3	36.3
5'	72.0	72.1	74.5	105.1	103.6	78.4
6'	122.7	122.8	38.7	62.7	63.6	129.6
7'	138.5	138.6	35.9	64.0	63.5	149.3
8'	25.8	25.8	17.3	98.4	98.3	10.5
9'	18.6	18.6	176.7	12.0	12.4	174.0
10'	26.1	26.2	24.8	25.3	25.8	23.2
11'	-	-	52.0	-	-	

Annex 8

^{1}H NMR spectroscopic data of compounds **51**–**56** [500 MHz, $CDCl_3$, δ ppm (J =Hz)]

Position	51+52	53	54	55	56
6	7.01, d (8.0)/7.02 d (8.0)	7.10, d (7.8)	7.10, d (8.0)	7.11, d (7.9)	7.08, d (8.0)
7	7.33, br t (8.0)	7.39, t (7.8)	7.38, t (8.0)	7.38, t (7.9)	7.38, t (8.0)
8	7.17, d (8.0)	7.19, d (7.8)	7.17, d (8.0)	7.18, d (7.9)	7.18, d (8.0)
9	2.68, s	2.72, s	2.74, s	2.74, s	2.67, s
1'a	2.60, m (2H)	5.22, d (17.5)	5.06, d (17.3)	4.96, d (17.4)	5.06, d (17.4)
1'b	1.98, dd (13.4, 6.2) /2.03, dd (13.4, 6.2)	5.10, d (10.3)	5.09, d (10.5)	5.09, d (10.8)	5.14, d (10.6)
2'	2.10, dd (13.4, 6.2) /2.13, dd (13.4, 6.2)	6.19, dd (17.5, 10.3)	6.18, dd (17.3, 10.5)	6.02, dd (17.4, 10.8)	6.11, dd (17.4, 10.6)
4'α	3.05, d (16.0)/2.99, d (16.6)	3.45, d (15.3)	3.61, d (14.0)	2.91 d (13.7)[a,b]	3.19, d (13.2)[a]
4'β	2.91, d (16.0)/2.94, d (16.6)	2.68, d (15.3)	2.41, d (14.0)	2.74 d (13.7)[a,b]	3.03, d (13.2)[a]
6'	3.36, s/3.38, s	4.30, s	4.29, s	-	4.55, d (17.3)[a]
				-	4.51, d (17.3)[a]
8'	1.41, s/1.43 s	1.41, s	1.44, s	2.06, s	-
9'	1.27, s	1.27, s	1.31, s	1.70, s	-
10'	1.60, s/1.57, s	1.66, s	1.65, s	1.57, s	1.66, s
7'-OH		3.54, s	3.86, br s	-	-

[a] signals may be reversed

[b] data obtained from ^{1}H NMR record in benzene-d_6 at 328 K

Annex 9

^{13}C NMR data of compounds **51**–**56** [125 MHz, $CDCl_3$, δ ppm]

Position	51+52	53	54	55	56
2	162.8	161.1	161.1	161.1	160.9
3	161.2	114.2	116.4	109.6	116.6
4	99.98/99.95	168.9	168.2	166.1	167.0
4a	114.6/114.7	116.6	116.6	116.4	114.
5	136.59/136.61	135.4	135.3	135.9	137.1
6	127.6/127.7	128.1	128.1	128.3	128.3
7	130.7/130.8	131.2	131.1	131.2	131.6
8	115.3	114.8	114.8	114.9	115.0
8a	153.8	152.6	152.4	152.9	153.5
9	23.7/23.8	23.8	23.5	23.9	23.9
1'	17.4	115.1	113.4	113.6	113.9
2'	29.7/29.8	141.0	145.7	143.4	144.0
3'	78.8/78.9	44.2	42.4	42.9	42.8
4'	48.3/48.5	53.4	53.7	53.5	53.3
5'	203.2/203.0	208.4	210.6	196.3	207.4
6'	65.9/66.0	93.7	94.9	147.8	78.3
7'	61.6/61.7	72.0	72.5	137.5	-
8'	24.8/24.9	24.9	24.8	19.6	-
9'	18.5/18.7	26.9	27.1	20.3	-
10'	24.7/25.0	30.2	23.2	23.9	27.0

Annex 10

^{1}H and ^{13}C NMR data of compound **58** [500 MHz (^{1}H), and 125 MHz (^{13}C), $CDCl_3$, δ ppm (J = Hz)]

Position	^{1}H NMR	^{13}C NMR	Key HMBC correlations
2	-	161.0	
3	-	103.8	H-6’
4	-	167.6	H-6’
4a	-	111.2	H-6, H-8, H-9
5	-	142.2	H-7, H-9, H-1’
6	7.00, d (7.8)	124.9	H-9
7	7.38, t (7.8)	132.2	
8	7.20, d (7.8)	115.2	
8a	-	157.2	H-7, H-8
9	2.82, m 3.31, dd (13.2, 7.5)	34.2	H-6
1'	1.77, m 2.33, m	33.1	
2'	5.70, dd (12.4, 5.1)	128.8	H-10’
3'	-	130.4	H-10’
4'	2.17, d (13.5) 3.03, d (13.5)	37.6	H-2’, H-10’
5'	-	129.9	H-4’, H-8’
6'	3.50, d (10.1)	51.1	
7'	2.68, m	37.3	
8'β	3.54, d (10.5)	76.3	
8'α	4.27, d (8.3)		
9'	1.14, d (7.0)	12.2	H-8’
10'	1.98, s	26.9	H-2’, H-4’

Annex 11a

^{1}H NMR spectroscopic data of compounds **59**–**61** [500 MHz, $CDCl_3$, δ ppm (J =Hz)]

Position	59 (VP-54)	60 (VP-137)	61 (VP-138)
3	4.15, d (11.3)	3.21, d (11.6)	3.10, d (11.6)
6	6.71, d (8.0)	7.05, d (8.0)	7.04, d (8.0)
7	7.20, t (8.0)	7.30, t (8.0)	7.28, t (8.0)
8	6.78, d (8.0)	6.83, d (8.0)	6.80, d (8.0)
9	2.39, s	2.43, s	2.39, s
1'a	4.89, d (17.2)	5.12, d (17.5)	4.98, d (17.5)
1'b	4.78, d (10.6)	5.17, d (11.0)	5.04, d (11.0)
2'	5.65, dd (17.2, 10.6)	6.51, dd (17.5, 11.0)	5.90, dd (17.5, 11.0)
4'α	2.42, d (17.1)	2.51, d (18.0)	2.27, d (18.0)
4'β	2.23, d (17.1)	2.27, d (18.0)	2.60, d (18.0)
6'	3.43, d (11.3)	2.73, d (11.6)	2.72, d (11.6)
8'	1.56, s	1.51, s	1.50, s
9'	1.23, s	1.34, s	1.34, s
10'	1.04, s	1.12, s	1.73, s

Annex 11b

^{1}H NMR spectroscopic data of compounds **62** (**VP-145**) and **63** (**VP-140**)
[500 MHz, $CDCl_3$, δ ppm (J =Hz)]

Position	62 (VP-145)	63 (VP-140)
3	3.53, s	3.50, s
7	6.88, d (7.8)	6.87, d (7.8)
8	7.35, t (7.8)	7.34, t (7.8)
9	6.90, d (7.8)	6.90, d (7.8)
11	2.64, s	2.63, s
1a'	5.11, d (11.0)	5.09, d (17.4)
1b'	5.17, d (18.0)	5.05, d (10.7)
2'	6.26, dd (18.0, 11.0)	6.20, dd (17.4, 10.7)
4'α	2.50, d (13.0)	3.39, d (12.5)
4'β	3.36, d (13.0)	2.18, d (12.5)
6'	4.19, s	4.22, s
8'	1.54, s	1.56, s
9'	1.29, s	1.37, s
10'	1.60, s	1.37, s

Annex 12

^{13}C NMR data of compounds **59**–**63** (125 MHz, $CDCl_3$, δ ppm)

Position	59	60	61	62	63
2	–	–	–	123.8	123.7
3	59.2	58.4	59.1	63.3	62.7
4	205.9	204.5	205.9	191.7	191.1
54a	127.3	132.2	132.7	119.0	119.1
65	137.5	140.0	139.6	142.4	142.5
76	123.4	128.5	128.4	126.1	126.3
87	132.6	132.2	132.0	134.8	134.7
98	116.4	123.5	123.3	115.8	115.9
108a	156.4	154.4	154.0	158.3	158.4
119	21.5	20.6	20.1	23.0	23.1
1'	113.4	112.1	115.0	114.3	111.3
2'	143.1	145.7	140.8	142.3	148.6
3'	43.9	43.7	44.0	41.0	40.6
4'	55.7	54.4	53.8	57.2	56.2
5'	214.4	213.4	213.5	211.0	211.8
6'	59.7	56.3	56.8	87.0	86.7
7'	73.1	80.5	80.6	85.1	84.9
8'	30.4	26.1	26.1	27.8	27.6
9'	23.8	22.4	22.3	21.1	21.2
10'	20.4	20.7	27.3	32.2	20.0